Harpur Hill, Buxton, SK17 9JN
Telephone: +44 (0)114 289 2000
Facsimile: +44 (0)114 289 2050

A Review of the State-of-the-Art in Gas Explosion Modelling

HSL/2002/02

Project Leader: C. J. Lea

H. S. Ledin MSc PhD DIC

Fire and Explosion Group

Summary

Objectives

1. To identify organisations involved in gas explosion research in the U.K. and Europe.
2. To survey these organisations, to determine their areas of current and proposed work.
3. To collate their responses in a report, which also provides an up to date literature review of gas explosion modelling.
4. To critically assess the strengths and weaknesses of available gas explosion models.
5. To recommend areas where further work is needed to improve the accuracy of the gas explosion models.

Main Findings

1. There are a wide range of class of models available - from empirical and phenomenological, through to those which are Computational Fluid Dynamics (CFD) based. The latter category falls into two areas: 'simple' - many obstacles not resolved and 'advanced' - all obstacles resolved by the 3-D CFD grid.
2. Generally as one moves from empirical to advanced CFD, models become based on more fundamental physics, are able to more accurately represent the real geometry, but require increasing resource to set-up, run and interpret the results.
3. Models in each class embody a number of simplifications and assumptions, limiting their ability to be used as reliable predictive tools outside their range of validation against test data. It appears that only those models falling into 'advanced' CFD class could in principle be capable of being truly predictive tools outside their immediate range of validation. However, even here the existing models have limitations and require further development and testing before this capability is fully realised - which even then will currently be limited to relatively simple geometries by the required computer resources.
4. Many of the CFD-based explosion models in current use employ relatively crude approximations of the modelled geometry, relying on calibrated sub-grid models.
5. Most of the 'simple' CFD codes and some of the 'advanced' CFD codes most commonly used for explosion prediction use simple, dated numerical schemes for both the computational grid and the finite differencing, which could lead to substantial numerical errors.
6. The combustion model used in CFD-based approaches to predict the reaction rates are also subject to a considerable degree of uncertainty. Models, which

employ prescribed reaction rate, could be more sound than those relying on an Eddy Break-Up model, because the latter requires a resolution of the flame front unlikely to be achieved in practice. Work is currently under way on the incorporation of detailed chemical kinetics into a gas explosion model, but it will not be feasible to use such a model on a real complex plant geometry in the foreseeable future.

7. The simple eddy-viscosity concept is ubiquitous amongst the explosion codes for modelling turbulent transport, but this model of turbulent transport is not strictly applicable in high speed, combusting flows, leading to further possible errors. There is a move to full Reynolds stress turbulence models, these have either been implemented in research type codes - currently not available on general release, or have not been tested for explosions. There are numerical stability problems associated with Reynolds stress transport models which need to be addressed.

8. The accuracy expected from, say phenomenological and 'simple' CFD models, is generally fairly good (to within a factor of two), e.g. the models yield solutions which are approximately correct, but, importantly, only for a scenario for which the model parameters have been tuned. This limits the applicability of these models as truly predictive tools.

Main Recommendations

1. There is a range of modelling approaches available, each with their own strengths and weaknesses. In order to establish greater confidence in model predictions, it is clear that, for the future, improvements in the physics and the numerics are required, particularly for the CFD-based approaches. However, predictive approaches are needed now. It is thus important that the user be aware of the uncertainties associated with the different models. The following recommendations are essentially those needed to be taken on board by model developers and their funders. They primarily relate to CFD models, which, in principle, should offer the best hope of becoming truly predictive models of gas explosions, with wide applicability.

2. Ideally one would replace the Cartesian grid / PDR (Porosity / Distributed Resistance) based CFD models by models that are capable of representing a given geometry more accurately. However, the likely time scale for the necessary advances in computing power and code efficiency which will possibly allow geometries to be fully grid resolved is large, possibly of the order of ten years or more. Until this is possible a hybrid approach has to be adopted, whereby body-fitted grids are used to represent the larger objects within the explosion domain, with the PDR approach reserved for the regions that may not be resolved by the grid. It is therefore recommended that methodologies are developed to allow a seamless transition between resolved and PDR-represented solutions as grids are refined. There should be a move away from fixed grid cell size, because such models will require constant re-calibration for new scenarios due to physical and numerical errors associated with the large grid cell size always needing to be

compensated. This situation cannot improve until there is a move to a more soundly based methodology.

3. More work is needed to establish the reliability of the combustion models used. Presently, the majority of the explosion models investigated prescribe the reaction rate according to empirical correlations of the burning velocity. However, it should be recognised that these correlations are subject to a large uncertainty. The eddy break-up combustion model should ideally not be used if the flame front cannot be properly resolved or, the resulting errors should be recognised and quantified.

4. The sensitivity of model predictions to the turbulence model used should be investigated. Turbulence modelling has not yet received much attention in the field of explosion modelling. The commonly used two-equation, k-ε model has a number of known failings i.e. does not predict counter-gradient diffusion, but remains in use due to its economy and robustness. Large improvements in over-pressure prediction have been noted by including simple terms into the k-e model, to account for compressibility effects. However, inclusion of these terms is by no means universal. There is a wide range of advanced, non-linear k-e models now available. Ideally Reynolds stress transport modelling should be used but the models require much work to ensure that improvements are not offset by lack of numerical stability.

5. Model development should now be driven by repeatable, well defined, detailed experiments, focusing on key aspects of the physics of explosions. This tends to imply small or medium-scale experiments. Large-scale experiments are suitable as benchmark tests, but code calibration on the basis of macroscopic property measurements should be treated with caution, since it is quite possible to obtain approximately correct answers but for the wrong reasons due to gross features swamping finer details. Detailed comparisons of flame speeds, species concentrations, etc., should allow deficiencies in explosion model physics and numerics to be identified, and solutions developed and tested.

6. There are no, or few, technical barriers to implementation of the above model improvements, beyond a willingness and need to do so.

7. Perhaps the safest that can be advised at this point is that it would be unwise to rely on the predictions of one model only, i.e. better to use a judicious combination of models of different types, especially if a model is being used outside its range of validation.

Contents

1. INTRODUCTION 1
1.1. Background 1
1.2. A Description of Gas Explosions 1
1.3. Why Model Explosions? 2
1.4. Model Requirements 3
1.5. Review Methodology 4

2. DESCRIPTION AND DISCUSSION OF CURRENT MODELS 7
2.1. Empirical Models 7
2.1.1. Introduction 7
2.1.2. TNT Equivalency Method 7
2.1.3. TNO Method 8
2.1.4. Multi-Energy Concept 8
2.1.5. Baker-Strehlow Method 9
2.1.6. Congestion Assessment Method 10
2.1.7. Sedgwick Loss Assessment Method 11
2.2. Phenomenological Models 12
2.2.1. Introduction 12
2.2.2. SCOPE 12
2.2.3. CLICHE 14
2.3. CFD Models 17
2.3.1. Introduction 17
2.3.2. EXSIM 18
2.3.3. FLACS 20
2.3.4. AutoReaGas 22
2.4. Advanced CFD Models 24
2.4.1. Introduction 24
2.4.2. CFX-4 24
2.4.3. COBRA 26
2.4.4. NEWT 27
2.4.5. REACFLOW 29
2.4.6. Imperial College Research Code 31

3. DISCUSSION 34
3.1. Overview of Model Constraints 34
3.2. Empirical Models - Main Capabilities and Limitations 36
3.3. Phenomenological Models - Main Capabilities and Limitations 37
3.4. Simple CFD Models - Main Capabilities and Limitations 37
3.5. Advanced CFD Models - Main Capabilities and Limitations . . . 39
3.6. Model Accuracy 39
3.7. Recommendations for Future Work 42
3.7.1. Grid Improvements 42
3.7.2. Combustion Model Improvements 42
3.7.3. Turbulence Model Improvements 43
3.7.4. Experimental Input to Model Development 43

3.7.5. Miscellaneous Issues 43

4. CONCLUSION 44

5. REFERENCES 46
5.1. References Cited in the Report 46
5.2. References Used but not Cited 53

APPENDIX A - THEORETICAL DESCRIPTION OF GAS EXPLOSIONS 54
A1. Conservation Equations 54
A2. Turbulence Modelling 56
A3. Reaction Rate Modelling 57
A3.1. Turbulent Flame Speed 58
A3.2. Turbulent Reaction Rate 59
A4. Numerical Modelling 61

APPENDIX B - COMBUSTION MODEL IN SCOPE CODE 66

APPENDIX C - COMBUSTION MODELS IN CFD CODES 68
C1. Exsim 68
C2. FLACS 69
C3. CFX-4 70
C4. COBRA 73
C5. NEWT 74

APPENDIX D - DISCRETISATION OF PARTIAL DIFFERENTIAL EQUATIONS 77
D1. Introduction 77
D2. First-Order Discretisation Schemes 77
D3. Second-Order Discretisation Schemes 78
D3.1. Central Differencing Scheme 78
D3.2. Total Variation Diminishing Schemes 78
D4. References 79

APPENDIX E - COMMUNICATIONS WITH CHRISTIAN MICHELSEN RESEARCH 80
E1. Introduction 80
E2. Comments from J. R. Bakke on 20 June 2001 80
E3. Reply from O. R. Hansen on 9 July 2001 80

List of Figures

Figure 1 - Example of a congested geometry 40

Figure 2 - Comparison of calculated and measured maximum over-pressures for MERGE medium-scale experiments, (×) - COBRA predictions and (◇) - EXSIM predictions; a) all experiments and b) experiments with maximum over-pressures below 1.5 bar, see also Popat *et al.* (1996) 40

Figure 3 - Comparison of calculated and measured maximum over-pressures for MERGE large-scale experiments, (×) - COBRA predictions, (◇) - EXSIM predictions, (●) - FLACS predictions and (○) AutoReaGas predictions; a) all experiments and b) experiments with maximum over-pessures below 1 bar, see also Popat *et al.* (1996) 41

Figure A1 - Schematic description of the flame reaction zone 58

Figure A2 - A non-orthogonal structured grid 62

Figure A3 - A multi-block, non-orthogonal structured grid 62

Figure A4 - An unstructured grid with prismatic grid in the boundary layer 63

Figure A5 - Control volume in one dimension 64

List of Tables

Table 1 - Numerical Model Summary 5

1. INTRODUCTION

1.1. Background

The aim of this review is to inform the Hazardous Installations Directorate about the current status and future direction of gas explosion numerical models presently in use. Gas explosions are a major hazard in both the on-shore and off-shore environments.

The 1974 explosion at the Nypro plant at Flixborough is one of the most serious accidents to afflict the chemical processing industry. The explosion at Flixborough was caused by the ignition of a flammable cloud containing about 50 tons of cyclohexane, the cyclohexane release was probably due to the failure of a temporary pipe. The blast has been estimated to be equivalent to about 16 tons of TNT, with the result that 28 people were killed, 89 injured, the plant was totally destroyed, and damage was caused to nearly 2000 properties external to the site.

In 1988 on the offshore platform Piper Alpha a small explosion in a compressor module caused fires which resulted in the rupture of a riser. Most of the platform was subsequently destroyed by fire, causing the death of 167 people. The over-pressure generated by the initial explosion has been estimated to be only 0.3 bar, Cullen (1990).
This report describes empirical models, phenomenological models and Computational Fluid Dynamics (CFD) based models. Empirical models are the simplest way of estimating deflagration over-pressures. These models contain correlations and contain little or no physics. Phenomenological models are simplified models which represent the major physical processes in the explosion. CFD models involve numerical evaluation of the partial differential equations governing the explosion process and yield a great deal of information about the flow field.

The report is further restricted to numerical models of deflagrations. Detonations are not included. A deflagration is the name given to the process of a flame travelling through a combustible mixture where the reaction zone progresses through the medium by the processes of molecular (and / or turbulent) diffusion of heat and mass. The burning velocity - i.e. the velocity of the combustion front relative to the unburnt gas is sub-sonic relative to the speed of sound in the unburnt gas. A detonation is a self-driven shock wave where the reaction zone and the shock are coincident. The combustion wave is propagating at super-sonic velocity relative to the speed of sound in the unburnt gas. The chemical reaction is initiated by the compressive heating caused by the shock, the energy released serving to drive the compression wave. Propagation velocities of the combustion wave for a detonation can be up to 2000 m s^{-1} with a pressure ratio across the detonation front of up to 20.

This is a update and extension of the gas explosion model review by Brookes (1997).

1.2. A Description of Gas Explosions

An explosion is the sudden generation and expansion of gases associated with an increase in temperature and an increase in pressure capable of causing structural damage. If there is only a negligible increase in pressure then the combustion phenomena is termed a flash-fire.

Gas explosions are generally defined as either confined or unconfined. An explosion in a process vessel or building would be termed as confined. If the explosion is fully confined - i.e. if there is no venting and there is no heat loss, then the over-pressure will be high, up to about eight times higher than the starting pressure. The pressure increase is determined mainly by the ratio of the temperatures of the burnt and unburnt gases. Explosions in confined but un-congested regions are generally characterised by low initial turbulence levels and hence low flame speeds. If the region contains obstacles, the turbulence level in the flow will increase as the fluid flows past the objects, resulting in a flame acceleration. If the confining chamber is vented, as is usually the case, then the rate of pressure rise and the vent area become factors that will influence the peak pressure. The rate of pressure rise is linked to the flame speed, which in turn is a function of the turbulence present in the gas.

The over-pressure generated by an unconfined explosion is a function of the flame speed, which in turn is linked to the level of turbulence in the medium through which the flame progresses. As the flame accelerates the pressure waves generated by the flame front begin to coalesce into a shock front of increasing strength. If the explosion occurs in a medium of low initial turbulence, is fully unconfined, and there are no obstacles present then the generated over-pressure is very low. If obstacles are present then expansion-generated flow, created by the combustion, of the unburnt gas passing through the obstacles will generate turbulence. This will increase the burning velocity by increasing the flame area and enhancing the processes of molecular diffusion and conduction, and this will in turn increase the expansion flow which will further enhance the turbulence. This cycle, so called Schelkchkin mechanism, continues generating higher burning velocities and increasing over-pressures.

1.3. Why Model Explosions?

Deflagrations are unwanted events. Models containing physical descriptions of deflagrations are a complement to experiments in risk assessments and/or when designing or assessing mitigating features. The more complex models have the wherewithal to be applied to diverse situations, but must not therefore be assumed to be more accurate.

The effects of an explosion depends on a number of factors, such as maximum pressure, duration of shock wave interaction with structures, etc. These factors in turn depend on a number of variables:

- Fuel type
- Stoichiometry of fuel
- Ignition source type and location
- Confinement and venting (location and size)
- Initial turbulence level in the plant
- Blockage ratios
- Size, shape and location of obstacles

- Number of obstacles (for a given blockage ratio)
- Scale of experiment/plant

The reactivity of fuel has a profound effect on the overpressures generated in a given geometry. The least reactive gas is methane, while acetylene and especially hydrogen give rise to very high pressures.

The stoichiometry of the gas cloud is also important. Lean mixtures produce lower overpressures than rich or stoichiometric mixtures, while slightly rich mixtures yield the highest over-pressures for a given plant layout.

Ignition source type also affects the strength of the explosion; jet-type, or bang-box-type, ignition sources give rise to higher over-pressures than a planar or point source. The location of the ignition is also important, but must be viewed in conjunction with information about the plant geometry, e.g. how confined and/or congested is the plant. Confinement leads to pressure build-up and influences the way the flame front advances through the geometry. Venting is one way of reducing the over-pressure generated by the combustion. Strategically placed vents can greatly reduce the impact of a deflagration.

Explosions situated in a quiescent environment will generally lead to lower over-pressures than those occuring in turbulent flow environments. This is due to the enhanced burning rate experienced by the flow.

One can define a blockage ratio, which is measure of how congested the plant is. Explosions in plants with large blockage ratios usually yield higher over-pressures than small blockage ratios. However, the size and shape of the obstacles are also important factors to take into account. In general, for a given blockage ratio, many small objects results in higher pressures than larger objects. Furthermore, the location of the obstacles also affects the pressure. The more tortuous route the flame has to travel through the domain, the higher pressure is likely to be produced, due to turbulence enhancement of the burning velocity.

Finally, the scale of experiment/plant is also an important factor. Large-scale experiments generally yield higher pressures than small-scale ones. This makes it difficult to predict, from a small-scale experiment, what the pressures are likely to be in real plants.

Ideally, explosion risks should be considered at the plant design stage, but for various reasons this might not be possible. Unfortunately accidents do happen, but research programmes consisting of experiments and modelling should hopefully result in a better understanding of why the accident happened and how the impact can be minimised or the risk of explosion be mitigated or eliminated completely. In most cases, a great number of scenarios needs to be investigated, which is one justification for developing and using models of varying degrees of complexity.

1.4. Model Requirements

A number of factors influencing the strength of the deflagration were identified in the previous section. A model should ideally take all these variables into account. In addition to

this, the model should contain appropriate physics, be able to deal with different fuels and ambient conditions without special tuning of constants, and be easy to use. Furthermore, the computer code in which the model is implemented should be numerically accurate, allow for an accurate representation of the geometry, be easy to use and the run times should be short.

Some of these requirements are contradictory. Complex models are unlikely to run very quickly. In some cases the understanding of the underlying physics is sketchy, at best. Turbulent premixed combustion is an active area of research and new findings may find their way into the models currently in use. However, there are limitations in terms of computer resources. A real world plant is very complex, with a large number of pipes, tanks and other equipment of various shapes and sizes, and it is not possible today to resolve all the features of the geometry - due to the demands on computer memory and processor speed. The flame acceleration due to turbulence generated when the flow has to make its way past obstacles is partly down to a more intense combustion, but also an increase in flame area. Most of the CFD codes do not allow for flame front tracking, neither would these codes be able to properly resolve the flame front.

However, the models currently in use do contain some physics and chemistry. In many situations, the results of the simulations are in good agreement with experiments, but it is important to remember that the models have their limitations. The choice of model depends on the level of detail required, on the level of accuracy required, and time available for the calculations.

The turbulence models implemented in the CFD codes can perform well for some types of flows, mainly high Reynolds number, isothermal, isotropic, incompressible flows. These models have no mechanism for modelling transition from laminar to turbulent flow. Deflagrations in confined spaces might start in a quiescent environment. A transition from laminar to turbulent flow is a distinct possibility, which can contribute to inaccurate solutions.

1.5. Review Methodology

This review was conducted by following three approaches. The HSL Sheffield Information Centre was asked to carry out an on-line search seeking information on gas explosion modelling. A number of key words and phrases, as well as a large number of possible authors, were provided

A paper based literature survey was conducted. Relevant reports and papers were collected, the reference lists of which were used to discover further useful sources of information. The survey continued to 'fan out' in this manner, generating a large quantity of useful material. This search has been mainly used to provide the background to this report, but some recent information on certain models was also discovered in the open literature.

Finally, the most recent information on each of the models has been obtained directly from the model developers. This was achieved by sending a standard letter to a number of organisations, inviting comment on the current status and future development of their gas explosion modelling. Further letters were sent to organisations that failed to respond to the original request. Letters were sent to around twenty organisations, over half of which eventually responded to the request for information. Generally, however, the organisations

that did reply showed some reluctance to divulge full technical details of their models, most probably due to the increasing commerciality of their operations - either through consultancy or code sales. The numerical models reviewed in the present report are listed in Table 1.

Table 1 - Numerical Model Summary

Name	Type	Grid	Accuracy	Reaction Model
TNT Equivalency	Empirical	N/A	N/A	None
TNO	Empirical	N/A	N/A	None
Multi Energy	Empirical	N/A	N/A	None
Baker-Strehlow	Empirical	N/A	N/A	None
Congestion Assessment Method	Empirical	N/A	N/A	None
Sedgwick Loss Assessment Method	Empirical	N/A	N/A	None
SCOPE	Phenomeno-logical	N/A	N/A	Empirical Correlation
CLICHE	Phenomeno-logical	N/A	N/A	Empirical Correlation
EXSIM	3D CFD Finite Volume	Structured, Cartesian, PDR Treatment of Sub-Grid Scale Objects	First Order Temporal Second Order Spatial	Eddy Break-Up
FLACS	3D CFD Finite Volume	Structured, Cartesian, PDR Treatment of Sub-Grid Scale Objects	First Order Reaction Progress Variable Second Order	Empirical Correlation
AutoReaGas	3D CFD Finite Volume	Structured, Cartesian, PDR Treatment of Sub-Grid Scale Objects	First Order Temporal and Spatial	Empirical Correlation
CFX-4	2D and 3D CFD Finite Volume	Structured, Body-fitted	Higher Order Temporal and Spatial	Eddy Break-Up and Thin Flame

COBRA	2D and 3D CFD Finite Volume	Unstructured, Cartesian, Cylindrical Polar or Hexahedral, Adaptive, PDR Treatment of Sub-Grid Scale Objects	Second Order Temporal and Spatial	Empirical Correlation
Imperial College Research Code	2D CFD Finite Volume	Unstructured, Adaptive	Implict Temporal, Second order (TVD) Spatial	Laminar Flamelet and PDF Transport
NEWT	3D CFD Finite Volume	Unstructured, Adaptive	Higher Order Temporal and Second Order Spatial	Eddy Break-Up and Laminar Flamelet
REACFLOW	2D and 3D CFD Finite Volume	Unstructured, Adaptive	First or Second Order Temporal and Spatial	Eddy Break-Up

2. DESCRIPTION AND DISCUSSION OF CURRENT MODELS

2.1. Empirical Models

2.1.1. Introduction

Empirical models are based on correlations obtained from analysis of experimental data. The models described below constitute a selection of methods commonly used in industry for risk assessment, etc. It does not purport to be an exhaustive selection.

2.1.2. TNT Equivalency Method

The TNT equivalency method is based on the assumption that gas explosions in some way resemble those of high charge explosives, such as TNT. However, there are substantial differences between gas explosions and TNT. In the former the local pressure is much less than for TNT detonations. Furthermore, the pressure decay from a TNT detonation is much more rapid than the acoustic wave from a vapour cloud explosion. Nevertheless the model has been used extensively to predict peak pressures from gas explosions. The TNT equivalency model uses pressure-distance curves to yield the peak pressure. One must use a relationship, see below, to find the mass of TNT equivalent to the mass of hydrocarbon in the cloud.

$$W_{TNT} \approx 10\ \eta\ W_{HC}\ , \qquad \text{[kg]} \tag{1}$$

Where W_{TNT} is the mass of TNT, W_{HC} is the actual mass of hydrocarbons in the cloud, and η is a yield factor ($\eta \approx 0.03$-0.05) based on experience. The factor 10 represents the fact that most hydrocarbons have ten times higher heat of combustion than TNT. In the original TNT equivalency model no consideration was taken of the geometry and therefore it is recommended that this model should not be used, Bjerketvedt, Bakke and van Wingerden (1997).

A TNT equivalency model which does take geometry effects into account has been proposed, Harris and Wickens (1989). Results from experiments formed the basis for the new formulation. The yield factor was increased to 0.2 and the mass of hydrocarbon in stoichiometric proportions was to correspond to the mass of gas in the severely congested region of the plant. For natural gas the mass of TNT can be arrived at using

$$W_{TNT} = 0.16\ W_{eff}\ , \qquad \text{[kg]} \tag{2}$$

where $V_{eff} = \min(V_{con}, V_{cloud})$ is the total volume of the congested region and $_{Vcloud}$ is the total volume of the gas cloud. The equation will hold for most hydrocarbons. It is recommended that the TNT equivalency model should not be used.

Weaknesses:

- Non-unique yield factor is needed
- Weak gas explosions not well represented
- Information only of the positive phase duration

- Not suited for gas explosions, since the physical behaviour of gas explosions differs substantially from that of solid explosives

- Difficult to define a sensible charge centre

2.1.3. TNO Method

The TNO method, Wiekema (1980), resembles the multi-energy method described in Sect. 2.1.4 below. The main difference between the two methods is that the TNO method assumes that the whole vapour cloud contributes to the over-pressure, rather than just the portion which happens to be in a confined and/or congested area. The TNO model and TNT equivalency model were used in the Dutch CPR14E handbook of methods for calculation of physical effects of the escape of dangerous materials, CPR14E (1979). The multi-energy method has replaced the TNO model in the revised CPR14E handbook, Mercx and van den Berg (1997). The TNO method will not be discussed further, but see Sect. 2.1.4 for details and comments.

2.1.4. Multi-Energy Concept

The multi-energy concept, van den Berg (1985), can be used to estimate the blast from gas explosions with variable strength. The method assumes that only that part of the gas cloud which is confined or obstructed will contribute to the blast. The rationale being that unconfined vapour clouds give rise to only small over-pressures if ignited. The over-pressure increases with increasing confinement. In essence, the method is based on numerical simulations of a blast wave from a centrally ignited spherical cloud with constant velocity flames.

There are two parameters feeding into the model. Firstly, a combustion-energy scaled distance, R_{ce} , related to the distance to the explosion centre can be defined as

$$R_{ce} = R_0 / (E/P_0)^{1/3}, \quad [\text{m}] \tag{3}$$

where R_0 is the distance to the explosion centre, E is the total amount of combustion energy, e.g. the combustion energy per volume times V_{cloud}, where V_{cloud} is the volume of vapour cloud in the congested area, and P_0 is the atmospheric pressure. The total amount of energy for a stoichiometric hydrocarbon-air mixture does not vary significantly with the type of hydrocarbon. Thus for a hydrocarbon-air mixture, the total combustion energy an be estimated from

$$E \approx 3.5\ V_{cloud}, \quad [\text{MJ}] \tag{4}$$

Where V_{cloud} is measured in m^3. It is important to note that only the confined and/or congested areas contribute to the blast. Secondly, the strength of the explosion can be estimated by taking into account the layout of the explosion source. The charge strength is given a number between one and 10, where 10 represents a detonation.

The two parameters can then be used to read a non-dimensional maximum "side-on" over-pressure and a non-dimensional positive phase duration from diagrams, where the source strength is represented by a set of curves.

Strengths:

- Fast method
- Conservative approximation can be made

Weaknesses:

- Setting a sensible value for the charge strength is difficult.
- Setting a sensible value for the total combustion energy, e.g. charge size is difficult.
- Not ideally suited to weak explosions, i.e. partly confined clouds.
- Difficult to accurately represent complicated geometries
- Not clear how to deal with several congested regions
- Not clear how to deal with multiple blast waves

In light of the weaknesses listed above, the choice of charge size and strength must ideally be based on other simulations, experimental data or by making a conservative assumption. Van den Berg (1991) suggested that V_{cloud} should be chosen to encompass the total volume of gas, that is both the confined and the unconfined part. This will in many cases lead to an overestimation of the over-pressure caused by the blast.

2.1.5. Baker-Strehlow Method

The Baker-Strehlow method, Baker, Tang, Scheier and Silva (1994), was developed to provide estimations of blast pressures from vapour cloud explosions. The model was further extended by Baker, Doolittle, Fitzgerald and Tang (1998). The methodology consists of a number of steps, assessing flame speed, fuel reactivity, confinement, etc.

- Walk through plant identifying potential explosion sites
- Decide on the dimensionality of the confined areas to work out flame speed
- Calculate burning velocity for fuel mixtures

The blast pressure and impulse are the read from a series of graphs. The revisions proposed by Baker *et al.* (1998) were the results of experience gained from plant walk throughs and hazard assessments.

Strengths:

- Easy to use
- Fast
- Takes into account some geometrical details, with regards to confinement
- Can handle multi-ignition points

Weaknesses:

- Can be over conservative

2.1.6. Congestion Assessment Method

The Congestion Assessment Method (CAM) was developed at Shell Thornton Research Centre, Cates and Samuels (1991). The model has been enhanced and further extended by Puttock, (1995, 1999).

Cates and Samuels (1991) devised a decision tree procedure as guidance for estimating the source pressure, taking into account the layout of the plant, e.g. degree of confinement and congestion and the type of fuel involved. The accuracy of the estimations was variable, but the method was designed to yield conservative pressures.

The method comprises three steps:

1) An assessment of the congested region is carried out to assign a reference pressure, P_{ref}, which is an estimation of the maximum over-pressure generated by a deflagration of a vapour cloud of propane.

2) The type of fuel is taken into account through a fuel factor, which is then multiplied by the reference pressure worked out in step i) to determine the maximum source pressure.

3) It is now possible to estimate the pressure experienced at various distances from the ignition point. Cates and Samuels (1991) assumed a simple decay law inversely proportional to the distance. Puttock (1995) generated pressure decay curves by fitting polynomials to detailed computations, which in turn had been validated by experimental data.

Puttock (1999,2000b) further improved the model when the results from the MERGE (Modelling and Experimental Research into Gas Explosions) project, which involved small scale, medium scale and large scale experiments were published, Mercx (1993). Development of CAM 2, Puttock (1999,2000b) also addressed the problems of i) non-symmetric plants, ii) plants which are much longer in one spatial direction than the other two, iii) making allowance for partial fill, e.g. where the gas cloud size is smaller than the

congested volume, and iv) how to deal with sharp-edged rather than rounded objects. The congestion assessment method is the most advanced empirical model reviewed in the present report. However, it is not known how well the model would perform for a new scenario for which the model has not been calibrated.

The user must assess the level of congestion and the level of confinement in the plant. This is not a problem for simple geometries, but many plant installations are highly complex in nature. There are guidelines for how to assess the congestion and the confinement of the plant. Nevertheless, it is quite possible that two people could independently make sufficiently different assessments of the plant which could lead to potentially significantly different predicted explosion generated over-pressures.

Strengths:

- Easy to use
- Short run times
- Calibrated against a large number of experiments
- Approaches sensible maximum over-pressure as severity index goes to infinity
- Can deal with non-symmetrical congestion and long, narrow plant

Weaknesses:

- Allows only a relatively crude representation of the geometry
- No uniqueness in the specification of level of congestion and level of confinement

2.1.7. Sedgwick Loss Assessment Method

Thyer (1997) tested the vapour cloud explosion model developed by Sedgwick Energy Ltd. The Sedgwick model is based on Puttock's CAM model, see Section 2.1.6, with some refinements. Thyer (1997) noted that the degree of resemblance with the CAM method was not easy to assess, in part due to scarce amount of details in their promotional leaflets. The package allows the user to set up a simple computer representation of the plant, using a graphical interface.

2.2. Phenomenological Models

2.2.1. Introduction

Phenomenological models are simplified physical models, which seek to represent only the essential physics of explosions. The greatest simplification made is with respect to the modelled geometry. Generally, no attempt is made to model the actual scenario geometry, which is instead represented by an idealised system - e.g. a single vented chamber containing a number of turbulence generating grids. This is a reasonable approximation for certain types of geometry (an offshore module for example), but may not be adequate for more complex situations. The physics of the explosion process may be described either empirically or theoretically. Phenomenological models fall somewhere between empirical correlations and CFD models, in terms of complexity. CFD models may in fact share some of the embedded physics with phenomenological models, but of course are in principle better able to model complex, arbitrary geometries. The run times for phenomenological models are short, of the order of a few seconds. This type of model is well suited to running through large number of different scenarios and can be used to pick out particular situations which can then be investigated using a CFD code to obtain further details.

2.2.2. SCOPE

The SCOPE (**S**hell **C**ode for **O**ver-pressure **P**rediction in gas **E**xplosions) model is under continuing development at Shell's Thornton Research Centre. The SCOPE model was initially designed for modelling explosions in offshore modules. However, the model may be applied to any geometry where a single flame path may be identified. SCOPE 2 was released in March 1994. It is based on the original version of SCOPE described by Cates and Samuels (1991). The present incarnation of SCOPE is SCOPE 3 which went live in early 1997, Puttock, Yardley and Cresswell (2000). This section will describe the SCOPE 2 code and then highlight the revisions which have been incorporated in SCOPE 3. Appendix B contains the differential equations solved in SCOPE.

SCOPE 2

The SCOPE code seeks to model gas explosions by representing the essential physics in a simplified form. Models of this type are to be distinguished from empirical models that are nothing more than 'fits' to existing experimental data and are of limited applicability. The model is one-dimensional and is based on the idealised geometry of a vented vessel containing a series of obstacle grids. The flow through each of these grids determines the turbulence and hence the rate of turbulent combustion downstream from the grid.

The flows from the vents are modelled using standard compressible vent flow relations. Vent opening may also be modelled using SCOPE 2. The vent area is taken to be zero until the vent opening pressure is reached, at which point the vent area is increased linearly with time until the vent is fully open at a pre-set value of the vent opening time.

The external explosion, generated by combustion in the unburnt gas pushed from the box, may exert a large influence on the internal pressure felt by the box. The vented gas forms a mushroom-shaped jet and the highest external pressure is generated when the flame burns in

the vortex at the mushroom head. The last of the gas to be vented from the box forms the stem of the mushroom. Therefore, the gas vented in the last stages of the explosion event contributes little to the external over-pressure. The external over-pressure calculated by the model is related to the vent flow (which in turn is related to the box internal pressure) when the flame has traversed 70 % of the box length. The ratio of the external pressure to the internal pressure also depends on the vent area, this ratio is taken as

$$\frac{P_{ext}}{P_{0.7}} = 3.75 \left(\frac{A_v}{V^{2/3}} \right)^{0.85}, \qquad (5)$$

where V is the box volume, P_{ext} is the external explosion over-pressure, and $P_{0.7}$ is the maximum internal pressure for $X/L \leqslant 0.7$. Finally, the maximum internal pressure is determined by

$$P_{max} = P_{emerg} + 0.7\, P_{ext}, \qquad (6)$$

where P_{emerg} is the internal pressure at the time that the flame emerges from the box.

SCOPE 2 has received extensive experimental calibration by comparison with experiments in idealised geometries similar to that modelled by SCOPE 2. The experiments have been conducted at various scales and include a 2.5 m^3 box, a 35 m^3 box, and the 550 m^3 SOLVEX experiments, Puttock *et al.* (1996).

SCOPE 3

One of the most significant changes from SCOPE 2 is the ability to handle mixed scale objects. Generally objects will be of mixed scale and in characterising these objects in terms of a blockage ratio and a shape (round or sharp edged) information has been lost. The main effect of obstacles of various sizes is on the flame surface area which increases as it passes between the objects; the flame area affects the consumption rate of the unburnt gas (cf. eqn. B1). This is referred to as 'obstacle complexity' in SCOPE. SCOPE 3 will allow rear venting, in addition to the side and main vents allowed by SCOPE 2. Venting behind the ignition point can have a large effect on the development of the explosion over-pressure. Rear venting allows some of the initial combustion generated expansion flow to leave the box, decreasing the flow of unburnt gas through the obstacles. This reduces the turbulence level in the unburnt gas, which reduces the turbulent burning velocity and hence the over-pressure. Improvements have also been made to the basic combustion model which now has a better treatment for variations in stoichiometry as well as allowing mixtures of fuel gases. A pressure dependency has been implemented for the expansion ratio and the laminar burning velocity. SCOPE 3 has been validated against more than 300 experiments, Puttock *et al.* (2000). Further developments of SCOPE 3 involves modelling of un-confined but congested plant, with central ignition, and modelling the effect of water deluge on explosion development, Puttock *et al.* (2000).

Strengths:

- Can handle venting and external explosions
- Imposed limits to flame self-acceleration yield sensible flame speeds
- Validated against a large number of small-, medium- to large-scale experiments involving different gases and various degrees of congestion
- Contains less geometrical detail than CFD models
- A fast tool for evaluating different scenarios during plant design phase

Weaknesses:

- Does not provide the same wealth of information about the flow field as do CFD models
- Contains less geometrical detail than CFD models
- Can deal with single enclosures only

2.2.3. CLICHE

The CLICHE (**C**onfined **LI**nked **CH**amber **E**xplosion) code has been developed by Advantica Technologies Ltd. The status of its present development is unknown. CLICHE was developed to study confined explosions in buildings but its use has been extended to modelling explosions in off- and on-shore plant. The basis of CLICHE is well established in applications to vented vessels explosions, Fairweather and Vasey (1982) and Chippett (1984), however, the CLICHE code represents a generalisation of this concept to a sequence of interlinked explosion chambers. Typically process plant consist of semi-confined areas congested with pipework and process vessels. The expansion induced flow in an explosion will be subject to a large pressure gradient caused by the drag from these obstacles. Regions are represented in the CLICHE code by a series of linked chambers, the pressure gradients are modelled by applying appropriate resistance terms at the inter-chamber vents. The necessary parameters to model the drag and flame / obstacle interaction are determined from a numerical database containing a detailed description of the plant geometry. A combustion sub-model based on the local flow properties is used to determine both laminar and turbulent burning velocities. Any external burning, caused by vented gases, is treated by a separate external combustion model.

The explosion model formulation used in CLICHE was developed by applying the conservation laws to the unburnt and burnt gas volumes in each chamber, assuming that the properties within each chamber are uniform and that any momentum changes occur only at the perimeter of these volumes. This latter assumption does not allow the prediction of the flow distribution within the volume, and hence the flame distortion. Consequently a flame shape is empirically prescribed, based on the geometry and the volume of burnt gas. The equation set describing the series of chambers forms a system of coupled ordinary differential

equations which are solved numerically. Equilibrium properties are assumed for the burnt gas and these properties are calculated during the CLICHE simulation, taking into account the pressure and temperature dependence. CLICHE uses a numerically generated flame area, which enables the model to simulate ignition from any position, with the initial flame assuming a spherical shape. Flame distortion effects are treated by empirical correlations. When the flame interacts with obstacles it develops 'folds' or 'fingers', which grow as the flame passes the obstacles and within which the burning rates are locally higher due to the turbulence generated in the obstacle wakes. CLICHE calculates the rate of growth of flame folds from the mean velocity of unburnt gas past the obstacles.

The burning velocity is assigned the value of the maximum of the laminar and turbulent burning velocities, calculated from the known flame radius, root mean square turbulence velocity and turbulence integral length scale. Ignition in an initially quiescent medium results in laminar flame propagation, until the flame intersects an obstacle at which point the flame downstream of the obstacle becomes turbulent. Turbulence parameters are based upon the mean flow velocities and the characteristics of the wake turbulence shed by the obstacles. The model also allows an initial non-zero turbulence field to be present.

The laminar burning velocity is based upon empirical correlations of the flame speed as a function of flame radius. The turbulent burning velocity is based upon a Kolmogorov, Petrovsky and Piskounov analysis of the combustion model of Bray (1987) which has been calibrated against measurements made by Abdel-Gayed, Bradley and Lawes (1987). The model is based upon the assumption that the turbulent flame is an ensemble of laminar flamelets and takes account of the quenching of the flamelets by the turbulence strain field.

Combustion in the semi-confined region causes unburnt gas ahead of the flame to be expelled through perimeter vents. When the flame propagates through a vent an external explosion is triggered, which as well as providing an external source of pressure generation may increase the pressure inside the semi-confined region by impeding the escape of further gas. The external explosion and the propagation of the pressure wave towards the vent are described by an acoustic model, Strehlow, Luckritz, Adamczyk and Shimpi (1979) and Catlin (1985) for peak over-pressures below 300 mbar. This assumes a spherical flame and an empirically derived peak over-pressure and flame speed.

Strengths:

- Allows ignition location anywhere within a cuboidal volume
- Simple combustion model, based on a mixture of some fundamental physics and empirical correlations
- Flame distortion effects due to vents, etc., are included
- Can handle external explosions
- Can generate its own input parameters from an obstacle database
- Short run times

Weaknesses:

- Simplified representation of the geometry, through a series of inter-linked chambers
- Does not provide the same wealth of information about the flow field as do CFD models

2.3. CFD Models

2.3.1. Introduction

Computational Fluid Dynamics (CFD) models find numerical solutions to the partial differential equations governing the explosion process. Appendix A describes the Navier-Stokes equations, which govern the fluid flow, and the sub-models used to represent the terms which are not modelled exactly. The numerical solutions are generated by discretizing the solution domain (in both space and time). The conservation equations are applied to each of the sub-domains formed by the discretization process, generating a number of coupled algebraic equations that are normally solved by an iterative procedure.

Solutions obtained with CFD codes contain a great wealth of information about the flow field, i.e. velocities, pressure, density, species concentrations, etc. Surface pressure data can be used for structural analysis. CFD is widely applicable and can be used in many different disciplines - from designing aeroplanes, cars or artificial heart valves, to weather forecasting and environmental modelling. CFD simulations can offer insight into the flow behaviour in situations where it is impractical or impossible to carry out experiments. In principle, it is possible to try out many different scenarios, with little extra effort. CFD and experiments should be viewed as complementary means of investigating flow situations. It is vitally important that the sub-models used are properly validated against well-controlled, well-defined and repeatable experiments. If the models have not been validated, confidence in the results obtained from calculations with CFD codes must be low, and the results used with prudence, if at all. The importance of solving the right problem, i.e. using the correct geometry, correct initial and boundary conditions, can not be over emphasised. CFD codes are immensely powerful and useful tools, if applied correctly.

The main drawbacks associated with the use of CFD are caused by the limitations imposed by the available computing hardware, for example it is currently impractical (if not impossible) to simulate exactly a turbulent combusting flow. Hence, sub-models of combustion and turbulent transport have been developed that simplify the calculation process. Small-scale (relative to the explosion domain) objects may cause significant over-pressure generation in a gas explosion, due to the turbulence generated. Explicit representation of small-scale features is demanding in terms of computer memory and computing speed, hence an alternative method of modelling turbulence generation caused by small-scale objects has been developed, the so-called Porosity/Distributed Resistance, or PDR, method. The CFD models presented in this section rely heavily on sub-models for the representation of small-scale objects, coupled with relatively simple numerical schemes for the solution of the governing flow equations.

The rate of progress in model development in the field has been relatively slow. Turbulence remains a highly active topic of research. The mathematical understanding of the subject is improving, but there are still a number of issues which have not been fully resolved, i.e. transition from laminar to turbulent flow. Furthermore, the process of incorporating the new findings into the existing turbulence models has been slow. This is to some extent due to the fact that most of these models are relatively crude approximations of reality and can therefore not easily accommodate the mechanisms involved. The first papers discussing second moment closure modelling appeared in the early 1970's. In principle, second moment closures should be more general that the simpler turbulence models, Models of that

complexity should able to better represent many different types of flows. But thirty years on, Reynolds stress transport models are still not applied routinely. The implementations of Reynolds stress models in the currently available commercial CFD codes lack one of the most important properties to industry, namely robustness.

In fairness, some of the outstanding issues are to do with numerical aspects, i.e. discretisation of the transport equations, etc., rather than to do with the numerical modelling. It seems unlikely that fully simulating a turbulent combusting flow in a real plant - with all its associated time and length scales, and involving a great number of obstacles and other configurational complexities, will be possible for several decades, judging by the current rate of progress. However the rapid development of faster processors with more random access memory, and parallel processing - but which might require rewriting of parts of the CFD codes to take full advantage of massively parallel architecture, may go some way to alleviate matters.

2.3.2. EXSIM

The EXSIM code is under continuing development at the Telemark Technological R&D Centre (Tel-Tek) in Norway and Shell Global Solutions in United Kingdom. The current version of the EXSIM code is version 3.3. EXSIM is a structured Cartesian grid, semi-implicit, finite volume code that relies on the Porosity / Distributed Resistance method for the representation of small-scale objects. The main effect of these obstacles is to obstruct the flow and generate additional turbulence. Using the PDR approach, small scale objects are represented by a volume porosity, an area porosity, and a drag coefficient. The drag generated by the obstacles feeds into the k-ε turbulence model, via a modified generation rate of turbulence term, and subsequently into the Navier-Stokes equations. Sect. C1 of Appendix C describes how the PDR method is implemented in the code and gives details on the implemented combustion model. EXSIM, version 3.3, is using AUTOCAD 14 as pre-processor with an additional LISP program called EXCAD.

The scalar variables are stored at positions within the control volumes, whereas the velocity components and the area porosities are stored at the control volume boundaries. First or second order accurate upwind differencing schemes may be used to generate the numerical approximations to the governing equations. The second order upwind scheme is bounded by the van Leer limiter. Time integration is performed using the implicit Euler scheme, which is first order accurate. The resulting system of non-linear algebraic equations is solved by applying the tri-diagonal matrix algorithm in the three co-ordinate directions. A version of the SIMPLE, (Patankar and Spalding (1972), algorithm, modified for compressible flows, Hjertager (1982), is used to solve the pressure/velocity/density coupling of the momentum equations and the mass balance. The method introduces a pressure correction, which makes the necessary corrections to the velocity components, pressure and density to ensure that mass is conserved at the new time step.

The pre-processor in older versions, pre 3.3, of EXSIM only allowed geometry specification with standard obstacles. A box shaped domain is specified, the subsequent geometry being built up by the addition of variations of eight basic objects. These objects are:

1) Large box, resolved by the grid.

2) Cylinder aligned with one of the co-ordinate directions.

3) Pipe bundle in the form of a box.

4) General porous box.

5) Louvered wall

6) Box beam or box that is not resolved by the grid.

7) Sharp edged beam.

8) Grating.

The pre-processor in version 3.3 of EXSIM makes it possible to convert data from a number of different CAD formats, extracted from CAD databases, to EXSIM format which allows for a quicker setting up of the geometry, Chynoweth (2000).

Version 3.3 of Exsim, Chynoweth and Ungut (2000) has been extensively validated against the experimental data from Phase 2 of the Flast and Fire Engineering for Topside Structures, experiments carried out by DNV, Shell Solvex full and 1/6-th scale tests, tests carried out by CMR on their M24 and M25 modules, further tests carried out by Shell at their Buxton site, etc. The code can also be applied to congested configurations with varying degrees of confinement, including a completely unconfined geometry.

Current developments include implementation of an adaptive mesh algorithm to improve the resolution of areas of interest, i.e. flame fronts, and inclusion of a gas dispersion model so that the shape of a vapour cloud and the gas concentration, i.e. from a pipe rupture, can be estimated.

Strengths:

- Allows the user to specify (arbitrary?) spatial resolution of obstacles
- Has been compared against small-scale, medium-scale and large-scale experiments
- Can be applied to congested but unconfined geometries
- Can be applied to external explosions
- Can read in CAD data

Weaknesses:

- Using standard k-ε model
- Does not have a local grid refinement / de-refinement facility yet

2.3.3. FLACS

The FLACS (**FL**ame **AC**celeration **S**imulator) code has been developed at the Christian Michelsen Research Institute in Norway, now CMR-GEXCON. FLACS is a finite volume code based on a structured Cartesian grid. The Porosity / Distributed Resistance approach is used to model sub-grid scale obstacles. Transport of scalars and momentum through turbulent processes is modelled using the k-ε turbulence model. The discretisation of the governing equations follows a weighted upwind / central differencing scheme, which is first order accurate. However, for the reaction progress variable the second order accurate van Leer scheme is used - van Leer (1974) - to prevent artificial flame thickening, caused by numerical diffusion.

The combustion model originally employed in FLACS was a version of the eddy break-up model. This has recently been replaced by a model, called β flame model, based on correlations of turbulent burning velocities with turbulence parameters - Arntzen (1995,1998). The β flame model assumes that the flame propagates at a constant burning velocity and has a specified constant flame thickness, e.g. three grid cells, Arntzen (1998). Furthermore, the flame model uses correction functions to account for flame thickness, due to numerical diffusion, flame curvature and burning towards walls, Arntzen (1998). The reaction rate and the turbulent viscosity are set in the transport equation for the reaction progress variable so as to ensure that the burning velocity matches that given by a correlation - this is similar to the method employed in COBRA.

An advanced user interface to FLACS has been developed. This consists of Computer Aided Scenario Design (CASD) and Flowvis. CASD is used to generate the scenario definition for FLACS and Flowvis presents the results from the FLACS simulations. The scenario is defined by simplifying the geometry - for example pipes are represented by long cylinders, beams which are not vertical or horizontal are represented by horizontal or vertical beams with a blockage similar to the original beams. In general all objects with a dimension greater than 0.03 m are included, although areas which contain a high density of smaller obstacles will have to be represented as well. Obstacles which are not resolved by this grid are represented as an area blockage and a volume blockage. Walls and decks may be modelled in four different ways: solid unyielding surface, porous surface, blow out / explosion relief panel, or open.

Earlier versions of FLACS - up to 1993, required that the geometry be meshed with a grid of cells of 1 m^3 volume (1 m sides), as the code was calibrated for cells of this size. This is contrary to generally accepted CFD practice, in which it should - at least in principle, be possible to perform a grid dependency study to ensure that the solution does not contain gross numerical errors due to grid coarseness. In FLACS-93 and later versions the grid resolution is based on a certain number of cells across the gas cloud. This means that the cells can be smaller than 1 m cube, see Appendix E. However for a 'typical' offshore module a cell size of 1 m would still be used, with 2 m x 2 m x 2 m cells employed for large offshore modules and onshore plants, see Appendix E.

FLACS does not have adaptive meshing capabilities. However, the user can, a priori, refine the grid in the region where it is deemed to be needed, i.e. the grid cells could be of the order of 2 to 5 cm near a jet leak, Hansen (2001) - Appendix E. FLACS does not have multi-grid

capability per se. However, for blast waves in the far field FLACS has a multi-block concept, allowing turbulence and combustion equations to be solved in the explosion block and the Euler equations in the blocks where the flow is essentially inviscid, Hansen (2001) - Appendix E.

CMR state that FLACS has been validated against a wide range of experiments. Unfortunately many of these results are confidential. However, comparisons of FLACS predictions with measurements were undertaken and published as part of the MERGE, Mercx (1993), EMERGE and BFETS, Selby and Burgan (1998), projects.

CMR state that they are content if the accuracy with which the code predicts explosion over-pressures is of the order of ± 30 %, see Section E3 of Appendix E. They also note that in some cases the discrepancy can be a factor of two. Hansen (2001), in Section E3 of Appendix E, states that, since average over-pressure measurements can vary by a factor of two between tests which are essentially identical, it is difficult to see how accuracies can be substantially improved. The need for accurate measurements and high repeatability has been discussed elsewhere, see Section 3.6, in the present report.

There have apparently been further developments in the FLACS code, van Wingerden (2001), i.e. to the laminar and turbulent combustion modelling, to the modelling of turbulence generation at walls and implementation of a subgrid model describing turbulence length scale as a function of obstacle size. Unfortunately, these developments are not published in the open literature - being kept confidential to clients and sponsors. It is therefore not possible to comment on the impact of these developments.

Strengths:

- Have been compared against a range of small-scale, medium-scale and large-scale experiments
- Uses second order accurate discretisation scheme, a van Leer Upwind scheme, but for the reaction progress variable only
- Can be applied to congested, but unconfined geometries
- Can be applied to external explosions
- Can read in CAD data
- Incorporates a water deluge model

Weaknesses

- Uses k-ε model, but with modifications to deal with near-wall flows, etc.
- Uses a first-order accurate, weighted upwind/central differencing scheme for all variables except for the reaction progress variable

- Versions of the code up to 1993 were calibrated for 1 m cube grid cell size - thus not allowing grid dependency to be examined.

- Recent developments not in the open literature, hence not possible to comment on present theoretical basis.

2.3.4. AutoReaGas

AutoReaGas is the result of a joint venture, between Century Dynamics Ltd. and TNO, that began in 1993. The code integrates features of the REAGAS and BLAST codes developed by TNO and have been incorporated into an interactive environment based on the AUTODYN-3D code developed by Century Dynamics Ltd. REAGAS is a gas explosion simulator whereas BLAST simulates the propagation of blast waves. The REAGAS and BLAST software were implemented in AutoReaGas as the gas explosion solver and blast solver, respectively. AutoReaGas can be used on most computer platforms running under either UNIX, Windows 95 or later versions or Windows NT operating systems.

The gas explosion solver is a three dimensional finite volume CFD code based on a structured, Cartesian grid. Discretization is achieved by use of the first order accurate Power Law scheme, with the SIMPLE algorithm implemented for pressure correction. Turbulent transport is modelled by use of the standard two equation k-ε model. Large objects may be resolved by the grid, but sub-grid scale obstacles are modelled as a source of turbulence and drag (a Porosity / Distributed Resistance approach). The code also allows blow-out panels to be included in a simulation. The combustion model assumes that the combustion reaction takes place as a single step process. Transport equations are solved for the fuel mass fraction and the mixture fraction, which is a conserved quantity (i.e. a quantity that is unaffected by chemical reactions). The addition of the mixture fraction transport equation allows the modelling of explosions in non-uniform gas mixtures. The reaction rate is determined from an empirical correlation for flame speed (Bray (1990) and see also section 2.2.3), where the transition from laminar to turbulent combustion is based upon the local flow conditions.

The blast solver solves the three dimensional Euler equations for blast wave propagation using the Flux Corrected Transport technique. An automatic 'remapping' facility is available to take the output from a gas explosion simulation into a larger domain for a study of the far-field blast effects.

Scenario geometry may be supplied to the code by defining a combination of object primitives, such as boxes, cylinders and planes (cf. EXSIM, section 2.3.2), or alternatively may be imported from a CAD package.

Present development work is concerned with improving important aspects of the solver; in particular a higher order numerical discretization scheme will be implemented in the near future. A new improved combustion model will also be implemented. In addition, a wall friction model will be incorporated for modelling gas explosions in geometries with no sub-grid scale obstacles. In the longer term a number of developments are planned; these include:

- A dynamic structural response capability coupled with the explosion and blast processor

- Gas dispersion modelling

- Multi-block mesh, which allows a more efficient grid structure to be used

The latest release, version 3.0, contain a number of new features: the pre- and post-processing has been improved and a new flow solution and geometry visualizer has been implemented. The objects database uses dynamic memory allocation, e.g. there is no restriction on the number of objects. Furthermore, object modelling has been enhanced, i.e. non-orthogonal objects can now be used. Pressure surfaces (when specifying blow out panels), cold front quenching and a water deluge model have been implemented.

Considerable effort has gone and continues to go into model validation against the medium-scale and large-scale experiments carried out within the MERGE/EMERGE projects and the Joint Industry Project Blast and Fire Engineering for Topside Structures (phases 2 and 3), respectively.

Significantly, a validation manual is supplied with the latest release of AutoReaGas, version 3.0.

Strengths:

- Has been compared against small-scale, medium-scale and large-scale experiments

- Incorporates a water deluge model

- Can read in CAD data

- Can accept a large number of objects through dynamic memory allocation of the objects database

Weaknesses:

- Currently uses a first-order accurate discretization scheme for all variables

- Uses standard k-ε turbulence model

2.4. Advanced CFD Models

2.4.1. Introduction

The CFD models presented in this section attempt a more complete description of the explosion process. The differences between these models and those presented in the previous section mainly lie with the representation of the geometry and the accuracy of the numerical schemes used. The CFD codes presented in this section (with the exception of the COBRA code) allow an exact geometric representation of the explosion scenario, limited by the available computer memory. The memory limitations can limit the applicability of the code to less complex configurations or might force the user to omit objects to stay within the available memory. All of the codes detailed in this section use numerical schemes of increased accuracy, when compared with the CFD codes described in the previous section.

2.4.2. CFX-4

CFX-4 is a general purpose, commercially available CFD code, under development at AEA Technology Engineering Software at Harwell. An explosion module has been developed for this code by the code vendors, funded by the HSE. This module was initially available to the HSE, but has now been released commercially in release 3, December 1999. CFX-4 is a finite-volume, structured grid code. To facilitate the modelling of complex geometries the code allows multi-block, non-orthogonal grids. A variety of equation solvers may be used along with a wide selection of first order and bounded second order accurate differencing schemes. As well as the commonly used k-ε turbulence model, the code also includes a full Reynolds stress turbulence model, which has not been tested for explosion modelling. Further information on the basic code may be obtained from the solver manual. A CFD code using unstructured grids, called CFX-5, is also under development at AEA Technology Engineering Software. However, at present CFX-5 does not contain the physical models necessary to model an explosion.

Before release 3, the standard CFX-4 software included many options for spatial differencing, but only two for temporal differencing. These are the first order accurate implicit Euler and the second order Crank-Nicolson schemes. The Crank-Nicolson scheme is not bounded for positive definite variables and therefore very small time steps must be used when a turbulence model is included (turbulence kinetic energy and its dissipation rate are strictly positive quantities). Therefore, a new higher order backward differencing scheme has been included in release 3, that guarantees positivity. The temporal differencing scheme is also adaptive, failure to meet the convergence criteria at a particular time step results in the time step being reduced for another attempt at convergence. Successful convergence at five successive time steps results in the time step being increased.

Mesh generation for CFX-4 may be accomplished by using either of two codes written for this purpose, CFX-MESHBUILD and CFX-BUILD. To allow further flexibility the CFX-BUILD code allows the user to import geometry files from a wide range of CAD packages.

The code has been used for prediction of explosion over-pressure in a series of small-scale baffled and vented enclosures - Pritchard, Freeman and Guilbert (1996). The agreement reported by Pritchard *et al.* (1996), between the CFD predictions and the experimentally

determined over-pressures for these enclosures, is very good. Pritchard, Lewis, Hedley and Lea (1999) stressed that great care must be taken when applying models to other gases than the one for which the model has been "tuned", or calibrated. Pritchard *et al.* (1999) found that the agreement between calculations and experiments was poor when changing gas from methane, the gas for which the model was calibrated, to propane. A recent paper, Rehm and Jahn (2000), presented good agreement between over-pressures calculated by CFX-4 and measured over-pressures in hydrogen explosion experiments.

Pritchard *et al.* (1999) contains a detailed discussion on the deficiencies with the ignition model and the thin flame model implemented in CFX-4. The ignition model gives physically implausible results. One would expect the gas velocity ahead of the approaching flame to increase with time until the flame reaches the observer. The ignition model implemented in CFX-4 predicts that the gas velocity reaches a peak and then decreases before flame arrival. Moreover the flame is not fully developed by the end of the ignition period. Thus the model does not provide a suitable precursor to the thin flame model. There is also an exponential growth in numerical error in all conservation equations due to the steep gradient in volume expansion at the boundary of the ignition region. The thin flame model will give rise to unwanted oscillations which are caused by the abrupt initiation of reaction in each new cell entering the reaction zone. Furthermore, the steep gradient in volume expansion between neighbouring reacting and non-reacting cells at the cold front is a source of exponential growth in numerical error.

Strengths:

- Offers multi-block capability for greater control over the meshing
- Wide selection of discretization schemes
- A number of turbulence models, including Reynolds stress transport models, are implemented
- Can read in CAD data
- Has an integrated geometry building front-end
- Performs adequately for CH_4 and H_2 deflagrations

Weaknesses:

- Yields poor agreement with experiments for gases other than methane and hydrogen, to which the model appears to have been tuned.
- Uses a thin flame model which is not well suited to explosion modelling
- Uses an ignition model with deficiencies
- The explosion model and ignition model are not thoroughly validated

2.4.3. COBRA

The COBRA CFD code has been developed by Mantis Numerics Ltd. in conjunction with Advantica Technologies Ltd. It appears that there has been no development of the code since 1997, although its Advantica Technologies Ltd application continues.

COBRA uses an explicit or implicit, second order accurate (spatial and temporal), finite-volume integration scheme coupled to an adaptive grid algorithm. The grid is effectively unstructured and may be refined and de-refined automatically locally within the flow, in principle allowing features such as flame fronts and shear layers to be resolved accurately. The grid is updated after each time-marching cycle, ensuring that a fine grid resolution follows moving flow features, Catlin, Fairweather and Ibrahim (1995). Despite this adaptive grid capability COBRA employs the PDR approach for modelling sub-grid scale obstacles - see the discussion of EXSIM (section 2.3.2) for a description of this approach. The PDR approach has its deficiencies, but if there is a need for practical simulations for real complex geometries, then PDR is, in many cases, the only viable approach. The turbulent reaction rate is prescribed using burning velocity correlations.

In addition to the conventional ensemble averaged, density-weighted equations for continuity and momentum, COBRA also solves transport equations for a reaction progress variable and the total mixture energy. Closure of this equation set in the turbulent flow is achieved through use of the k-ε turbulence model, which is modified to include compressibility effects, Jones (1980), or a Reynolds stress transport model.

COBRA is a finite volume code, with the cell average values of the dependent variables stored in the computational cells. To second order, these cell averages correspond to values at the centroids of computational cells. Diffusion and source terms are approximated using central differencing and the convective and pressure fluxes are obtained using a second order accurate variant of Godunov's method - Godunov (1959) - derived from a conventional first order Godunov scheme by introducing gradients within the computational cells. The mesh employed within COBRA is Cartesian, cylindrical polar or curvilinear and may be refined, where necessary, by successively overlaying layers of refined mesh. Each layer is generated from the previous layer by doubling the number of cells in each co-ordinate direction. The mesh can also be de-refined, but only to its original fineness.

Mantis Numerics has supplied a simple visualisation program called MUVI, which is command line driven. It is possible to dump out data from the solution by means of adding a lines of code to a user subroutine.

Results with the COBRA code has been compared to experimental data from Phase II of the BFETS project, Popat et al. (1996), to experiments carried out by Advantica in 1 m long tubes of 1m length, and to experiments carried out by CMR in a 10 m long tube, Catlin, Fairweather and Ibrahim (1995), Fairweather, Ibrahim, Jaggers and Walker (1996), and Fairweather, Hargrave, Ibrahim and Walker (1999). Catlin, Fairweather and Ibrahim (1995) showed good agreement, to within 50 %, between the calculations and the experiments for the over-pressure at two different locations in the explosion tube; however, at two other locations the calculated maximum over-pressure was twice the measured over-pressure. The calculations underpredicted time of arrival of the pressure wave, at the four pressure transducers, by about

20 ms, equivalent to an error of the order of 20 %. Moreover, the pressure decay was much more rapid in the experiments than in the COBRA calculations.

Strengths:

- Second order accurate spatial and temporal discretization
- Cartesian mesh, which makes meshing particularly easy, but can also handle cylindrical polar or arbitrary hexahedral meshes
- Advanced grid refinement/de-refinement facility enabling flame front tracking and shock wave capturing.
- Can read in CAD generated geometries

Weaknesses:

- Uses the standard k-ε model, but offers Wolfshtein's two-layer k-ε turbulence model, which uses an algebraic expression for the energy dissipation rate, ε, in the near-wall region and the standard k-ε model elsewhere
- Setting up complex geometries can be time-consuming and difficult
- Does not have a model for transition from laminar to turbulent flow, which might affect the initial growth of the flame
- Visualisation of flow fields with the MUVI program is slow and laborious, being command line driven, compared to commercially available visualisation tools, i.e. EnSight and Fieldview

The underlying numerical methods available within COBRA have recently been updated to improve computer run times, particularly for complex three-dimensional geometries, by Mantis Numerics Ltd. This new code, called PICA, is currently being developed as an explosion model by Mantis Numerics Ltd. and the University of Leeds independently of Advantica Technologies Ltd.

2.4.4. NEWT

NEWT is an unstructured adaptive mesh, three dimensional, finite volume (tetrahedral volumes), computational fluid dynamics code. The unstructured mesh makes it amenable to the modelling of very complex geometries. NEWT was originally developed for non-combusting, turbomachinery applications but is now being adapted for explosion prediction at the Engineering Department of Cambridge University, the work being part-funded by the Offshore Safety Division of the Health & Safety Executive.

Due to its adaptive grid capabilities, the NEWT code should allow explosion prediction in very congested environments containing, of the order, one hundred obstacles. Current objectives of the work on NEWT are to refine the code and also to use the model to help

refine current PDR methods. The first phase of the OSD, HSE sponsored work has concentrated on implementing into NEWT models developed for the CFX-4 code by AEA Technology Engineering Software, Harwell in collaboration with the Health & Safety Laboratory, Buxton.

A second-order accurate discretisation scheme is used for the convective fluxes. Artificial dissipation - a combination of second-order and fourth-order derivatives - is added to control shock capture and solution decoupling. The fourth-order smoothing takes place throughout the domain, while the second-order smoothing is only used in regions of large pressure gradients. A fourth-stage Runge-Kutta time integration approach is used for the time dependent calculations. Maximum local time steps can be used in order to enhance convergence, when a steady state solution is sought.

The NEWT code uses a modified Lam and Bremhorst variant of the k-ε turbulence model where the near wall damping function is dependent on the turbulence Reynolds number and not the wall normal distance, Watterson, Connell, Savill and Dawes (1998).

The combustion is modelled using the eddy break-up model or a laminar flamelet model, Bray *et al.* (1985). The eddy break-up model can give rise to spurious ignition ahead of the flame. This is countered by suppressing the flame leading edge at each time step, Watterson *et al.* (1998). Ignition of the gas mixture is achieved through a ramping of the reaction progress variable, from zero to unity, in the specified ignition region during the specified ignition period. The laminar flamelet model does not requires fixes, like the leading edge suppression described above, and yields better agreement between the predicted and experimentally observed flame shapes for baffled channel test cases, Birkby, Cant and Savill (1997), while incurring slightly higher computational overheads than the EBU model.

Special treatment was needed for low Mach number flows ($Ma \leqslant 0.3$), due to convergence problems with density based flow solvers. This was a particular problem for the laminar flame propagation phase, Watterson *et al.* (1998).

Also currently in progress at Cambridge University is a research project that will lead to the development of a CAD interface to NEWT. This interface will automatically mesh the CAD generated geometry, allowing the modelling of more complex scenarios. The first implementation of the adaptive grid only allowed a single level of refinement (and de-refinement), whereby one parent cell may split into up to eight child cells. However, to increase the accuracy of the code, and to reduce the memory requirements, a multi-level refinement algorithm has been implemented, Watterson *et al.* (1998).

Watterson *et al.* (1998) presented calculations where they claimed to achieved qualitative agreement in terms of flame brush propagation and flame brush shape with small-scale experiments in the HSE baffled channel, Freeman (1994), and with large-scale experiments in Shell SOLVEX box, Puttock, Cresswell, Marks, Samules and Prothero (1996). However, the calculated maximum over-pressure was overpredicted by between 2 and 15 times. The maximum flames speed was also overpredicted, by about 50 % or more, while time to maximum overpressure in the SOLVEX test case was substantially underpredicted by NEWT. These discrepancies can perhaps be explained by a number of factors: an inaccurate ignition

model, inaccurate modelling of the initial development of the laminar flame and a crude approximation of the transition from laminar to turbulent flow.

Strengths:

- Incorporates an adaptive mesh algorithm
- Uses unstructured meshes which reduces the amount of effort required to generate a mesh, even for complex geometries
- Any 3D tetrahedral mesh generator can be used, provided that the output from the generator is converted to the format expected by NEWT

Weaknesses:

- Uses the standard k-ε model, but with a better near-wall damping
- Uses a crude ignition model
- Uses a crude transition model

2.4.5. REACFLOW

REACFLOW is a CFD code developed over the last nine years at the Joint Research Centre of the European Union in Ispra, Italy. The code is designed to simulate gas flows with chemical reactions. REACFLOW is a finite-volume, unstructured mesh code, which may be used to model two or three dimensional geometries. An advantage of the unstructured mesh approach is that the code is more easily able to handle geometries of arbitrary complexity. The code is still under development. Hence, the following code description contains features that are still in the process of being implemented. The present status of the code is given at the end of this description.

REACFLOW initially divides the flow domain into elements which are triangular in 2-D and tetrahedral in 3-D. The control volumes are defined by the medians of these elements. Within each control volume only the averages of the flow variables are known. These averages may be interpreted as constants or as linearly varying functions through the control volume. The first interpretation results in a discretization method that is first order accurate in space, whereas the second interpretation yields a method that is second order accurate. Given the variation through the control volumes the fluxes across the control volume boundaries are calculated as an approximation to a Riemann problem on each interface. REACFLOW incorporates two methods, Roe's approximate Riemann solver, Roe (1981), and van Leer's flux vector splitting, van Leer (1982). The discretization of the transient term is performed by a simple finite difference formulation, which may be either explicit or implicit.

To be better able to calculate slow-flow phenomena, REACFLOW contains a module for simulating incompressible, variable density flows. The incompressible flow solver takes as its control volumes the basic elements (triangles in 2-D). The fluxes are calculated at the boundaries of each triangular element. The flux calculation is done in a fully upwind manner,

which means that the flux calculation is not necessarily conservative. The incompressible solver exists in versions that are first order accurate in space (variables assumed to be constant within the elements) or second order (variables assumed to vary linearly through each element). Time discretization may be first order (Euler) or second order (Lax-Wendroff correction).

Presently, only two types of source terms are present in REACFLOW. These are body forces due to gravity and chemical reaction source terms. REACFLOW employs two methods for the calculation of the chemical source terms, the first is based on finite rate chemistry and the other is based on the eddy dissipation concept (eddy break-up model). The use of finite rate chemistry is more applicable when the influence of the turbulence on the chemical reactions is negligible, such as in the case of a laminar flame. For flames that are turbulent, a different approach is necessary. The eddy dissipation concept may be used to model this turbulent combustion rate. The eddy dissipation concept, leading to the eddy break-up model of turbulent combustion, is discussed in appendix A3.2. The implementation in REACFLOW is very similar to that in the EXSIM code (section 2.3.2). The disappearance rate of fuel is given by

$$\overline{\omega}_f = -A\,\overline{\rho}\,\frac{\varepsilon}{k}\,\widetilde{Y}_{\min}. \qquad (7)$$

A cut-off criterion based on the Damköhler number is applied to set the reaction rate to zero if the temperature becomes too low (this is the same cut-off criterion as applied in EXSIM).

The effect of the turbulence on the flowfield is modelled using the standard k-ε turbulence model, incorporating a correction for variable density / compressible flows.

In studies of explosions the regions of interest are generally much smaller than the total flow domain. It is therefore advantageous to be able to concentrate the computational effort in these regions. REACFLOW has an adaptive grid capability, which allows regions of the grid to be refined or coarsened locally, depending on the local conditions. For example a steep gradient in the reaction progress variable indicates the reaction zone, and this may be resolved with more cells for greater accuracy. Grid adaptation in REACFLOW is dynamic and fully reversible. However, to avoid excessive refinement a minimum grid size is specified.

The present status of REACFLOW may be summarised as:

2-D Solvers. This module of the code is nearly complete. There are 2-D solvers for compressible and incompressible flows, including convective and diffusive processes, as well as the models for turbulence and chemistry. The compressible solver exists in both explicit and implicit versions. The implementation of adaptive gridding has been completed. Arienti, Huld and Wilkening (1998) describe the grid adaptation methodology implemented in REACFLOW. Arienti et al. (1998) showed comparisons between 2D calculations and experiments for shock tube tests; the advantage of using grid adaptation was highlighted by the better representation of the shock wave.

2-D Axisymmetric solver. An axisymmetric version of the 2-D solver is presently under development.

3-D Solver. The three dimensional solver is presently under development. The geometry has been implemented and an explicit compressible solver is under development. So far this solver includes diffusion and chemistry, but not yet the turbulence model. Grid adaptation is under development. Wilkening and Huld (1999) present results from calculations of large scale Hydrogen explosions. The grid adaptation was used to good effect, keeping the number of elements down and thus minimising the runtime. Wilkening and Huld (1999) found good agreement between the simulations and experiments in terms of generated overpressure, pressure time history and detonation velocity.

Future plans for REACFLOW:

The plans for the near future are to finish the development work outlined above under the heading 3-D Solver. In the longer term there is the possibility that some form of joint Probability Density function (PDF) combustion model will be implemented (see appendix A3.2). This combustion model is highly parallelizable (i.e. the calculation may be split into smaller parts running simultaneously on different processors) and its computationally intensive nature will demand a parallel implementation of the code. A graphical user interface (GUI) will developed to make it easier for the user to define and create a mesh for plant configuration.

Strengths:

- Unstructured mesh capability for easier meshing
- Adaptive meshing for better obstacle representation and flame front resolution
- Accurate solver and second-order, van Leer discretisation scheme has been used

Weaknesses:

- Standard k-ε turbulence model
- Simple combustion models

2.4.6. Imperial College Research Code

Professor Lindstedt, in the Mechanical Engineering Department, has studied premixed flames, including explosions, for a number of years. He and his group have developed a 2D computer code, for research purposes, which incorporates all the latest findings with respect to the combustion model, a sophisticated gradient/flame front tracking refinement and de-refinement mesh algorithm, as well as using an accurate time (implicit Euler) and spatial discretisation (Total Variation Diminishing - TVD) schemes. A parallelized version the code, for greater speed, exists.

The k-ε model is the turbulence model being used in most explosion calculations, though shortcomings of the model are well known. Lindstedt and Váos (1998, 1999) have used second order moment closures to calculate premixed turbulent flames with prescribed PDF to good effect. In the two papers Lindstedt and Váos have improved the modelling of the terms,

focusing on the pressure redistribution/scrambling in the scalar flux equation. Previously the terms in the scalar flux equation have been treated analogously to those of an isothermal constant density flow, but combusting flows, with reacting scalars and large heat release, are of the variable density variety and behaves differently to constant density flows. The Reynolds stress/scalar flux model performs appreciably better than the k-ε model, Lindstedt and Váos (1998, 1999), but more work is still needed on the second order moment closure methods. However, the present closure does provide, arguably for the first time, the ability to model the dynamics of turbulent flames, e.g. burning velocity and flame thickness, with good accuracy.

In non-premixed combustion, quantities like density and species mass fractions, etc., have traditionally been obtained from flamelets and a prescribed probability density function (PDF), often a β−PDF, whose form is dependent on, say, the mixture fraction and the mixture fraction variance. The flamelets are effectively tables of data relating density and species mass fractions to some variable for which a transport equation is solved, i.e. mixture fraction. The data can be obtained from laminar flame calculations with detailed or reduced kinetics or from equilibrium calculations. For premixed combustion the use of laminar flamelets with a prescribed PDF was proposed by Bray and Moss (1981) and has been further extended by, amongst others, Bray *et al.* (1985). The model is often referred to as the Bray-Moss-Libby model. The Bray-Moss-Libby model has not been used extensively, the eddy break-up model being the preferred choice, despite its shortcomings.

A very promising approach is the PDF-transport combustion model, which allows detailed chemical kinetics to be used, Hulek and Lindstedt (1996). Solving a transport equation for the PDF should lead to more accurate combustion predictions. There are experimental uncertainties in the kinetics data, but those are modest in this context and sensitivity studies can reveal whether these uncertainties will greatly affect the predictions. The results of the research will filter into existing combustion models, but it is currently not tractable to use the PDF-transport technique for large industrial problems. The disadvantages with the PDF transport approach is that a large number of "particles" must be used to obtain sensible statistics if using a Monte Carlo approach (commonly used), which leads to long run times, calculations of reaction rates, which feed into the source terms in species transport equations, can be done at run time (leading to long run times) or the data can be tabulated which for detailed kinetics necessitates access to computers with large memory. Development of other ways of obtaining reaction rate data is likely, but probably on a three to five year time scale. However, the advent of faster computers with large memory and running jobs in parallel on multi-processor machines might make it feasible, though unlikely within the next ten years, to use PDF transport models to simulate explosions in large-scale installations on- and off-shore. However, it should be pointed out that the method currently is the only way to account for direct kinetic effects in the context of high Reynolds number flows. The latter are typical of gaseous explosions and finite Damköhler effects have a direct influence on heat release and turbulent burning velocities. The latter property clearly control the severity of gaseous explosions.

Strengths:

- Higher order spatial and temporal discretization techniques are used

- Has adaptive meshing capability
- Use of second-order moment closures, with more accurate modelling of variable ensity flows
- Incorporates detailed chemical kinetics
- Realistic method of obtaining the PDF (through a transport equation)
- Is available in a parallelized form

Weaknesses:

- Long run times with transported PDF method for large-scale problems of interest to industry
- Great requirements for computer memory, if using tabulated rate data
- Not readily available as it is, strictly, a research code

3. DISCUSSION

3.1. Overview of Model Constraints

The empirical model constraints are twofold. Firstly the geometrical representation is quite crude, and secondly, the relative lack of physics incorporated in these models means that they have to be calibrated for every fuel. One of the models, the TNT equivalency model, even assumes that gas explosions behave like TNT explosions, which is not the case. It is necessary to make assumptions about the explosion source strength and degree of confinement, etc., when using some of the models, leading to a range of possible answers, i.e. uncertainties. There are guidelines for how to estimate source strength and confinement, but it is inevitably a much simplified approach. These approaches are open to abuse by inexperienced users or extrapolation beyond bounds of applicability, but many of constraints forced by use of a simple method designed to generate answers with the minimum of effort.

The phenomenological models contains more physics than the empirical models. Moreover, it is still necessary to carry out calibrations for all fuels of interest. The geometry is not represented in as a great detail as in the CFD codes reviewed in the present report, though one of the codes, CLICHE, calculates its input parameters from an obstacle database, which in principle allows a more accurate representation. There is also uncertainty introduced by non-unique obstacle representation - the choice of obstacle representation dependent on the experience of the user.

There are several fundamental constraints imposed on the CFD models discussed in this report.

The first constraint applies to the representation of the modelled geometry. (This is not applicable to the empirical and the phenomenological model type, as these attempt no detailed representation of the actual geometry.) Desktop computers presently have only a limited amount of memory, the maximum capacity being of the order 10^9 bytes. However, the latest desktop PC's, even with more than 1 Gb of random access memory, are becoming very affordable, and offer fast processor speeds, compared to many (more expensive) workstations. It is also possible to reduce the amount of memory required (per processor) by partitioning the mesh into a number of smaller parts, e.g. use a parallelized version of the CFD code. Clusters of PC's, i.e. Beowulf clusters, running the Linux operating system, are now making parallel computing affordable. In light of this, memory constraints might become less of an issue in the next decade.

Experience has shown that each finite volume used by a CFD code requires around 10^3 bytes of computer memory. Hence, the maximum number of finite volumes available to represent a geometry on a poweful desktop PC is around 10^6. In three dimensions this would allow approximately 100 volumes in each co-ordinate direction, equating to equal sized cells of around 0.1 to 1.0 m per side for typical process plant. Many of the objects within a process plant that are important for turbulence production in an explosion will be this size or smaller. Fitting the grid around these objects would clearly require an even larger number of grid cells. This has resulted in the development of various techniques, in particular the Porosity / Distributed Resistance (PDR) approach, to allow some form of geometric representation for

large-scale scenarios, but there are uncertainties in the PDR approach as to how drag induced by the obstacles feeds into the source terms in the turbulence transport equations. However, smaller domains (e.g. flame proof enclosures) can be fully grid-resolved using current computers.

There are also the effects of the grid size on the flow calculation to be considered. Numerical studies have shown that, if the eddy break-up description is used to represent the turbulent reaction rate, then for the flame speed to be grid independent the reaction zone must be resolved by at least four cells, Catlin and Lindstedt (1991). The turbulent reaction zone thickness is around the same size as the turbulence integral length scale, which amongst obstacles may be taken as being equal to a characteristic obstacle dimension. Thus the obstacles would have to be few and large in relation to the overall geometry for the eddy break-up model to be a fundamentally sound practical approach.

The transport equations are discretized using finite differences. An idealised general requirement for the solution to a given problem, generated by a CFD code, is that the solution is grid independent - i.e. that the solution no longer varies as the grid is progressively refined. This may be impractical to demonstrate rigorously. Nevertheless, a grid dependency investigation should ideally form an integral part of CFD studies, certainly at the validation stage. The problem of obtaining a grid independent burning velocity, using the eddy break-up combustion model, is only one of the problems that may occur due to a lack of grid resolution. For example, lack of grid resolution around grid resolved obstacles could smooth the velocity profile in the shear layer caused by these obstacles, reducing the predicted turbulence generation - lowering the predicted flame speed and hence lowering the predicted explosion over-pressure. The simple CFD models do not allow grid independent solutions to be found, as these codes are generally calibrated for a fixed cell size (which is usually very large).

All of the CFD models presented in this report, without exception, model turbulent transport processes by applying the gradient transport assumption and using the two-equation, k-ε turbulence model to generate an effective turbulent viscosity. However, this model was developed over twenty-five years ago and not surprisingly there are several deficiencies associated with this turbulence model. First, it is important to remember that this is only a model of turbulent transport, one that has been validated / calibrated against only a limited number of fundamental flow types - e.g. planar shear layer, axisymmetric jet, etc. The model constants used for prediction of the turbulent mixing in a planar shear layer are actually different to those needed for an axisymmetric jet. Such a model is not expected, therefore, to accurately represent the turbulent processes in an arbitrary three dimensional geometry. Also, this turbulence model was developed for non-reacting, constant density flows. Hence, there is the basic question of whether or not such a model may be applied to a combusting flow without modification. Evidence suggests - Libby and Bray (1980) - that the conventional gradient transport expression (equations A13 and A14, appendix A) may not even correctly predict the sign of the turbulent flux in premixed flames - i.e. that there may be counter-gradient diffusion. Lindstedt *et al.* (1997) have conducted a numerical modelling study of flame propagation in a simple geometry (a long rectangular section tube containing a single flat plate obstacle, aligned perpendicularly to the flow) using the k-ε turbulence model and a form of the eddy break-up combustion model. Lindstedt *et al.* (1997) find that although the large-scale features of the flow are well predicted, such as the over-pressure and mean

flow velocities, the turbulence intensities are not at all well predicted. Such good agreement for the macroscopic parameters may then be merely fortuitous, but further work is needed.

The eddy break-up combustion model, used by some of the 'simple' and 'advanced' CFD codes, requires a high grid resolution to yield a grid independent value of the burning velocity. The model also requires corrections to prevent unphysical behaviour near to surfaces and also at the flame leading edge to prevent numerical detonation. This has led most CFD explosion model developers to use empirical correlations for the flame speed which are grid independent and implicitly include strain rate effects. Implementation of detailed chemical kinetics through the use of a PDF transport equation holds great promise for the future, but due to the heavy demand on computer resources in terms of both processor speed and computer memory, it is unlikely that this approach will be feasible for calculations of real complex geometries for perhaps another ten or more years. Furthermore, there are large uncertainties with regards to rate data for many combustion related reactions; the combustion chemistry is extremely complex and may involve many tens of reactants and intermediate species in over one hundred reactions. It is possible to reduce the detailed kinetics schemes to a smaller number of species (maybe only five or six species), but the resulting set of species conservation equations can become mathematically stiff, with the associated sensitivity to small changes in the dependent variables. Generally, explosion models represent the combustion reactions by a single reaction step involving fuel and oxidant species only. This simplification is necessary due to present constraints in terms of both computer memory and computer speed (cf. appendix A3.2).

The models investigated fall naturally into four basic categories, empirical models, phenomenological models, Computational Fluid Dynamics (CFD) models, and 'advanced' CFD models. The differences between the three groups lie in the simplifications introduced to ease the problem solution. The phenomenological model types compromise geometric accuracy, by approximating a given geometry with an idealised model geometry, but do include reasonably advanced models for the underlying physics. The simple CFD models rely heavily on sub-grid models, such as the Porosity / Distributed Resistance model, to represent objects and, in some cases, the reaction zone. The 'advanced' CFD models allow a more realistic representation of the modelled geometry, through the use of body-fitted or unstructured grids. Grid efficiency for these latter models may be further enhanced by the use of adaptive grids, where a high grid resolution is generated only in those regions that require it. This feature also allows the reaction zone to be fully grid resolved, even for large-scale scenarios.

3.2. Empirical Models - Main Capabilities and Limitations

The main focus will be on the limitations of the empirical models, while the capabilities are described in Sect. 2.1.1 to Sect. 2.1.7. Empirical models are based on correlations of experimental data. The main effort involved in their use is spent deciding on source strengths, degree of confinement, etc. Once the different parameters have been given sensible values, calculations of overpressures, pulse duration and shape are fast. Another advantage is, in some cases, that as long as the representation is good and one is working within the bound of the empiricism, then answers may be adequate. Non-uniqueness in how the parameter values are chosen means that different risk assessors can arrive at very different answers. Also, many empirical models tend to be over conservative.

The models are limited in their applicability and give only a few details of the flow conditions and pressure. The TNT equivalency model does not incorporate the correct physics, since gas explosions behave very differently from TNT detonations.

For all their shortcomings, empirical models have a role to play. The run times are short, of the order of seconds, which means that a number of different scenarios can be quickly tested. Scenarios of particular interest can then be singled out for further analysis with a CFD code or a phenomenological model. The required degree of accuracy and the required level of flow detail may well be such that these simple models will suffice. Extensive calibration against, predominantly, large-scale experiments ensures that the accuracy is, in many situations, acceptable.

3.3. Phenomenological Models - Main Capabilities and Limitations

The main focus will be on the limitations of the phenomenological models, while the capabilities are described in Sect. 2.2.1 to Sect. 2.2.3. The phenomenological models have been extensively calibrated against medium-scale and large-scale experiments . They should be suitable for calculations of geometrical scenarios similar to the ones for which the models have been calibrated. These model may be used in conjunction with both empirical and CFD models

The phenomenological models are subject to a number of uncertainties arising mainly from the simplified geometrical descriptions employed. For example, an accurate representation of plant layouts by a sequence of obstacle grids relies on the judgement of the code operator. This applies to a far lesser extent to the CLICHE code which calculates its input parameters from an obstacle database. The modelling approach taken by these phenomenological models disregards the presence of shock waves. Hence, the pressure distribution within a volume may be incorrectly predicted if shock waves are present.

The over-pressure predicted by the phenomenological codes is generated for the worst case scenario, that of the explosion volume being filled with a uniform gas mixture corresponding to stoichiometric proportions. The more general case, of a non-uniform cloud of fuel and oxidant, may not be modelled. One advantage of CFD codes is that gas explosions in non-uniform clouds can be modelled. In principle, CFD codes are also capable of performing a dispersion calculation prior to ignition.

3.4. Simple CFD Models - Main Capabilities and Limitations

The main focus will be on the limitations of the 'simple' CFD models, while the capabilities are described in Sect. 2.3.1 to Sect. 2.3.4. The 'simple' CFD models have been extensively calibrated against medium-scale and large-scale experiments. They should be suitable for calculations of geometrical scenarios similar to the ones for which the models have been calibrated. These model may be used in conjunction with both 'simple' models and 'advanced' CFD models to yield an insight into the flow. These models benefit from relatively short run times, compared to the 'advanced' CFD models, but which may still be several hours or overnight.

The main limitation of the 'simple' CFD models lies with the simple grids used for discretising the computational domain. All of the 'simple' CFD models presented in this report use Cartesian grids, with sub-grid scale objects represented by the PDR approach. Cartesian meshes are easy to generate and do not incur large computational overheads. However, even objects that are similar in size to the grid cells, or larger, can then only be crudely represented. A sphere, for example, when represented by a Cartesian grid, can be represented only as either an equivalent cube or as a volume / area porosity and resistance. Obviously, neither of these descriptions is an accurate representation of the sphere and the effect of such a simplification on the flowfield and flame development is uncertain.

The other point to consider is the effect of grid resolution on the predicted reaction rate. The FLACS and AutoReaGas codes employ a prescribed burning velocity, obtained from an empirical correlation, whereas the EXSIM code uses the eddy break-up expression to model the turbulent reaction rate. However, it has been shown that a grid independent value of the burning velocity is not obtained for the eddy break-up expression unless the reaction zone is resolved by at least four cells. In practice the developers of the majority of PDR based CFD codes recommend a single cell size. The codes are then compared and developed against experimental data for this size of cell. This effective calibration introduces an element of uncertainty: The codes may work well for scenarios that are similar to the calibration situation but in other instances the performance would be uncertain. Such a strategy does not guarantee grid independence of the final solution and, given the large recommended cell size, grid independence is unlikely. The end result is that these codes may be concealing large numerically generated errors.

The 'simple' CFD codes tend to use first order accurate numerical schemes, see Appendix D for a brief introduction. These schemes cause 'numerical diffusion', which may be greater than the real turbulent diffusion, leading to flame front thickening, increased flame spread and the smoothing of velocity profiles. Numerical diffusion is entirely artificial and may be largely eliminated by the use of numerical schemes of higher order accuracy. The EXSIM code is the only 'simple' CFD code which uses second order accurate schemes for all spatial differencing. The AutoReaGas code is currently first order accurate only, although a version incorporating higher order spatial differencing schemes is under development.

There are other problems associated with this approach. Code validation exercises have tended to concentrate on the measurement of macroscopic explosion properties - i.e. explosion over-pressure and time of flame / over-pressure arrival. The recent Joint Industry Project on Blast and Fire Engineering for Topside Structures Phase II, Selby and Burgan (1998), is an example of this type of exercise. One of the problems with this type of benchmarking is that the code may be forced to give the right result for the wrong reasons. At the microscopic level, the processes of turbulence generation, combustion, flame area enhancement, etc. may not be represented correctly at all. Small scale experiments, concentrating on key areas of the explosion process, coupled with detailed measurements of microscopic properties would provide a more useful tool for code development - cf. Lindstedt and Sakthitharan (1993), as well as another source of data for code evaluation.

3.5. Advanced CFD Models - Main Capabilities and Limitations

The main focus will be on the limitations of the 'simple' CFD models, while the capabilities are described in Sect. 2.4.1 to Sect. 2.4.6. The 'advanced' CFD models use more complicated numerical schemes to improve the representation of the geometry and / or the reaction zone. The COBRA code, for example, uses the PDR approach to represent the explosion geometry, but the code's adaptive grid capability allows the reaction zone to be fully resolved. The NEWT and REACFLOW codes use an adaptive, unstructured mesh, which (in principle at least) allows a full representation of the modelled geometry and of the reaction zone. However, both of these codes are under development and it will be some time, perhaps another ten years, before such a fully resolved approach can take over from the PDR based codes, further developments in both computing power and the codes being required. NEWT was used to calculate two experiments with reasonable success within a factor of 2, after some adjustments for laminar burning, for flame arrival time, flame speed and time to maximum over-pressure, but significantly overpredicted the maximum over-pressure, Watterson *et al.* (1998).

The CFX-4 code uses a structured grid that may be fitted to a given geometry, this allows a much better representation of a given geometry than any of the PDR based codes, but is not as memory efficient as the unstructured, adaptive grid approach. The CFX-4 code also allows regions to be modelled using the PDR approach, although this has not yet been proven in application to an explosion.

3.6. Model Accuracy

Many of the code developers claim extensive model 'validation' for their codes, by making comparison with many experiments. In practice much of what is termed validation is in fact calibration. Most of the models contain a certain degree of empiricism that must be calibrated by making comparisons with experimental measurement. However, there have been some studies to independently determine the accuracy of commonly used explosion models. These studies include the EU co-funded projects MERGE and EMERGE, as well as the more recent Joint Industry Project on Blast and Fire Engineering for Topside Structures Phase 2 (JIP-2). The CFD component of the MERGE project was split into three phases. The first phase was concerned with the evaluation of the various sub-models incorporated into the CFD codes. The second phase involved verification of the CFD explosion models against small and medium scale geometries. For the third phase the code developers submitted 'blind' (i.e. before the experiments were carried out) predictions of the explosion over-pressures in the large scale MERGE geometry. The MERGE geometry consisted of a regular cuboidal pipe array, that was filled with the combustible gas mixture - see Figure 1.

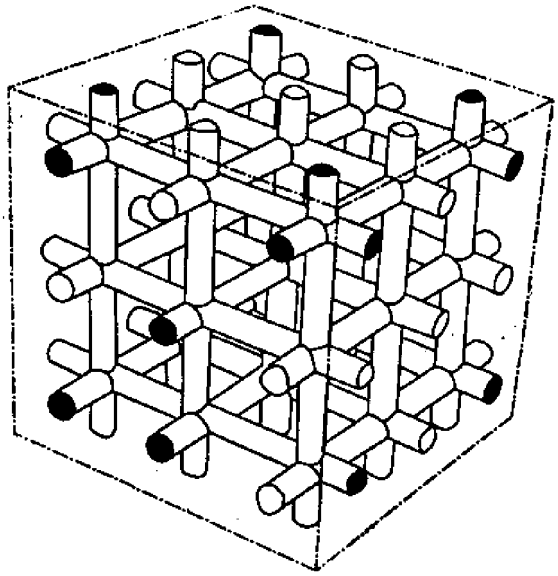

Figure 1 - Example of a congested geometry

The ignition point was at floor level, in the centre of this array, resulting in an expanding hemispherical flame front moving through the obstacles. Predictions generated by four of the codes detailed in this report were submitted for this geometry. Figure 2 shows comparisons between calculated and measured over-pressures for MERGE medium-scale experiments, see also Popat, Catlin, Arntzen, Lindstedt, Hjertager, Solberg, Sæter, van den Berg (1996). Figure 3 shows the calculated and measured maximum over-pressures for MERGE large-scale experiments, see also Popat *et al.* (1996). The results presented in Figures 2 and 3 are representative of the accuracy that may be generally expected from simple CFD explosion models in blind predictions. There is considerable scatter in the results.

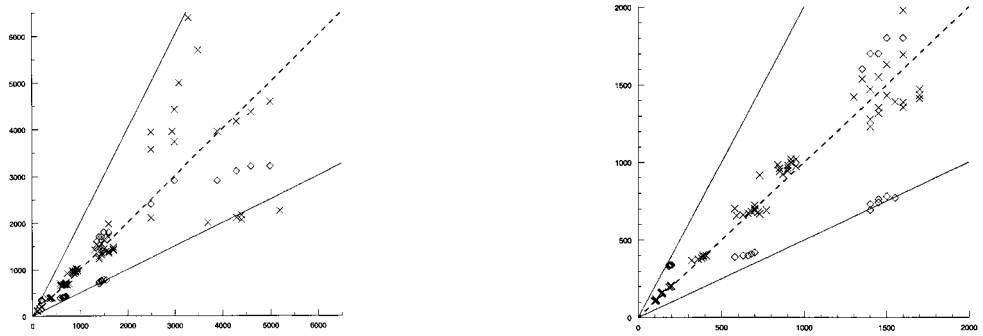

Figure 2 - Comparison of calculated and measured maximum over-pressures for MERGE medium-scale experiments, (×) - COBRA predictions and (◇) - EXSIM predictions; a) all experiments and b) experiments with maximum over-pressures below 1.5 bar, see also Popat *et al.* (1996)

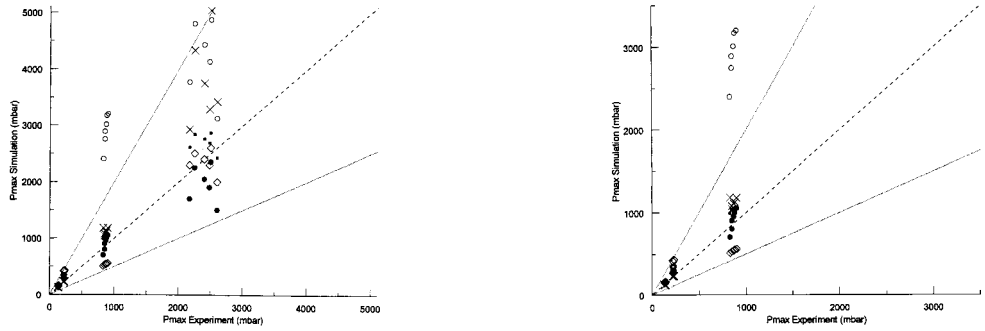

Figure 3 - Comparison of calculated and measured maximum over-pressures for MERGE large-scale experiments, (×) - COBRA predictions, (◇) - EXSIM predictions, (●) - FLACS predictions and (○) AutoReaGas predictions; a) all experiments and b) experiments with maximum over-pressures below 1 bar, see also Popat *et al.* (1996)

The JIP-2 programme was sponsored by 10 offshore operators and the Health & Safety Executive, Selby and Burgan (1998). The programme consisted of an experimental part and a modelling part. The experimental phase consisted of 27 large-scale experiments in an offshore module with varying 'equipment density'. One of the important findings of the experiments was the profound effect water deluge has on the mitigation of explosion overpressures. There is now a database of large-scale experiments against which CFD models can be calibrated. The modelling part consisted of three phases, A) blind predictions on an 8 m wide geometry, which unfortunately did not correspond exactly to the actual experimental geometry, B) predictions of the same geometry as in Phase A but after the tests had been carried out and the models developed / re-tuned and C) blind predictions of a 12 m wide geometry using the correct experimental geometry.

The results of calculations carried out as part of JIP-2, Selby and Burgan (1998), suggest that small changes, or inaccuracies in the representation of the geometry, can lead to over predictions in one case and under predictions (or vice versa) when the geometry changes have been implemented. The findings of the modelling phase were:

- Large scatter in the predictions from the models evaluated in Phase A
- Better agreement between the predictions and the experiments after the models had been re-tuned in Phase B
- Slightly reduced scatter in the predictions from the models, with their re-tuned parameters from Phase B, evaluated in Phase C
- Some models were sensitive to small changes in the geometry
- Some models were very sensitive to small changes in the input conditions
- All models have associated uncertainties, which vary widely between models

JIP-2 did not enhance fundamental understanding of the underlying physics of explosions. Instead of being a true blind predictive test of models, it could perhaps be said that Parts A and B became refocused as a model calibration exercise. In Part A, the maximum over-pressure was, in general, underpredicted and the rise time and duration overpredicted. In Part C as many models underpredicted each parameter as overpredicted. This observation that the models exhibited a completely opposite behaviour for two different geometries, even development and re-tuning in Part B, raises the question whether it would not also have been useful to carry out an experimental investigation into the fundamental physical aspects of explosions as well. My interpretation of the outcome of JIP-2 is that confidence can be attached to the model predictions only if the new geometry strongly resembles one of the two geometries in the database.

It must be emphasised that even with the use of what appears to be in principle a more advanced model, i.e. CFD-based, outside its area of validation/calibration it may in fact give little overall reduction in uncertainties over the use of simpler modelling approaches.

3.7. Recommendations for Future Work

There is a range of modelling approaches available, each with their own strengths and weaknesses. In order to establish confidence in model predictions, it is clear that, for the future, improvements in the physics and the numerics are required, particularly for the CFD-based approaches. However, predictive approaches are needed now. It is thus important that the user be aware of the uncertainties associated with the different models. The following recommendations are essentially those needed to be taken on board by model developers and their funders. They primarily relate to CFD models, which, in principle, should offer the best hope of becoming truly predictive models of gas explosions, with wide applicability.

3.7.1. Grid Improvements

Ideally one would replace the Cartesian grid / PDR based CFD approach by models that are capable of representing a given geometry more accurately. However, the likely time scale for the necessary advances in computing power and code efficiency which will possibly allow geometries to be fully grid resolved is large, possibly of the order of ten years or more. Until this is possible, a hybrid approach could be adopted, whereby body-fitted grids are used to represent the larger objects within the explosion domain, with the PDR approach reserved for the regions that may not be resolved by the grid. It is therefore recommended that methodologies are developed to allow a seamless transition between resolved and PDR-represented solutions as grids are refined. There should be a move away from fixed grid cell size, because such models will require constant re-calibration for new scenarios due to physical and numerical errors associated with the large grid cell size always needing to be compensated. This situation cannot improve until there is a move to a more soundly based methodology.

3.7.2. Combustion Model Improvements

More work is needed to establish the reliability of the combustion models used. Presently, the majority of the explosion models investigated prescribe the reaction rate according to

empirical correlations of the burning velocity. However, it should be recognised that these correlations are subject to a large uncertainty.

The eddy break-up combustion model should ideally not be used if the flame front cannot be properly resolved or, the resulting errors should be recognised and quantified.

Incorporation of detailed or reduced chemical kinetics with a PDF transport approach is appealing, but it is unlikely that this will be feasible for real complex configurations in the foreseeable future - due to the heavy demand placed by this approach on computer resources, in terms of processor time and memory.

3.7.3. Turbulence Model Improvements

The sensitivity of model predictions to the turbulence model used should be investigated. Turbulence modelling has not yet received much attention in the field of explosion modelling. The commonly used two-equation, k-ε model has a number of known failings (i.e. does not predict counter-gradient diffusion), but remains in use due to its economy. Large improvements in over-pressure prediction have been noted by including simple terms into the k-ε model, to account for compressibility effects. However, inclusion of these terms is by no means universal. There is a wide range of advanced k-ε models now available. Ideally Reynolds stress transport modelling should be used but the models require much work to ensure that improvements are not offset by lack of stability.

3.7.4. Experimental Input to Model Development

Model development should now be driven by repeatable, well defined, small-scale, detailed experiments, focusing on key aspects of the physics of explosions. This tends to imply small or medium-scale experiments. Large-scale experiments are suitable for benchmarking, but code calibration on the basis of macroscopic property measurements should be treated with caution, since it is quite possible to obtain approximately correct answers but for the wrong reasons due to gross features swamping finer details. Detailed comparisons of microscopic properties, i.e. initial flame growth, should allow deficiencies in explosion model physics and numerics to be identified, and solutions developed and tested.

3.7.5. Miscellaneous Issues

There are no or few technical barriers to implementation of the above model improvements, beyond a willingness and need to do so.

Perhaps the safest that can be advised at this point is that it would be unwise to rely on the predictions of one model only, i.e. better to use a judicious combination of models of different types, especially if a model is being used outside its range of validation.

4. CONCLUSION

A wide ranging review of numerical models for explosion over-pressure prediction has been conducted and a number of numerical models have been outlined in this report. The models are of varying degrees of complexity, but naturally fall into four distinct groups - i.e. empirical models, phenomenological models, 'simple' CFD models and 'advanced' CFD models.

The limitations associated with the empirical and phenomenological models. i.e. simplified physics and relatively crude representations of the geometry, can only be overcome through additional calibration. This limits the scope for improvements.

The codes comprising the group 'simple' CFD models (EXSIM, FLACS, and AutoReaGas) are in widespread use, as is the phenomenological model SCOPE.

The main limitation of codes in the 'simple' CFD group lies with the crude representation of the explosion geometry. In the long term, ten years hence perhaps, unstructured, adaptive mesh codes may replace the PDR based approaches as the codes and computer hardware develop. In the short term constraints imposed by computing hardware necessitate the use of the PDR approach. However, in the near future the PDR approach could be enhanced by the use of codes employing body-fitted grids, allowing large-scale objects to be fully resolved by the grid, with the PDR description reserved for regions containing very small-scale objects. However, there are uncertainties in how the PDR based approaches feed drag induced by the obstacles into the turbulence transport equations.

It is widely accepted CFD practice that a grid dependency study should ideally be carried out for CFD applications. This is not possible with all 'simple' CFD models as some of these models appear to have been essentially calibrated for a single cell size, with the model developers recommending that this cell size is used throughout. This procedure is likely to lead to large numerically generated errors, which the use of first order accurate numerical schemes is likely to exacerbate. This situation seems, to the author, to lead to the conclusion that 'simple' CFD models will require continual calibration for new scenarios.

The eddy break-up combustion model, used in some 'simple' and 'advanced' CFD codes, has been found to have a number of shortcomings. This combustion model requires a high grid resolution to yield a grid independent value of the burning velocity. The model also requires corrections to prevent unphysical behaviour near to surfaces and also at the flame leading edge to prevent numerical detonation. Most of the explosion model developers have therefore opted to use combustion models based on empirical correlations for the flame speed. Such models have the major advantage that they are grid independent and implicitly include the effects of turbulent strain. However, the experiments upon which the correlations are based show considerable scatter around the correlation function (typically a factor of 2). Hence, even this model should not be thought of as yielding totally reliable values of the reaction rate. A laminar flamelet combustion model has been implemented in the NEWT code. Qualitatively this model shows much better agreement with experiment than the previously used eddy break-up model. Overall, considerable uncertainty still exists in the specification of the reaction rate.

All of the CFD-based explosion models presented use the well known k-ε turbulence model. This model of turbulent transport is known to be deficient even for some aspects of non-combusting flows. In reacting and/or compressible flows, such as those occurring in an explosion, the use of this model is even less well founded. The effects of these model deficiencies, on explosion predictions, are uncertain. Further work is needed to quantify the limitations of this model and to determine whether or not, for example, a full Reynolds stress turbulence model would improve the agreement between CFD model results and experiments. Early indications from the work carried out at Imperial College by Prof. Lindstedt and co-workers suggest that full Reynolds stress/scalar flux transport calculations lead to much better results when applied to deflagrations than the traditional eddy viscosity models. Preliminary results also show that more work is needed, especially for the modelling of the terms in the scalar flux equations for variable density flows, and to improve numerical stability.

Experimental measurements for gas explosions have tended to concentrate on macroscopic properties, such as peak over-pressure. Model development would now be better served by more detailed experimental measurements, such as measurements of turbulence parameters in an explosion and the detailed interaction of a propagating flame front with obstacles. Such measurements would aid the calibration of the PDR approach to explosion modelling as well as providing a sound experimental basis for the development of more advanced physical sub-models. It would be of benefit to both 'simple' and 'advanced' CFD models. This should not in any way be seen as taking a defeatist view, but rather a pragmatic one, as CFD models using the PDR approach are unlikely to be replaced by the next generation of CFD codes, which will be able to resolve all important obstacles, until perhaps the next decade.

In light of the fact that gas explosion predictions are needed now, but that it will probably be ten or more years before the CFD-based models will incorporate fully realistic combustion models, be able to more adequately model turbulence and turbulence-combustion interaction as well as being able to accurately represent all important obstacles in real, complex geometries, one must make the best use of the currently available models. However, it may be unwise to rely on the predictions of one model only, given the uncertainties which remain - especially if the model is used outside its range of validation. One must also be aware of the uncertainties associated with whatever modelling approach is used.

5. REFERENCES

5.1. References Cited in the Report

Abdel-Gayed, R.G., and Bradley, D. (1976)
16th Symposium (International) on Combustion, The Combustion Institute, Pittsburgh, Pennsylvania, U.S.A., pp. 1725-1735

Abdel-Gayed, R. G., and Bradley, D. (1989)
Combustion and Flame **76**:213

Abdel-Gayed, R. G., Al-Khishali, K. J., and Bradley, D. (1984)
Turbulent burning velocity and flame straining in explosions
Proceedings of the Royal Society of London **A391**:393-414

Abdel-Gayed, R. G., Bradley, D., and Lawes, M. (1987)
Turbulent burning velocities: a general correlation in terms of straining rates
Proceedings of the Royal Society of London **A414**:389-413

Abu-Orf, G. M. (1996)
Laminar Flamelet Reaction Rate Modelling for Spark-Ignition Engines
PhD Thesis, University of Manchester Institute of Science and Technology, Manchester, U.K.

Andrews, G. E., Bradley, D., and Lwakabamba, S. B. (1975)
15th Symposium (International) on Combustion, The Combustion Institute, Pittsburgh, Pennsylvania, U.S.A., pp. 655-664

Arienti, M., Huld, T., and Wilkening, H. (1998)
An adaptive 3-D CFD solver for simulating large scale chemical explosions
Proceedings of the 4th ECCOMAS Computational Fluid Dynamics conference, 7-11 September, 1998, Athens, Greece

Arntzen, B. J. (1995)
Combustion Modelling in FLACS 93
HSE Offshore Technology Report, **OTN 95 220**

Arntzen, B. J. (1998)
Modelling of turbulence and combustion for simulation of gas explosions in complex geometries
Dr. Ing. Thesis, Norges Tekniske-Naturvitenskapelige Universitet, Trondheim, Norway

Baker, Q. A., Tang, M. J., Scheier, E. A., and Silva, G. J. (1994)
Vapor Cloud Explosion Analysis
AIChE Loss Prevention Symposium, Atlanta, Georgia, U.S.A.

Baker, Q. A., Doolittle, C. M., Fitzgerald, G. A., and Tang, M. J. (1998)
Recent developments in the Baker-Strehlow VCE Analysis Methodology
Process Safety Progress **17**(4):297-301.

Bakke, J. R. (1986)
Numerical Simulations of Gas Explosions in Two-dimensional Geometries
Christian Michelsen Institute, **CMI 865403-8**.

Berg, A. C. van den (1985)
The Multi-Energy Method - A Framework for Vapour Cloud Explosion Blast Prediction
Journal Hazardous Materials **12**:1-10.

Birkby, P., Cant, R. S., and Savill, A. M. (1997)
Initial HSE Baffled Channel Test Case Results with Refined Combustion and Turbulence Modelling
1st Milestone Report on the HSE Research Contract Research at Cambridge University under Agreement No. **HSE/8685/3278**

Bjerketvedt, D, Bakke, J. R., and Wingerden, K. van (1997)
Gas Explosion Handbook
Journal Hazardous Materials **52**:1-150

Bradley, D., Kwa, L. K., Lau, A. K. C., and Missaghi, M. (1988)
Laminar Flamelet Modelling of Recirculating Premixed Methane and Propane-Air Combustion
Combustion and Flame **71**:109-122.

Bradley, D., Lau, A. K. C., and Lawes, M. (1992)
Flame Stretch Rate as a Determinant of Turbulent Burning Velocity
Philosophical Transactions of the Royal Society of London **A338**:359

Bray, K. N. C. (1987)
9th Australasian Fluid Mechanics Conference, Auckland, New Zealand

Bray, K. N. C., Champion, M., and Libby, P. A. (1989)
The Interaction Between Turbulence and Chemistry in Premixed Turbulent Flames
Turbulent Reactive Flows, Lecture Notes in Engineering No. 40, Springer Verlag, pp. 541-563

Bray, K. N. C. (1990)
Studies of the turbulent burning velocity
Proceedings of the Royal Society of London **A431**:315-325

Bray, K. N. C. and Moss, J. B. (1977)
A Unified Statistical Model of the Turbulent Premixed Flame
Acta Astronautica **4**:291-320

Bray, K. N. C., Libby, P. A., and Moss, J. B. (1985)
Unified Modelling Approach for Premixed Turbulent Combustion - Part 1: General Formulation
Combustion and Flame, **61**:87-102

Brookes, S. J. (1997)
A Review of Gas Explosion Models
HSL Report No. **FS/97/12 - GE/97/05**

Cates, A. T., and Samuels, B. (1991)
A Simple Assessment Methodology for Vented Explosions
Journal of Loss Prevention in the Process Industries **4**:287-296

Catlin, C. A. (1985)
IChemE Symp. Series No. **93**

Catlin, C. A., and Lindstedt, R. P. (1991)
Premixed Turbulent Burning Velocities Derived from Mixing Controlled Reaction Models with Cold Front Quenching
Combustion and Flame **85**:427-439

Catlin, C. A., Fairweather, M., and Ibrahim, S. S. (1995)
Predictions of Turbulent, Premixed Flame Propagation in Explosion Tubes
Combustion and Flame **102**:115-128

Chippett, S. (1984)
Modeling of Vented Deflagrations
Combustion and Flame **55**:127-140

Chynoweth, S. (2000)
Private communication.

Chynoweth, S., and Ungut, A. (2000)
Private communication.

Connell, I. J., Watterson, J. K., Savill, A. M., Dawes, W. N., and Bray, K. N. C. (1996a)
An Unstructured Adaptive Mesh CFD Approach to Predicting Confined Premixed Methane-Air Explosions
Proceedings of the 2nd International Specialists Meeting in Fuel-Air Explosions

Connell, I. J., Watterson, J. K., Savill, A. M., and Dawes, W. N. (1996b)
An Unstructured Adaptive Mesh Navier Stokes Solution Procedure for Predicting Confined Explosions
19th IUTAM Congress of Theoretical and Applied Mechanics, Kyoto, Japan

CPR14E (1979)
Methods for Calculation of the Physical Effects of the Escape of Dangerous Materials
Commission for the Prevention of Disasters, Dutch Ministry of Social Affairs, Directorate-General of Labour, Voorburg, the Netherlands.

Cullen, Hon. Lord (1990)
The Public Inquiry into the Piper Alpha Disaster
The Department of Energy, HMSO, London, UK

Damköhler, G. (1940)
Zeitschrift für Elektrochemie **46**:601-626

Fairweather, M., Hargrave, G. K., Ibrahim, S. S., and Walker, D. G. (1999)
Studies of Premixed Flame Propagation in Explosion Tubes
Combustion and Flame **116**(4):504-518

Fairweather, M., and Vasey, M. W. (1982)
A Mathematical Model for the Prediction of Overpressures Generated in Totally Confined and Vented Explosions
19th Symposium (International) on Combustion, The Combustion Institute, Pittsburgh, Pennsylvania, U.S.A., pp. 645-653

Fairweather, M., Ibrahim, S. S., Jaggers, H. and Walker, D.G. (1996)
Turbulent Premixed Flame Propagation in a Cylindrical Vessel
26th Symposium (International) on Combustion, The Combustion Institute, Pittsburgh, Pennsylvania, U.S.A., pp. 365-371

Freeman, D. J. (1994)
Visualisation of explosions in a baffled plate, vented enclosure
HSL Report **IR/L/GE/94/08**

Godunov, S. K. (1959)
A Finite Difference Method for the Computation of Discontinuous Solutions of the Equations of Fluid Dynamics
Mat. Sb. **47**:271-290

Gouldin, F. C. (1987)
An Application of Fractals to Modelling Premixed Turbulent Flames
Combustion and Flame **68**:249-266

Guilbert, P. W., and Jones, I. P. (1996)
Modelling of Explosions and Deflagrations
HSE Contract Research Report No. **93/1996**

Gülder, O. L. (1990a)
23rd Symposium (International) on Combustion, The Combustion Institute, Pittsburgh, Pennsylvania, U.S.A., pp. 743-750

Gülder, O. L. (1990b)
Turbulent Premixed Combustion Modelling Using Fractal Geometry
23rd Symposium (International) on Combustion, The Combustion Institute, Pittsburgh, Pennsylvania, U.S.A., pp. 835-842

Hansen, O. R. (2001)
Private communication

Hjertager, B. H. (1982)
Numerical Simulation of Flame and Pressure Development in Gas Explosions
SM study no. 16, University of Waterloo Press, Ontario, Canada, pp. 407-426

Hjertager, B. H. (1982)
Simulation of Transient Compressible Turbulent Reactive Flows
Combustion Science and Technology **41**:159-170

Hulek, T., and Lindstedt, R. P. (1996)
Computations of Steady-State and Transient Premixed Turbulent Flames Using pdf Methods
Combustion and Flame **104**:481-506

Jones, W. P. (1980)
Models for turbulent flows with variable density and combustion
in *Prediction Methods for Turbulent Flows* (Ed.: Kollmann W.), Hemisphere, Washington D.C., U.S.A., pp. 423-458

Leer, B. van (1974)
Towards the Ultimate Conservative Difference Scheme. II. Monotonicity and Conservation Combined in a Second-Order Scheme
Journal of Computational Physics **14**:361-370

Leer, B. van (1982)
Flux Vector Splitting for the Euler Equations
Lecture Notes in Physics, Springer-Verlag, **170**:507-512

Leuckel, W., Nastoll, W., and Zarzalis, N. (1990)
Experimental Investigation of the Influence of Turbulence on the Transient Premixed Flame Propagation Inside Closed Vessels
23rd Symposium (International) on Combustion, The Combustion Institute, Pittsburgh, Pennsylvania, U.S.A., pp. 729-734

Libby, P. A., and Bray, K. N. C. (1980)
Counter-Gradient Diffusion in Premixed Turbulent Flames
AIAA 18th Aerospace Sciences Meeting, Pasadena, California

Lindstedt, R. P., and Sakthitharan, V. (1993)
Transient Flame Growth in a Developing Shear Layer
9th Symposium on Turbulent Shear Flows, Kyoto, Japan

Lindstedt, R. P., Hulek, T., and Váos, E. M. (1997)
Further Development of Numerical Sub-models and Theoretical Support
EMERGE Project Report, Task 10

Lindstedt, R. P., and Váos, E. M. (1998)
Second Moment Modeling of Premixed Turbulent Flames Stabilized in Impinging Jet Geometries

27th Symposium (International) on Combustion, The Combustion Institute, Pittsburgh, Pennsylvania, U.S.A., pp. 957-962.

Lindstedt, R. P., and Váos, E. M. (1999)
Modeling of Premixed Turbulent Flames with Second Moment Methods
Combustion and Flame **116**:461-485

Magnussen, B. F., and Hjertager, B. H. (1976)
On Mathematical Modelling of Turbulent Combustion with Special Emphasis on Soot Formation and Combustion
16th Symposium (International) on Combustion, The Combustion Institute, Pittsburgh, Pennsylvania, U.S.A., pp. 719-729

Mandelbrot, B. B. (1975)
On the Geometry of Homogeneous Turbulence, with Stress on the Fractal Dimension of the Iso-surfaces of Scalars
Journal of Fluid Mechanics **72**:401-416

Mercx, W. P. M. (1993)
Modelling and experimental research into gas explosions: overall final report on the MERGE project
Commission of the European Communities Report, Contract **STEP-CT-011** (SSMA)

Mercx, W. P. M., and Berg, A. C. van den (1997)
The Explosion Blast Prediction Model in the Revised CPR 14E (Yellow Book)
Process Safety Progress **16**(3):152-159

Patankar, S. V., and Spalding, D. B. (1972)
A Calculation Procedure for Heat, Mass and Momentum Transfer in Three-dimensional Parabolic Flows
International Journal of Heat and Mass Transfer **15**:1787-1806

Popat, N. R., Catlin, C. A., Arntzen, B. J., Lindstedt, R. P., Hjertager, B. H., Solberg, T., Sæter, O., and Berg, A. C. van den (1996)
Investigations to Improve and Assess the Accuracy of Computational Fluid Dynamic Based Explosion Models
Journal of Hazardous Materials **45**:1-25

Prandtl, L. (1925)
Bericht über Untersuchungen zur ausgebildete Turbulenz
Zeitschrift für Angewandte Mathematik und Mechanik **3**:136-139

Pritchard, D. K., Freeman, D. J., and Guilbert, P. W. (1996)
Prediction of Explosion Pressures in Confined Spaces
Journal of Loss Prevention in the Process Industries **9**:205-215

Pritchard, D. K., Lewis, M. J., Hedley, D., and Lea, C. J. (1999)
Predicting the effect of obstacles on explosion development
HSL Report No. **EC/99/41 - CM/99/11**

Puttock, J. S. (1995)
Fuel Gas Explosion Guidelines - the Congestion Assessment Method
2nd European Conference on Major Hazards On- and Off-shore, Manchester, UK, 24-26 September 1995.

Puttock, J. S. (1999)
Improvements in Guidelines for Prediction of Vapour-cloud Explosions
International Conference and Workshop on Modeling the Consequences of Accidental Releases of Hazardous Materials, San Francisco, Sept-Oct, 1999

Puttock, J. S. (2000a)
Private communication

Puttock, J. S. (2000b)
Private communication

Puttock, J. S., Cresswell, T. M., Marks, P. R., Samuels, B., and Prothero, A. (1996)
Explosion Assessment in Confined Vented Geometries. SOLVEX Large-Scale Explosion Tests and SCOPE Model Development
HSE Offshore Technology Report, **OTO 96 004**

Puttock, J. S., Yardley, M. R., and Cresswell, T. M. (2000)
Prediction of Vapour Cloud Explosions Using the SCOPE Model
Journal of Loss Prevention in the Process Industries **13**:419-430

Rehm, W., and Jahn, W. (2000)
CFX German User Conference

Roe, P. L. (1981)
Approximate Riemann Solvers, Parameter Vectors, and Difference Schemes
Journal of Computational Physics **43**:357-372

Sæter, O. (1994)
Implementation of New Laminar Model in EXSIM
Shell UK and EMERGE Progress Report, Tel-Tek

Selby, C. A., and Burgan, B. A. (1998)
Blast and Fire Engineering for Topside Structures - Phase 2 (Final Summary Report)
SCI Publication No. **253**, The Steel Construction Institute, Ascot, U.K.

Smith, K. O., and Gouldin, F. C. (1978)
Experimental Investigation of Flow Turbulence Effects on Premixed Methane-Air Flames in Turbulent Combustion
Progress in Astronautics and Aeronautics, Vol. 58, ed. by Kennedy L. A.

Spalding, D. B. (1971)
Concentration Fluctuations in a Round Turbulent Free Jet
Chemical Engineering Science **26**:95-107

Strehlow, R. A., Luckritz, R. T., Adamczyk, A. A., and Shimpi, S. A. (1979)
The Blast Wave Generated by Spherical Flames
Combustion and Flame **35**:297-310

Thyer, A. M. (1997)
Updates to VCE Modelling for Flammable Riskat: Part 1
HSL Report No. **RAS/97/04 - FS/97/01**

Watterson, J. K., Savill, A. M, Dawes, W. N., and Bray, K. N. C. (1996)
Predicting Confined Explosions with an Unstructured Adaptive Mesh Code
Joint Meeting of the Portuguese, British and Spanish Sections of the Combustion Institute

Watterson, J. K., Connell, I. J., Savill A. M., and Dawes, W. N. (1998)
A Solution-Adaptive Mesh Procedure for Predicting confined Explosions
International Journal for Numerical Methods in Fluids **26**:235-247

Wiekema, B. J. (1980)
Vapour Cloud Explosion Model
Journal of Hazardous Materials **3**:221-232

Wilkening, H., and Huld, T. (1999)
An adaptive 3-D CFD solver for explosion modelling on large scales
17th International Colloquium on the Dynamics of Explosions and Reactive Systems,
25-30 July, 1999, Heidelberg, Germany

Wingerden, K. van (2001)
Developments in Gas Explosion Safety in the 1990's in Norway
FABIG Newsletter, Article R397, Issue no. **28** (April 2001), pp. 17-20

5.2. References Used but not Cited

Bray, K. N. C. (1980)
Turbulent Flows with Premixed Reactants
in *Turbulent Reacting Flows*, Topics in Applied Physics, Vol. **44**, Springer-Verlag

British Gas Plc (1989)
Review of the Applicability of Predictive Methods to Gas Explosions in Offshore Modules
Department of Energy Offshore Technology Report **OTH 89 312**

Gardner, D. J. and Hulme, G. (1994)
A Survey of Current Predictive Methods for Explosion Hazard Assessments in the UK Offshore Industry
HSE Offshore Technology Report **OTH 94 449**

APPENDIX A - THEORETICAL DESCRIPTION OF GAS EXPLOSIONS

A1. Conservation Equations

The basic equations describing the instantaneous state of a reacting flow are, for mass continuity

$$\frac{\partial \rho}{\partial t} + \nabla \bullet (\rho \boldsymbol{u}) = 0, \tag{A1}$$

for momentum conservation

$$\rho \frac{\partial \boldsymbol{u}}{\partial t} + \rho \boldsymbol{u} \bullet \nabla \boldsymbol{u} = \rho \boldsymbol{g} - \nabla P + \nabla \bullet \boldsymbol{\tau}, \tag{A2}$$

for species conservation

$$\rho \frac{\partial Y_n}{\partial t} + \rho \boldsymbol{u} \bullet \nabla Y_n + \nabla \bullet (\rho Y_n \boldsymbol{U}_n) = \omega_n, \tag{A3}$$

and for energy conservation

$$\rho \frac{\partial h}{\partial t} + \rho \boldsymbol{u} \bullet \nabla h = \frac{\partial P}{\partial t} + \boldsymbol{u} \bullet \nabla P - \nabla \bullet \boldsymbol{q} + \Phi + \dot{Q} + \rho \Sigma_{n=1}^{N} Y_n \boldsymbol{f}_n \bullet \boldsymbol{U}_n, \tag{A4}$$

where $\boldsymbol{\tau}$ is the deviatoric stress tensor, $\boldsymbol{q}$ is the heat flux vector, Φ is the dissipation of energy by viscous stresses, $\dot{Q}$ is the external heat input, $\boldsymbol{f}_n$ is the body force vector, and $\boldsymbol{U}_n$ is the diffusion velocity of species n relative to the mean mixture velocity. The enthalpy (h) is defined by

$$h = \Sigma_{n=1}^{N} h_n, \text{ where } h_n = \Delta h_{f,n}^{\circ} + \int_{T^{\circ}}^{T} C_{P,n} dT', \tag{A5}$$

$\Delta h_{f,n}^{\circ}$ is the heat of formation of species n at the reference temperature T° and $C_{P,n}$ is the specific heat capacity of species n. The heat flux vector is obtained from the summation of three components, conduction, diffusion, and the Dufour effect - a heat flux that arises from a concentration gradient. The Dufour effect is generally negligible. Hence, the heat flux vector is given by

$$\boldsymbol{q} = -\lambda \nabla T + \rho \Sigma_{n=1}^{N} h_n Y_n \boldsymbol{U}_n \tag{A6}$$

For closure of this system of equations relationships are needed for the equation of state for the gas and the rates of production of the chemical species. The equation of state for the gas is most easily approximated by the perfect gas law

$$\rho = \frac{MP}{RT}, \tag{A7}$$

where M is the molecular weight of the gas, P is the pressure and R is the universal gas constant. The production rate of each species may be approximated using the Arrhenius expression.

The complexity of this system of equations renders their solution intractable for all but the very simplest of situations. The chemical reaction time scales are generally smaller than the turbulence time scales, which in turn are smaller than the time scales characterising the mean flow. Explosions are transient phenomena, but to resolve the time scales of all the processes occurring within the explosion is beyond the capabilities of present computers and will remain so for the foreseeable future. Hence, the equations are averaged over a time period that is short in comparison with the macroscopic features of the explosion, but is long compared to the time scales of the chemical and turbulent processes. This averaging process results in additional correlations that need to be modelled. Also, closure of the mean chemical source terms presents a problem because of the non-linear dependence of these terms on temperature and species concentrations. The number of correlations introduced by the averaging process may be reduced by employing Favre (density weighted) averaging. The Favre mean of a variable is defined by $\tilde{x} = \overline{\rho x} / \overline{\rho}$. By replacing the instantaneous variables with their Favre mean plus a fluctuating component - i.e. $x = \tilde{x} + x''$ - and averaging over a suitable time period the conservation equations may be recast in the following form, for continuity and momentum conservation

$$\frac{\partial \overline{\rho}}{\partial t} + \nabla \bullet (\overline{\rho}\tilde{\boldsymbol{u}}) = 0 \qquad \text{(A8)}$$

$$\overline{\rho}\frac{\partial \tilde{\boldsymbol{u}}}{\partial t} + \overline{\rho}\tilde{\boldsymbol{u}} \bullet \nabla\tilde{\boldsymbol{u}} + \nabla \bullet \overline{\rho \boldsymbol{u}'' \otimes \boldsymbol{u}''} = \overline{\rho}\boldsymbol{g} - \nabla\overline{P} + \nabla \bullet \overline{\boldsymbol{\tau}}. \qquad \text{(A9)}$$

The third term on the left hand side represents the Reynolds stresses, these are additional stress terms that arise due to the turbulent transport of momentum. The last term on the right hand side, the molecular stress term, is generally small in comparison to the Reynolds stress term and may generally be neglected. Approaches for dealing with the Reynolds stress term are discussed in the next section.

For species and energy conservation the equations become

$$\overline{\rho}\frac{\partial \tilde{Y}_n}{\partial t} + \overline{\rho}\tilde{\boldsymbol{u}} \bullet \nabla\tilde{Y}_n + \nabla \bullet \overline{\rho \boldsymbol{u}'' Y_n''} = \bar{\omega}_n - \nabla \bullet (\overline{\rho}\tilde{Y}_n \boldsymbol{U}_n) \qquad \text{(A10)}$$

$$\overline{\rho}\frac{\partial \tilde{h}}{\partial t} + \overline{\rho}\tilde{\boldsymbol{u}} \bullet \nabla\tilde{h} + \nabla \bullet \overline{\rho \boldsymbol{u}'' h''} = \frac{\partial \overline{P}}{\partial t} + \tilde{\boldsymbol{u}} \bullet \nabla\overline{P} + \overline{\boldsymbol{u}'' \bullet \nabla P} - \nabla \bullet \overline{\boldsymbol{q}} + \overline{\Phi} + \overline{\dot{Q}} + \overline{\rho}\,\Sigma_{n=1}^{N}\, \tilde{Y}_n \boldsymbol{f}_n \bullet \boldsymbol{U}_n. \qquad \text{(A11)}$$

The third terms on the left hand side of these equations are the turbulent scalar fluxes of species and energy respectively. These terms arise from the transport of species and energy by turbulent motions in fluid. These terms will be discussed further in the next section.

It should be noted that all of the conservation equations have a similar form, i.e.

$$\overline{\rho}\frac{\partial \tilde{\phi}}{\partial t} + \overline{\rho}\tilde{\boldsymbol{u}} \bullet \nabla\tilde{\phi} + \nabla \bullet \overline{\rho \boldsymbol{u}'' \phi''} = \bar{S}_\phi + \bar{M}_\phi, \qquad \text{(A12)}$$

where ϕ represents the general variable, $\bar{S}_\phi$ the mean production rate of ϕ, and $\bar{M}_\phi$ is a term representing all the processes that occur at the molecular level. In a turbulent flow the molecular transport processes are usually negligible and the transport of momentum, species, and energy through turbulent action is dominant. The next section discusses the modelling of

turbulent transport processes and introduces the important models used for capturing turbulent transport.

A2. Turbulence Modelling

The Reynolds stresses and the turbulent scalar fluxes that appear in the averaged form of the transport equations for momentum, species, and energy require modelling for closure of this equation set. One of the simplest closure's models turbulent transport by making an analogy with molecular motion. Molecular momentum or scalar transport takes place by the random motion of molecules, turbulent transport may therefore be thought of as transport occurring through the random motion of macroscopic turbulent eddies - Prandtl (1925). Hence, the turbulent transport of a fluid property may be related to the gradient of its mean. The Reynolds stresses are given by

$$\overline{\rho u_i'' u_j''} = \tfrac{2}{3}\delta_{ij}(\bar{\rho}k + \mu_T \nabla \bullet \tilde{\boldsymbol{u}}) - \mu_T\left(\frac{\partial \tilde{u}_i}{\partial x_j} + \frac{\partial \tilde{u}_j}{\partial x_i}\right), \tag{A13}$$

where δ_{ij} is the Kronecker delta function ($\delta_{ij} = 1$ if $i = j$, $\delta_{ij} = 0$ if $i \neq j$) and k is the turbulence kinetic energy given by $k = \tfrac{1}{2}\overline{\rho \boldsymbol{u}'' \bullet \boldsymbol{u}''}/\bar{\rho}$. The turbulent scalar fluxes are given by

$$\overline{\rho u_j'' \phi''} = -\frac{\mu_T}{\sigma_\phi}\frac{\partial \tilde{\phi}}{\partial x_j}. \tag{A14}$$

The first constant introduced in these equations (μ_T) is the effective (or eddy) viscosity. The second constant (σ_ϕ) is the Prandtl / Schmidt number for the variable ϕ. The Prandtl number is defined as

$$\mathrm{Pr} = \frac{\mu}{\rho a}, \tag{A15}$$

where a is the thermal diffusivity. The Prandtl number is the ratio of momentum diffusion to energy diffusion. The Schmidt number is defined similarly

$$\mathrm{Sc} = \frac{\mu}{\rho D_\phi}, \tag{A16}$$

where D_ϕ is the diffusivity of species ϕ in the gas mixture. The Schmidt number is the ratio of momentum diffusion to mass diffusion.

From dimensional analysis the eddy viscosity is shown to be proportional to the product of a characteristic turbulence velocity and a turbulence length scale. Hence, the eddy viscosity may be given by

$$\mu_T = C_\mu \bar{\rho}\frac{k^2}{\varepsilon}, \tag{A17}$$

where ε is the dissipation rate of turbulence kinetic energy and C_μ is a model constant. The turbulence kinetic energy and its dissipation rate may be obtained from their respective balance equations. The transport equation for the turbulence kinetic energy is

$$\bar{\rho}\frac{\partial k}{\partial t} + \bar{\rho}\tilde{\boldsymbol{u}} \bullet \nabla k = -\overline{\rho \boldsymbol{u}'' \otimes \boldsymbol{u}''} : \nabla \tilde{\boldsymbol{u}} + \nabla \bullet (\frac{\mu_T}{\sigma_k}\nabla k) + \nabla \bullet \overline{\boldsymbol{u}'' \bullet \boldsymbol{\tau}} - \overline{\boldsymbol{u}'' \bullet \nabla \bullet \boldsymbol{\tau}^T} - \overline{\boldsymbol{u}'' \bullet \nabla P}, \tag{A18}$$

where the meanings of the terms on the right hand side are: i) production of turbulence kinetic energy due to the work done against the Reynolds stresses (which are generally modelled using the gradient transport assumption given above), ii) turbulent diffusion of turbulence kinetic energy (modelled by the eddy viscosity assumption), iii) molecular diffusion which is generally negligible, iv) removal of turbulence kinetic energy due to viscous effects, this term must be modelled and is often represented as $\overline{\boldsymbol{u}'' \bullet \nabla \bullet \boldsymbol{\tau}^T} = \bar{\rho}\varepsilon$, v) the pressure velocity correlation term, this represents a second source of turbulence kinetic energy. The velocity fluctuation-pressure gradient correlation term is generally ignored in most applications of the k-ε turbulence model. The equation for the dissipation rate of the turbulence kinetic energy may be modelled as

$$\bar{\rho}\frac{\partial \varepsilon}{\partial t} + \bar{\rho}\tilde{\boldsymbol{u}}\nabla \bullet \varepsilon = -C_{\varepsilon_1}\overline{\rho \boldsymbol{u}'' \otimes \boldsymbol{u}''} : \nabla \tilde{\boldsymbol{u}}\frac{\varepsilon}{k} - \bar{\rho}\, C_{\varepsilon_2}\frac{\varepsilon^2}{k} + \nabla \bullet (\frac{\mu_T}{\sigma_\varepsilon}\nabla \varepsilon), \qquad \text{(A19)}$$

where gradient diffusion has been assumed for the turbulent transport of the dissipation rate and C_{ε_1} and C_{ε_2} are model constants. The model constants for this turbulence model are normally given as $C_\mu = 0.09$, $C_{\varepsilon_1} = 1.44$, and $C_{\varepsilon_2} = 1.92$. In addition the turbulent Prandtl / Schmidt numbers for k and ε are normally given as 1.0 and 1.3 respectively.

Two-equations models of turbulence, such as the k-ε model outlined above, are commonly used due to their simplicity. However, eddy viscosity models have some serious deficiencies, partly in consequence of equations A13 and A14 not being strictly valid. In a three-dimensional flow the Reynolds stress and the strain rate are usually not related in a simple manner. This means that the eddy viscosity may no longer be a scalar but will in fact become a tensor. Models that account for the anisotropy are new and have not yet been applied to explosion modelling, so will not be further discussed here.

A more complicated, but potentially more accurate, approach is to model the transport of the Reynolds stresses and the turbulent scalar fluxes. These transport equations contain further triple correlations, which need to be modelled. In three dimensions an additional seven transport equations are required to model the Reynolds stresses, with another three additional equations for each scalar - there is one turbulent scalar flux in each co-ordinate direction. Reynolds stress modelling is being used in the field of combustion modelling, but has yet to make an impact on the more specialised application of explosion modelling.

A3. Reaction Rate Modelling

CFD models of explosions do not track the flame front directly. Instead the position of the flame front is inferred from a characteristic value for a certain scalar variable - e.g.. the reaction progress variable. The effect of the passage of a flame front through the gaseous medium is conveyed through the reaction rate source terms appearing in the equations for the species mass fractions and energy. Although the flame is not tracked directly, some CFD models (for example COBRA) infer the reaction rate from a locally fitted flame speed that is obtained from an empirical correlation. Hence, this section will begin by discussing ways of determining the turbulent flame speed.

A3.1. Turbulent Flame Speed

This sub-section will begin by explaining the relationship between the flame speed and the burning velocity. The burning velocity is defined as the mass consumption of unburnt gas divided by its density per unit area of flame. The flame speed is the speed of the flame relative to a stationary observer. Consider a planar combustion wave propagating through a premixed fuel / air mixture - fig. A1.

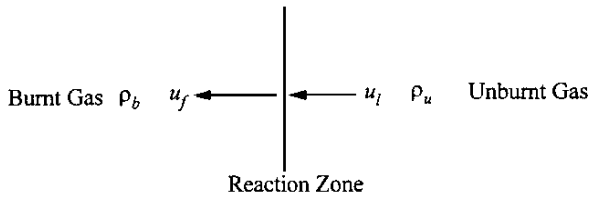

Figure A1 - Schematic description of the flame reaction zone

The mass consumption of reactant mixture must equal the mass production of product mixture. Hence, the speed of the flame is given by

$$u_f = \frac{\rho_u}{\rho_b} u_l, \qquad \text{(A20)}$$

where u_f is the flame speed, u_l is the burning velocity, and ρ_u and ρ_b are the densities of the unburnt and burnt gas mixtures respectively. The flame speed includes the expansion generated flow due to the decrease in density of the product gas mixture. Note that the burning velocity in this case is actually the laminar burning velocity, because an undisturbed combustion wave is considered. In a laminar gas mixture the flame speeds generated are fairly low. A burning velocity of 0.5 m s^{-1} is typical for a hydrocarbon fuel, with a density ratio of around 8. This yields a flame speed of approximately 4 m s^{-1}. Large scale experiments to measure flame speed have been conducted in initially quiescent media. The maximum flame speeds obtained in these experiments were between 7 and 15 m s^{-1} for various hydrocarbon / air mixtures. The increase over the expected value of around 4 m s^{-1} is caused by the formation of a 'cellular' flame surface. Flame front instabilities, of hydrodynamic or diffusional-thermal origin, cause the flame front to wrinkle with a characteristic cellular appearance. This wrinkling increases the surface area of the flame and hence the effective flame speed. The flame speed caused by this self-turbulization mechanism does not in itself generate a significant over-pressure. However, the enhanced expansion flow could potentially increase the turbulence level more in the unburnt gas, if obstacles were present.

An alternative approach to obtaining the turbulent burning velocity has been adopted by Gouldin (1987). The turbulent burning velocity is defined as the mean mass flux of unburnt

gas moving in to the flame divided by the unburnt gas density per unit area of flame. The flame area considered is a mean, smoothed flame area. However, at a small scale the flame front will be highly contorted. At low to moderate turbulence levels the reaction is known to occur in thin flame sheets ('flamelets') which are rough with multiple scales of wrinkling. Moreover, at a small scale the flame will be propagating at the laminar burning velocity, relative to the unburnt gas, in a direction normal to this flamelet surface (ignoring the effects of strain). Hence, the increase in burning velocity may be considered in terms of a flame area enhancement due to the turbulence. From continuity

$$\frac{u_T}{u_l} = \frac{A_l}{A_T} \,, \tag{A21}$$

where A_l is the 'exact' flame area and A_T is the flame area used to define u_T. Gouldin considers the flamelet surface to be a fractal surface - i.e. a surface that displays multiple scales of wrinkling. Consider a volume of dimension L^3 filled uniformly (in a statistical sense) with a wrinkled surface and with the scales of wrinkling being self-similar - Mandelbrot (1975), then if the volume is split into cubes with a length per side of ε, on average the number of cells touched by the surface is proportional to $(L/\varepsilon)^D$. If the surface is smooth the fractal dimension (D) will approach 2 (if it is rough then D will approach 3 and the surface will appear to fill the volume L^3). It follows that the surface area in L^3 as measured with a scale ε^2 is given by

$$A \sim \varepsilon^{2-D} L^D \,. \tag{A22}$$

Mandelbrot (1975) suggests two possible values for D, 8/3 for Gauss-Kolmogorov turbulence or 5/2 for Gauss-Bergers turbulence. More recent results, for the fractal dimension of an iso-surface in a turbulent shear flow, have suggested that the value should lie between 2.35 and 2.6. Eqn. A22 implies that if $D > 2$ then the flame surface area approaches infinity as ε approaches zero. In practice there is a lower limit for ε below which the flame surface area ceases to increase. Such a lower limit would be the Kolmogorov turbulence length scale. Similarly there is an upper limit for ε beyond which eqn. A22 will no longer describe the variation of the flame surface area with ε. This upper limit for ε is taken as the turbulence integral length scale, which may be thought of as the maximum scale of the surface wrinkling. Associating these two limiting values of the surface area with A_l and A_T above, then from eqn.s A21 and A22

$$\frac{u_T}{u_l} = \frac{A_l}{A_T} = \left(\frac{l}{\eta}\right)^{D-2} , \tag{A23}$$

where l is the integral length scale and η is the Kolmogorov length scale. The length scale ratio is given by $l/\eta = A_t^{1/4} R_l^{3/4}$ where A_t is a constant of order unity and $R_l = u' l/\nu$. Gouldin (1987) modifies this basic expression to account for the effects of flame propagation on the flamelet surface and also the effect of the strain on the laminar burning velocity.

A3.2. Turbulent Reaction Rate

The mean reaction rate for species n ($\bar{\omega}_n$) appears in the equation describing the transport of the species mass fraction (eqn. A10) and is a function of the gas mixture composition and its temperature (and pressure, as this will have an effect on the concentrations of the reacting

species). In general, the highly non-linear dependence of the reaction rate on these variables precludes the use of mean properties in generating the mean reaction rate, i.e.

$$\bar{\omega}_n \neq \omega_n(\overline{Y_n}, \overline{T}, \overline{P}), \tag{A24}$$

with the main non-linearity arising from the dependence of the reaction rate on temperature. The exact mean reaction rate may be written as a multiple integral of the instantaneous reaction rate weighted by the joint probability density function (PDF) describing the thermochemical state of the mixture

$$\overline{\omega} = \int_T \int_{Y_1} \ldots \int_{Y_N} \omega_n(Y_1, \ldots, Y_N, T)\, P(Y_1, \ldots, Y_N, T)\, dY_1 \ldots\, dY_N\, dT, \tag{A25}$$

where the effect of pressure has been neglected and $P(Y_1, .., Y_N, T)$ is the joint PDF of composition and temperature. Derivation of joint PDFs is possible, but has so far been limited to small scalar spaces and steady state calculations due to the very high computational overhead. Hence, approximations for the mean reaction rate are required.

Consider the simple reaction scheme

$$F + sO \rightarrow (1 + s)\, P, \tag{A26}$$

where s is the stoichiometric mass requirement of oxidant required to oxidise 1 kg of fuel. Magnussen and Hjertager (1976) propose a model for this reaction rate, based on the Spalding (1971) eddy break up model. Under the assumption of fast chemistry, it is assumed that the reaction rate will be determined by the mixing of the fuel and oxidant eddies at the molecular level. This small scale mixing is described by the dissipation rate of the eddies. The mean disappearance rate of the fuel is given by

$$\bar{\omega}_F = -A \tfrac{\varepsilon}{k} \bar{\rho}\, \tilde{Y}_{\min}, \text{ where } \tilde{Y}_{\min} = \min\left(\tilde{Y}_F,\ B \tfrac{\tilde{Y}_P}{1+s}\right), \tag{A27}$$

where A and B are constants. The function min indicates that the smallest of the terms within the brackets is to be used to determine the reaction rate. The presence of the product mass fraction within the brackets ensures that the flame propagation is determined by the turbulent diffusion of the product species into the reactants. This form of the reaction rate is widely used (in a modified form) in codes such as EXSIM and CFX-4.

The preceding sub-section introduced the laminar burning velocity, which is defined as the mass consumption of unburnt gas divided by its density per unit area of flame. It was also shown that the turbulent burning velocity may be determined from the laminar flame burning velocity if the instantaneous surface area of the flame is known. A knowledge of the flame surface area per unit volume may also be used to define a reaction rate, which is the product of the laminar burning velocity, the flame surface area, and the unburnt gas density

$$\bar{\omega}_F = -\rho_u\, Y_{F,u}\, u_l\, f \Sigma, \tag{A28}$$

where Σ is the mean flame surface area per unit volume, ρ_u is the density of the unburnt gas, $Y_{F,u}$ is the fuel mass fraction in the unburnt gas, and f is a correction factor for the effects of

strain on the laminar burning velocity. A transport equation may be derived for the flame surface area, which may be modelled and solved. However, the modelling process introduces uncertainties and an increase in computational effort. A simpler method is to obtain the flame surface area algebraically. An expression for Σ may be obtained by treating the passage of flame surfaces past a point in space as a stochastic process analogous to a random telegraph signal - Bray *et al.* (1989)

$$\Sigma = \frac{g\bar{c}(1-\bar{c})}{|\bar{\sigma}_y|\hat{L}_y}, \tag{A29}$$

where g and $\bar{\sigma}_y$ are model constants (assuming the values of 1.5 and 0.5 respectively), $\hat{L}_y$ is the integral length scale of the telegraph signal process, and the reaction progress variable c may be defined as

$$c = \frac{Y_{F,u}-Y_F}{Y_{F,u}-Y_{F,b}}, \tag{A30}$$

where $Y_{F,b}$ is the fuel mass fraction in the fully combusted mixture. One of the more recent codes, NEWT, uses this combustion model.

A4. Numerical Modelling

A brief description of the numerical methods applicable to CFD codes will be given in this section. The equations describing the explosion process have been given in the preceding sections. An analytical solution of this system of equations is not possible and one must resort to numerical methods. To obtain a numerical solution a discretization method is used. The solution domain (in both space and time) is discretized and the final solution yields values of the dependent variables at these discrete points. Three discretization approaches are commonly used in CFD. The first, the finite difference method, covers the solution domain by a grid. At each grid point the differential equations describing the explosion flow are represented by replacing the partial derivatives with values derived using the discrete grid point values. This results in one algebraic equation per variable for each grid node. The disadvantage of the finite difference method is that conservation is not automatically enforced. The most widely used approach is the finite volume method, which uses an integral form of the conservation equations. The spatial solution domain is divided into a number of control volumes to which the conservation equations are applied. At the centroid of each control volume is a computational node at which the variable values are calculated / stored. Variable values at the control volume faces are obtained by interpolation between neighbouring control volume centroid values. Advantages of the finite volume method include the ability to model complex geometries and conservation of the flow variables. Finally, the finite element method is similar to the finite volume method in that the spatial domain is split into a set of discrete volumes (finite elements). A simple piece-wise function, valid on each of the elements, is used to describe the local variations of the flow variables.

The discrete positions at which the variables are to be calculated are defined by a grid, which is a discrete representation of the flow geometry. Different types of grid may be used and these are described below. The first type of grid is the structured grid, which consists of families of grid lines with the property that grid lines belonging to the same family do not cross each other and only cross each member of the other families once. A simple example of

a Cartesian structured grid (in two dimensions) would be a series of lines crossing each other at right angles, forming a pattern of squares. It is not generally a requirement, however, that the grid lines are regularly spaced. Non-orthogonal (or body-fitted) grids do not have their grid lines crossing at right angles and are capable of modelling more complex geometries. An example of a non-orthogonal structured grid is shown in fig. A2.

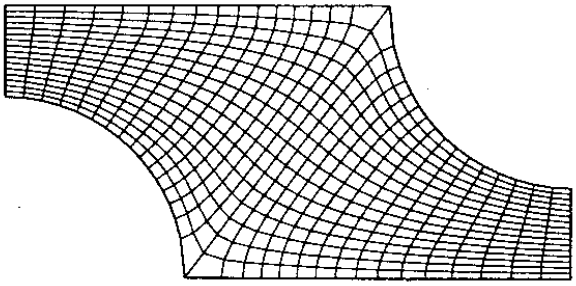

Figure A2 - A non-orthogonal structured grid

An increase in functionality is obtained by the use of multi-block structured grids. The flow geometry is split into a number of large scale regions, each of which is gridded with a structured mesh - which may or may not match the meshes on the other blocks at the block interfaces. This method is more adaptable than the previous single block method and may be used to model more complex geometries or to provide local grid refinement in regions where it is necessary to resolve the flow more accurately. Fig. A3 shows an example of a matched interface, multi-block, non-orthogonal structured grid.

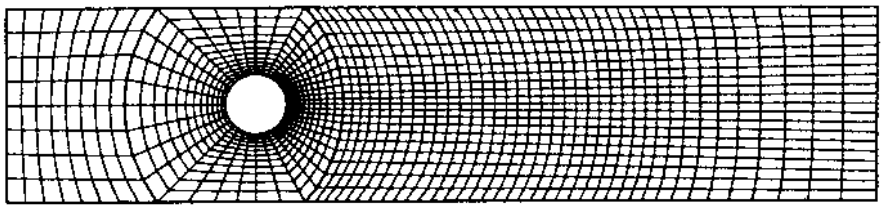

Figure A3 - A multi-block, non-orthogonal structured grid

For very complex geometries an unstructured mesh provides the best representation and works best with the finite volume or finite element approach. The control volumes may assume any shape and there is no limit to the number of neighbouring control volumes. However, a disadvantage of the unstructured grid approach is that the solution is slower than for a structured grid. An example of an hybrid grid with combination of a prismatic part in the boundary layer and an unstructured part is shown in fig. A4.

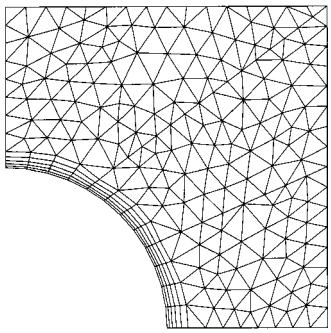

Figure A4 - An unstructured grid with prismatic grid in the boundary layer

The memory efficiency of any gridding technique may be further enhanced by use of adaptive gridding, whereby the grid is initially coarse, but during the calculation locally refines in order to resolve flow features. One advantage of adaptive gridding is that the optimum grid resolution need not be known a priori. Also, the local grid refinement increases memory efficiency, as the grid only refines where necessary. Codes that implement adaptive gridding generally also allow the grid to be de-refined, when there is no longer a need for a high grid resolution. During transient calculations this allows features to be tracked by the grid - e.g.. the flame front may be resolved by a fine mesh in an explosion calculation, whilst maintaining a relatively coarse mesh elsewhere in the solution domain.

Despite the increase in grid efficiency at representing arbitrary flow domains offered by each of these successive gridding techniques, it is not yet possible to represent the most complex geometries. The limit to the geometric complexity that may be modelled is imposed by computer memory and speed. A very high performance PC or workstation might be able to contain a model of one million cells, with the time taken for a solution of around a week. A three-dimensional grid containing one million nodes would only allow, for example, one hundred nodes in each co-ordinate direction. For a typical offshore module or chemical plant this would allow evenly spaced cells of 0.1 to 1.0 m side length. This is clearly too coarse to accurately represent all of the features present. Hence, sub-grid models have been introduced to model the effects of objects that are smaller than the grid spacing. Several of the codes presented in this report (EXSIM, FLACS, etc.) include the Porosity / Distributed Resistance (PDR) formulation of the governing equations. Sub-grid scale obstacles are represented by a volume fraction, an area fraction, and a drag coefficient. These obstacles offer an increased resistance to flow, a decreased flow area, and an increased production rate of turbulence, the effects of which need to be modelled. This modelling introduces additional uncertainty.

The most commonly used method of discretisation used by the explosion codes is the finite volume method. This uses an integral form of the conservation equation as its starting point. Eqn. A12 may be recast in the following form

$$\int_V \frac{\partial}{\partial t}\left(\bar{\rho}\tilde{\phi}\right) dV + \int_S \bar{\rho}\tilde{\phi}\tilde{\mathbf{u}} \bullet \mathbf{n}\, dS - \int_S \frac{\mu_T}{\sigma_\phi}\nabla\tilde{\phi} \bullet \mathbf{n}\, dS = \int_V \bar{S}_\phi\, dV, \qquad \text{(A31)}$$

where the molecular terms have been neglected, gradient transport has been assumed for the turbulent scalar fluxes, and **n** is the unit normal vector at the control volume surface. An approximated form of this integral equation is applied to each of the control volumes yielding a system of simultaneous equations, the solution of which describes the flow. Methods are therefore needed to numerically approximate the surface and volume integrals appearing in eqn. A31. The simplest method of approximating a volume integral is to replace the integral with the product of the cell centre value of the integrand and the cell volume - i.e.

$$\int_V \bar{S}_\phi \, dV \approx \bar{S}_{\phi,Centre} V. \tag{A32}$$

This method is second order accurate - i.e. the error is proportional to the square of the cell size. To evaluate the surface integrals the value of the integrand is required at each position on the surface. The simplest approximation (and one that is also second order accurate) is to replace the integral by the sum over all faces of the products of the integrand values at the cell face centres and the cell face areas - i.e.

$$\int_S \bar{\rho}\tilde{\phi}\tilde{\boldsymbol{u}} \bullet \boldsymbol{n} \, dS \approx \Sigma_i \left(\bar{\rho}\tilde{\phi}\tilde{\boldsymbol{u}} \bullet \boldsymbol{n}\right)_{i,Centre} S_i. \tag{A33}$$

However, the integrand values are not known at the cell faces, but are stored only at the cell centres. Values at the cell faces must be obtained by interpolation. It will be assumed that the velocity field and the fluid properties are known at all positions, the value of ϕ at the cell face centres must be found by interpolation. Consider fig. A5, which shows a one dimensional sequence of cells.

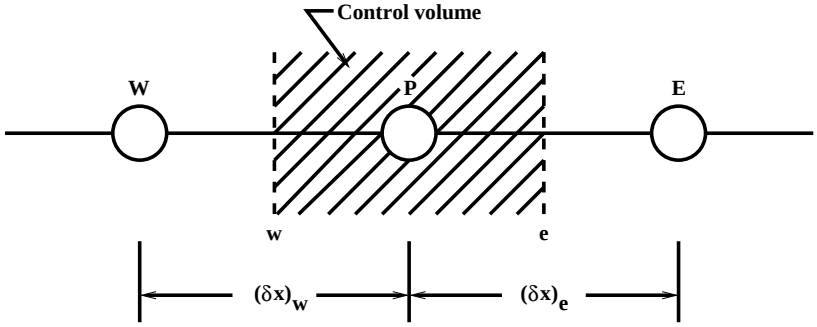

Figure A5 - Control volume in one dimension

The value of ϕ at face 'e' may be found most simply by linearly interpolating between the values at 'P' and 'E':

$$\phi_e \approx \alpha \, \phi_E + (1 - \alpha) \, \phi_P, \text{ where } \alpha = \frac{x_e - x_P}{x_E - x_P}, \tag{A34}$$

and the gradient of ϕ at face 'e' is simply given by

$$\left(\frac{d\phi}{dx}\right)_e \approx \frac{\phi_E - \phi_P}{x_E - x_P}. \tag{A35}$$

However, this method is unstable for the convective terms at high Reynolds numbers and is therefore not suitable for explosion flows. A simple scheme that is stable is the first-order

upwind differencing scheme. The value of ϕ at 'e' is taken as the value at the upstream node from 'e' - i.e.

$$\phi_e = \phi_P \text{ if } (\tilde{\boldsymbol{u}} \bullet \boldsymbol{n})_e > 0 \text{ and } \phi_e = \phi_E \text{ if } (\tilde{\boldsymbol{u}} \bullet \boldsymbol{n})_e < 0. \quad \text{(A36)}$$

However, this method is only first order accurate (the error is proportional to size of the control volume) and may also lead to numerical (false) diffusion. This is a particular problem for multi-dimensional flows, when the direction of flow is oblique to the grid. Numerical diffusion is then produced in directions both normal and aligned with the direction of the flow. Higher order schemes do exist, and are used by the more advanced CFD codes. These schemes use an increased number of nodal points to interpolate the cell-face values using curves. An example of such a higher order scheme is the QUICK scheme, which uses two upstream nodes and one downstream node to fit a local parabola. This scheme is third order accurate but if used with the simple approximation for the surface integral shown above is second order accurate overall.

The discretization process yields a set of algebraic equations that are generally non-linear and hence must be solved by an iterative technique. This technique involves guessing the solution, linearizing the equations about that solution, then improving the solution. The steps of linearization and solution improvement are repeated until the solution reaches (within a certain bound) a steady result - at which point the solution is said to be converged. Transient calculations, such as explosions, march through time in a sequence of time-steps. A converged solution must be obtained at each time-step. Convergence is not trivial, especially for the high speed flows typical of explosions. The choice of time step can be crucial in determining whether or not a converged solution is possible. Hence, adaptive time-stepping may be implemented to aid stability.

APPENDIX B - COMBUSTION MODEL IN SCOPE CODE

The following description of the models used in the SCOPE 2 code is summarised from Puttock *et al.* (1996). The explosion geometry is approximated by a box of length L and cross-sectional area A. At one end of the box is the main vent of area A_v and along the length of the box there is provision to incorporate side vents of total area A_s.

Ignition occurs at the centre of the face opposite the explosion vent, which corresponds to the worst possible case. The flame is assumed to be hemispherical until it reaches the walls of the box, at which point it ceases to increase in size and propagates along the box with a roughly hemispherical shape. The flame position, measured from the ignition point to the flame leading edge, is denoted by the variable X. In order to correctly predict the relationship between pressure generation and vent flow, the code records the evolution of two variables with time; representing the amounts of burnt and unburnt gas inside the box. From the point that the flame reaches the walls, these equations are

$$\frac{dM_u}{dt} = -s A u_T \rho_u - C_D u_v A_v \rho_u \qquad \text{(B1)}$$

and

$$\frac{dB}{dt} = P^{1/\gamma} s A u_T E, \qquad \text{(B2)}$$

where M_u is the mass of unburnt gas inside the box, the flame area is sA, C_D is the vent discharge coefficient, u_v is the velocity of the unburnt gas through the vent, P is the pressure inside the box, and E is the expansion ratio.

The quantity B is given by

$$B = P^{1/\gamma} V_b, \qquad \text{(B3)}$$

where V_b is the volume of burnt gas inside the box. The pressure and flame position is determined by the quantity of burnt and unburnt gas in the box.

The turbulent burning velocity (u_T) is obtained semi-empirically, allowing the model to be adjusted after comparison with experimental data. The basic form follows from Gülder (1990b)

$$\frac{u_T}{u_l} = 1 + \alpha \left(\frac{u'}{u_l}\right)^{1/2} \mathrm{Re}_l^{1/4}, \qquad \text{(B4)}$$

where α is a constant. The laminar burning velocity (u_l) is corrected for the effects of strain using the following expression, cf. Gouldin (1987),

$$\frac{u_l}{u_{l,0}} = 1 - \beta \, \mathrm{Ka}, \qquad \text{(B5)}$$

where $u_{l,0}$ is the unstrained laminar burning velocity, β is a constant which should be proportional to the Markstein number for the gas, and Ka is the Karlowitz stretch factor, which Bradley *et al.* (1984) define as

$$\mathrm{Ka} = 0.157 \left(\frac{u_l}{u_{l,0}}\right)^2 \mathrm{Re}_l^{1/2}, \qquad \text{(B6)}$$

The Markstein number is a physicochemical parameter that expresses the response of a flame to stretching - Bradley *et al.* (1992). The model constants (α and β) are obtained by fitting the model to experimental data provided by Gouldin (1987), Abdel-Gayed *et al.* (1984), and Leuckel *et al.* (1990).

The turbulence in the unburnt gas after each grid is calculated as the sum of the incident turbulence and the flow velocity ahead of the flame as the flame reaches the grid - i.e..

$$u'_{new} = (u'^2 + 0.01\, C_g\, u_u^2)^{1/2}, \qquad \text{(B7)}$$

where u_u is the velocity of the unburnt gas ahead of the flame. C_g is the drag coefficient, which is a function of the obstacle shape and blockage ratio.

APPENDIX C - COMBUSTION MODELS IN CFD CODES

C1. EXSIM

The PDR formulation of the transport equation for the general variable is

$$\frac{\partial}{\partial t}\left(\beta_v \bar{\rho}\tilde{\phi}\right) + \nabla \bullet \left(\boldsymbol{\beta}\bar{\rho}\tilde{u}\tilde{\phi}\right) - \nabla \bullet \left(\boldsymbol{\beta}\frac{\mu_T}{\sigma_\phi}\nabla\tilde{\phi}\right) = \bar{S}_\phi + \bar{R}_\phi, \qquad \text{(C1)}$$

where β_v is the volume porosity, $\boldsymbol{\beta}$ is the area blockage ratio vector, $\bar{S}_\phi$ is the non-obstructed component of the mean source, and $\bar{R}_\phi$ is the additional component of the source term caused by the obstructions. Gradient transport has been assumed for the turbulent diffusion. The effective viscosity (μ_T) is obtained using the two equation k-ε model, which has been modified to include the additional turbulence generation from the sub-grid scale objects. The production rate of turbulent kinetic energy is modelled as

$$\bar{S}_k = -\beta_v \rho \overline{\boldsymbol{u}'' \otimes \boldsymbol{u}''} : \nabla\tilde{\boldsymbol{u}} \text{ and } \bar{R}_k = C_s \mu_T |\tilde{\boldsymbol{u}}|^2 A_w^2 + \Sigma_n \boldsymbol{C}_T \bar{\boldsymbol{R}}_{\boldsymbol{u}} \bullet \tilde{\boldsymbol{u}}, \qquad \text{(C2)}$$

where C_s is a constant, A_w is the wetted area of the obstacles per unit volume, and $\boldsymbol{C}_T$ is a constant vector that gives the fraction of the pressure drop, in each co-ordinate direction, that contributes to the generation of turbulence kinetic energy. $\bar{R}_u$ is the drag force vector, and is given by

$$\bar{R}_{u,i} = -C_D \tfrac{1}{2} \bar{\rho} |\tilde{u}_i| \tilde{u}_i, \qquad \text{(C3)}$$

where C_D is the drag coefficient. In regions containing sub-grid scale obstacles the turbulence kinetic energy dissipation rate is not obtained from its transport equation, but is calculated from the following expression

$$\varepsilon = C_\mu^{3/4} \frac{k^{3/2}}{l}, \qquad \text{(C4)}$$

where $l = C_l D_{Ob}$, C_l is a constant and D_{Ob} is a typical obstacle dimension.

The turbulent combustion rate is modelled using the modified eddy break-up combustion model of Magnussen and Hjertager (1976). This is further modified by the inclusion of an ignition / extinction criterion - Hjertager (1982). The turbulent fuel consumption rate is given by

$$\bar{\omega}_f = 0, \text{ when } \frac{\tau_{ch}}{\tau_e} > D_{ie}, \qquad \text{(C5)}$$

or

$$\bar{\omega}_f = -\beta_v E_T A \frac{\varepsilon}{k} \rho Y_{min}, \text{ when } \frac{\tau_{ch}}{\tau_e} \le D_{ie}, \qquad \text{(C6)}$$

where A is a constant (A=20) and E_T is a combustion enhancement factor. The ignition / extinction criterion is based on the turbulent Damköhler number, which is the ratio of the chemical timescale (τ_{ch}) to the turbulent eddy mixing time scale (τ_e). These time scales are defined as

$$\tau_{ch} = A_{ch} \exp\{E_A/RT\} (\bar{\rho}\tilde{Y}_f)^a (\bar{\rho}\tilde{Y}_o)^b \quad \text{(C7)}$$

and

$$\tau_e = \frac{k}{\varepsilon}. \quad \text{(C8)}$$

The critical Damköhler number (D_{ie}) is taken to be 1000. If the turbulence Reynolds number is less than a critical value, the combustion rate is calculated from a quasi-laminar expression

$$\omega_f = -\beta_v E_L A_{lam} \frac{u_l}{\delta_l} \bar{\rho} Y_{\min}, \quad \text{(C9)}$$

where E_L is a flame area enhancement factor related to the instability induced wrinkling of the laminar flame, which varies linearly from 1 at a flame radius of 0 m to 2.5 at a flame radius greater than or equal to 0.5 m. A_{lam} is a constant, and δ_l is the laminar flame thickness.

C2. FLACS

The transport equation for the fuel may be written

$$\bar{\rho}\frac{D\tilde{Y}_F}{Dt} = \nabla \bullet (\bar{\rho} D \nabla \tilde{Y}_F) - Y_{F,0}\,\bar{\omega} \quad \text{(C10)}$$

The diffusion coefficient (D) is modelled as, Arntzen (1995),

$$D = 0.7\, S\, \Delta \quad \text{(C11)}$$

and the reaction rate ($\overline{\omega}$) as

$$\bar{\omega} = 3.5 \frac{S}{\Delta} \min\{c, 9 - 9c\}, \quad \text{(C12)}$$

where S is the burning velocity and Δ is the grid spacing. It is noted that eqn. C12 appears to be deficient by a factor of ρ. The turbulent burning velocity is obtained from one of the two following correlations, Bray (1990) and Abdel-Gayed and Bradley (1989),

$$u_{T_1} = 15\, u_l^{0.784}\, u'^{0.412}\, l^{0.196} \quad \text{(C13)}$$

and

$$u_{T_2} = u_l + 8\, u_l^{0.284}\, u'^{0.912}\, l^{0.196}, \quad \text{(C14)}$$

where $u_T = \min\{u_{T_1}, u_{T_2}\}$. An enhancement factor is applied to this turbulent burning velocity, to account for the flame area change as the flame passes through the sub-grid scale obstacles. This enhancement factor is

$$E_T = \max\{(R/P)^{0.4}, 1\}, \quad \text{(C15)}$$

where R is the radial distance of the flame front from the ignition point and P is a representative obstacle pitch. In some low-turbulence regions, or just after ignition in an

initially quiescent mixture, the flame will propagate in a quasi-laminar fashion. The burning velocity in this quasi-laminar phase is given by

$$u_{l,q} = \max\{1,\ \min\{R/P,\ 2\}.\} \qquad \text{(C16)}$$

The laminar burning velocity in FLACS is obtained from polynomial functions of the equivalence ratio and flammability limits.

C3. CFX-4

The explosion-modified code models the three important stages in the growth of an explosion. First, there is ignition and the establishment of an initial flame kernel. Second, the flame front expands as an initially laminar and then weakly turbulent reaction zone. Finally, if the flame encounters obstacles, or the turbulence level in the unburnt gas ahead of the flame otherwise increases, the flame will accelerate, propagating as a thick, highly turbulent reaction zone. Quenching of a flame is the reduction in reaction rate due to either flame stretch or turbulent time scales. Quenching due to flame stretch has been accounted for in both the thin flame and eddy break-up combustion models by a simple expression based on the Damköhler number.

Initially, the combusting region will be small compared to the volume of grid cells it occupies. A simple model treats this early flame as a laminar fire ball, which allows the fuel consumption rate to be estimated analytically as a function of time. The flame is assumed to be spherical and to burn at the laminar rate. The radius of the ignition region (R_{Ig}) is fixed and it is from this that the ignition time is determined

$$t_{Ig} = \frac{R_{Ig}}{u_f}, \qquad \text{(C17)}$$

where

$$u_f = \frac{\rho_u}{\rho_b} u_l.$$

The fuel mass fraction source term within the ignition region is given by

$$\overline{\omega}_F = \begin{cases} -\bar{\rho}\frac{\tilde{Y}_F}{t_{Ig}}\left(\frac{t}{t_{Ig}}\right)^2 \exp\{-\frac{t}{t_{Ig}}\} & \text{for } t \le t_{Ig} \\ 0 & \text{for } t > t_{Ig} \end{cases}. \qquad \text{(C18)}$$

This form for the ignition source does not give a smooth transition to the quasi-laminar phase, but does ensure that the ignition timescale is accurate. However, the exponential term in Eqn. C18 has not been implemented in CFX-4, release 3. Following ignition the flame propagates as a thin or quasi-laminar reaction zone. The actual physical width of this reaction zone (i.e.. for a real laminar flame) is likely to be smaller than the grid spacing. However, the simulated width of the reaction zone cannot be less than one cell, therefore it is necessary to model the heat release rate. Consider the reaction process to be characterised by a single progress variable (c) where, in this case, $c = 1$ is a property of the unburnt mixture. Now consider a set of values for this progress variable (c_i) at distances along a line normal to the flame front, separated by spacings of Δ_i. The equation describing the development of this progress variable is

$$\frac{dc_i}{dt} = \begin{cases} -\frac{c_i}{t_B} & \text{for } c_{i-1} \le \alpha \\ 0 & \text{for } c_{i-1} > \alpha \end{cases}, \tag{C19}$$

where t_B is the burning time and α is a constant bounded by zero and unity. The burning velocity is given by

$$u_B = \frac{\Delta_i}{t_b \ln\{1/\alpha\}}. \tag{C20}$$

The constant α determines the thickness of the modelled flame. If this constant is too large then the flame will be spread over several cells, whereas a small value will produce a flame that occupies only the thickness of one cell - yielding an undesirably large burning rate. Hence, a moderate value of this constant is used. The purpose of this transformation is to allow the modelled burning rate to be matched to a specified burning velocity - via t_b.

The laminar burning velocity of a combustible mixture is a function of the gas composition, its temperature and pressure, and may generally be easily specified. However, a small degree of turbulence will affect the flame propagation velocity greatly. The effects of mild turbulence are modelled by introducing the burning velocity correlation of Bradley *et al.* (1992), in a slightly modified form

$$u_B = u_l + 0.88 F \, \mathrm{Ka}^{-0.3} \sqrt{2k}, \tag{C21}$$

where F is a fitting factor, Ka is the Karlowitz stretch factor, and k is the turbulent kinetic energy. The Karlowitz stretch factor is given by

$$\mathrm{Ka} = 0.157 \frac{2k}{u_l^2} \left(\frac{\mu}{\mu_T}\right)^{0.5}. \tag{C22}$$

To enable the model to correctly predict the reaction rate of mixtures of differing equivalence ratios, the laminar burning velocity is obtained from a three point parabolic fit in terms of the equivalence ratio and the maximum laminar burning velocity, Bakke (1986),

$$\frac{u_l}{u_{l,max}} = \frac{(x-x_l)(x-x_r)}{(1-x_l)(1-x_r)}, \tag{C23}$$

where $x = \Phi/\Phi_{max}$. Φ_{max} is the equivalence ratio corresponding to the maximum laminar burning velocity ($u_{l,max}$) and x_l and x_r are the values of x at the lean and rich limits of flame propagation, respectively.

When the flow becomes fully turbulent, the combustion rate is modelled using a form of the eddy break-up expression

$$\bar{\omega}_F = -\rho \frac{\varepsilon}{k} C_R \, C_A \, Y_{min}, \tag{C24}$$

where C_R is given by

$$C_R = 23.6 \left(\frac{\mu \varepsilon}{\bar{\rho} k^2}\right)^{0.25} \tag{C25}$$

and C_A is given by

$$C_A = \begin{cases} 1 & \text{for } Y_P \geq Y_{P,i} \\ 0 & \text{for } Y_P < Y_{P,i} \end{cases}, \tag{C26}$$

where Y_P is the mass fraction of products and $Y_{P,i}$ is an ignition criterion based upon a product mass fraction threshold and Y_{min} which is defined as

$$Y_{min} = min\ (Y_{fu},\ Y_{ox}/s,\ BY_p/(1+s)),$$

where Y_{fu} is the mass fraction of fuel, Y_{ox} is the mass fraction of oxidant, Y_p is the mass fraction of product, s is the stoichiometric mass requirement of oxidant required to oxidise 1 kg of fuel, and B is a model constant. This is introduced to prevent propagation of the flame due to numerical effects. The quenching of the flame is also accounted for in CFX-4. The ratio of quenched and unquenched reaction rates is given by

$$\frac{\bar{\omega}_{F,q}}{\bar{\omega}_F} = \exp\left\{-\frac{D}{D_q}\right\}, \tag{C27}$$

where D is the Damköhler number and D_q is the quenching threshold. For the thin flame model the Damköhler number is the ratio of the turbulent rate of strain to the laminar flame crossing rate, for the eddy break-up model it is the ratio of the eddy dissipation rate to the laminar flame crossing rate. The quasi-laminar, thin flame model is used whenever the burning rate calculated by the thin flame model is greater than that calculated by the eddy break-up model. Hence, the thin flame model is not used only as a forerunner to the eddy break-up calculation, but is used throughout the entire life of the explosion to ensure that all low turbulence regions burn out correctly.

Currently, the turbulence model used in CFX-4 for explosion modelling is the two-equation k-ε model. Originally, the version of this turbulence model included in the standard CFX-4 code, in common with other explosion models and CFD codes, incorporated the effects of turbulence generation due to shear and (optionally) buoyancy only. However, two of the terms omitted from the exact transport equation for k may exhibit a large effect in an explosion situation. These terms appear as additional sources in the k equation and arise from compressibility effects, Jones (1980), not from the Rayleigh-Taylor instability as has been previously stated, Guilbert and Jones (1996). The terms are modelled as follows, see Bradley *et al.* (1988),

$$\overline{P' \nabla \bullet u''} = -\frac{9}{55}\ \bar{\rho}\ k \nabla \bullet \tilde{u} \tag{C28}$$

$$-\overline{u''} \bullet \nabla \bar{P} = -\frac{\mu_T}{\sigma_\rho}\frac{1}{\bar{\rho}^2} \nabla \bar{\rho} \bullet \nabla \bar{P}, \tag{C29}$$

where the term on the right hand side of each equation is the modelled form. These terms have been included in release 3 of the CFX-4 code. A large improvement in over-pressure prediction is noted after inclusion of these terms, the over-pressure increased (typically by an order of magnitude) compared with that predicted by the standard k-ε model, Pritchard *et al.* (1996).

C4. COBRA

The reaction progress variable (c) used in COBRA is bounded between zero and unity and is defined as $c = 1 - Y_F / Y_{F,u}$, where $c = 0$ corresponds to unburnt mixture. The combustion model may be considered as consisting of two distinct parts. The first part prescribes a local turbulent burning velocity based on the local flow properties and the second part ensures that the solution of the transport equations yields a propagating flame front that matches this prescribed burning velocity. The correlations of Bray (1990) and Gülder (1990a) are used to derive the turbulent burning velocity. The correlation of Bray (1990) is used in the regime where $\mathrm{Re}_l > 3200$ and $\mathrm{Re}_\eta > 1.5\,(u'/u_l)$ and is given by

$$\frac{u_T}{u_l} = 0.875\,\mathrm{Ka}^{-0.392}\,\frac{u'}{u_l}\,, \tag{C30}$$

where Ka, the Karlowitz stretch factor, is taken as

$$\mathrm{Ka} = 0.157\left(\frac{u'}{u_l}\right)\mathrm{Re}_l^{-1/2}, \tag{C31}$$

where

$$u' = \left(\frac{2k}{3}\right)^{1/2}.$$

Gülder (1990a) proposes three correlations for different turbulence regime

$$\frac{u_T}{u_l} = 1 + 0.62\left(\frac{u'}{u_l}\right)^{1/2}\mathrm{Re}_\eta \qquad \text{for } \mathrm{Re}_\eta \le 3200 \text{ and } \mathrm{Re}_\eta \ge 1.5\frac{u'}{u_l}, \tag{C32}$$

$$\frac{u_T}{u_l} = 1 + 0.62\exp\left\{0.4\left(\frac{u'}{u_l}\right)^{1/2}\right\}\mathrm{Re}_\eta \quad \text{for } \mathrm{Re}_l \le 3200 \text{ and } 0.6\frac{u'}{u_l} \le \mathrm{Re}_\eta \le 1.5\frac{u'}{u_l}, \tag{C33}$$

$$\frac{u_T}{u'} = 6.4\left(\frac{u_l}{u'}\right)^{3/4} \text{for } \mathrm{Re}_l \le 3200 \text{ and } \mathrm{Re}_\eta < 0.6\frac{u'}{u_l} \text{ or } \mathrm{Re}_l > 3200 \text{ and } \mathrm{Re}_\eta < 1.5\frac{u'}{u_l}, \tag{C34}$$

where the turbulence Reynolds number based on the Kolmogorov length scale (Re_η) is taken to be $\mathrm{Re}_l{}^{1/4}$. An enhancement factor is applied to the predicted burning velocity, based on the geometry of the sub-grid scale obstacles. This factor takes the form

$$E_T = 1 + \frac{\rho_b}{\rho_u}\,\frac{D}{P}\,, \tag{C35}$$

where D is representative obstacle diameter and P a representative obstacle pitch. Catlin and Lindstedt (1991) used numerical techniques to determine the burning velocities predicted by mixing controlled reaction models under idealised conditions. Their study focused on the limitation of such models caused by the problem associated with the boundary condition used at the cold front of the flame, i.e. the burning velocity predicted by these mixing controlled models is not uniquely defined unless the reaction rate falls to zero as the cold front is approached. Catlin and Lindstedt (1991) found that a quenching model based on the reaction progress variable was found to predict a limiting steady value for the burning velocity. Following guidelines established by the analysis of Catlin and Lindstedt (1991), the reaction rate in COBRA is specified as

$$\bar{\omega}_c = \bar{\rho} R \tilde{c}^4 (1-\tilde{c})(\tfrac{\rho_u}{\rho_b})^2. \qquad \text{(C36)}$$

The analysis of Catlin and Lindstedt (1991) shows that the turbulent burning velocity and the turbulent flame thickness can be expressed in terms of a turbulent diffusion coefficient (Γ) and the reaction rate constant (R) as

$$u_T = \Lambda_1 (\Gamma R)^{1/2} \qquad \text{(C37)}$$

and

$$\delta_T = \Lambda_2 (\Gamma R)^{1/2}, \qquad \text{(C38)}$$

where Λ_1 and Λ_2 are burning velocity and flame thickness eigenvalues. If the burning velocity is specified and the flame thickness is known, then the values of Γ and R required to reproduce the burning velocity are

$$\Gamma = \tfrac{u_T \delta_T}{\Lambda_1 \Lambda_2} \qquad \text{(C39)}$$

and

$$R = \tfrac{u_T \Lambda_2}{\delta_T \Lambda_1}. \qquad \text{(C40)}$$

Both eigenvalues have been calculated from one-dimensional numerical calculations of a planar flame propagating in a flowfield with constant levels of turbulence. These calculations demonstrate that unique values of these eigenvalues do exist and have the values of $\Lambda_1 = 0.346$ and $\Lambda_2 = 3.575$. In the calculations the flame thickness was taken as being equal to a turbulence length scale given by $l = C_\mu^{3.4} k^{3/2}/\varepsilon$, COBRA also uses this expression for the flame thickness.

C5. NEWT

Earlier work, sponsored by Shell Research Ltd., has applied NEWT to the modelling of two explosion geometries, the HSL baffled box, Connell *et al.* (1996a), and the Shell SOLVEX box, Watterson *et al.* (1996) and Connell *et al.* (1996b). This work highlighted deficiencies in the eddy break-up combustion model employed in NEWT. In particular it was found necessary to apply two constraints to the eddy break-up model. The first was required to yield correct flame behaviour near to walls. The reaction rate predicted by the eddy break-up model is proportional to the reciprocal of the turbulence time-scale ($\omega \propto \varepsilon / k$). Near wall boundary conditions force k to zero whilst ε remains finite, resulting in the combustion rate becoming unbounded as a wall is approached. However, experimental evidence shows that the opposite is true and in fact the combustion rate is decreased near surfaces. To prevent the combustion rate becoming unbounded near solid surfaces the eddy break-up term is modified so that when k becomes small the reaction rate is dependent on the Kolmogorov time scale

$$\bar{\omega}_c = C_{com} \bar{\rho} \tilde{c} (1-\tilde{c}) \left(\tfrac{k}{\varepsilon} + \sqrt{\tfrac{\nu}{\varepsilon}} \right)^{-1}, \qquad \text{(C41)}$$

where C_{com} is a constant and v is the kinematic viscosity of the gas mixture. The second constraint ensures that the combustion rate falls to zero as the leading edge of the flame is approached. This is achieved simply, and crudely, by setting the reaction rate to zero below a certain threshold for the reaction progress variable (leading edge suppression).

Within the HSE funded project, a parametric study has been undertaken to determine the sensitivity of the model to leading edge suppression and the eddy break-up constant. The value of the progress variable threshold, for the leading edge suppression, was set to be 0.001. This value yielded flame shapes that were qualitatively correct. However, with no leading edge suppression (equivalent to setting the threshold to zero) the flame was observed to become more distributed with spurious ignition, especially in high turbulence regions, whereas increasing the progress variable threshold by an order of magnitude was found to prevent flame propagation entirely. The calculations were also found to be sensitive to the eddy break-up model constant, with the flame speed increasing as this constant is increased. Leading edge suppression was found to be more important with higher values of C_{com}, as increasing this constant increased the tendency for the flame to run along the walls.

Further modifications have been made to the eddy break-up model as documented by Guilbert and Jones (1996). The first of these is a Damköhler number based quenching model, the second is a dependence on the turbulence Reynolds number combined with an ignition threshold - see section 2.3.2 for further details.

Presently the ignition treatment in NEWT is fairly simple, a point ignition is modelled by ramping up the value of the progress variable in a single cell at a wall. To more realistically model the ignition process, work is ongoing to implement the flameball approach described by Guilbert and Jones (1996) - see section 2.3.2. The quasi-laminar flame phase is modelled using the approach of Sæter (1994), where the combustion rate term is modified on the basis of an experimental correlation to ensure that the reaction rate over the whole domain is equal to that of the modelled laminar flame. This form of the reaction rate is used whenever the turbulence Reynolds number falls below a critical value - see section 2.2.2.

The deficiencies of the eddy break-up model have led to the inclusion of the alternative laminar flamelet combustion model, Bray *et al.* (1985), for the turbulent flame phase, in NEWT. The reaction zones are assumed to consist of thin, highly wrinkled surfaces that separate unburnt reactants from fully burnt products. These surfaces are stretched and transported by the turbulence, but retain the structure of a strained laminar flame - i.e.. the flame is propagating in a direction normal to its surface at the locally applicable laminar burning velocity. The reaction rate per unit volume may be formed as a product of the reaction rate per unit surface area (R) and the mean flame surface area per unit volume (Σ)

$$\bar{\omega}_c = R\,\Sigma. \qquad \text{(C42)}$$

It is possible to derive an exact transport equation for Σ, which may be modelled and solved. However, solution of this equation involves significant computational expense and the modelling assumptions introduce additional uncertainties. Presently in NEWT a simpler method is implemented whereby Σ is obtained algebraically. An algebraic expression for Σ may be derived by treating the passage of laminar flamelets past a point in space as a stochastic process analogous to a random telegraph signal, Bray *et al.* (1989),

$$\Sigma = \frac{g\bar{c}(1-\bar{c})}{|\bar{\sigma}_y|\hat{L}_y}, \tag{C43}$$

where g and $\bar{\sigma}_y$ are model constants with values of 1.5 and 0.5 respectively, and $\hat{L}_y$ is the integral length scale of the telegraph signal process. Abu-Orf (1996) proposes

$$\hat{L}_y = C_L L_L f\left(\frac{u'}{u_l}\right), \tag{C44}$$

where C_L is a constant (taken to be unity) and L_L is the laminar flamelet length scale. The empirical function f is included to reproduce experimentally observed behaviour where the turbulent flame speed first increases with the ratio u'/u_l, but then decreases for higher values of this ratio as flame stretch effects begin to cause local extinction. The laminar flame speed is obtained from an empirical correlation - Abu-Orf (1996). Qualitatively, results obtained using this combustion model are in much better agreement with experiment than with the eddy break-up model.

APPENDIX D - DISCRETIZATION OF PARTIAL DIFFERENTIAL EQUATIONS

D1. Introduction

The equations governing the fluid flow, the Navier-Stokes equations, are partial differential equations. It is necessary to cast the pde's into a set of algebraic equations. This is achieved by discretising the terms, both spatially and temporally, in the pde's. All terms are taken at time t_n, as indicated by a small superscript 'n', i.e. f_i^n, in an explicit finite difference formulation. In implicit finite differences, some if not all terms is taken at time step t_{n+1}. There are also semi-implicit schemes which treats some of the spatial directions implicitly while the other directions are treated in an explicit manner. For a more in-depth treatment, see e.g. Hirsch (1988) or Roache (1998). The following sections describe the process of discretising the equations, using some commonly used schemes.

D2. First-Order Discretization Schemes

Partial Taylor series expansion of partial derivatives yields the basic finite difference form. Assume that the problem is in 1D, the extension to 2D or 3D is trivial, and an explicit formulation is sought.

Carry out a forward expansion of a Taylor series of the first derivative, $\frac{\partial f}{\partial x}$ around point 'i', ignoring third-order and higher terms:

$$f_{i+1} = f_i + \left(\frac{\partial f}{\partial x}\right)_i (x_{i+1} - x_i) + \frac{1}{2}\left(\frac{\partial^2 f}{\partial x^2}\right)_i (x_{i+1} - x_i)^2 + \cdots \qquad \text{(D1)}$$

or

$$f_{i+1} = f_i + \left(\frac{\partial f}{\partial x}\right)_i \Delta x + \frac{1}{2}\left(\frac{\partial^2 f}{\partial x^2}\right)_i \Delta x^2 + HOT\,, \qquad \text{(D2)}$$

where HOT refers to higher order terms. Solve eqn. D2 for $\frac{\partial f}{\partial x}$

$$\left(\frac{\partial f}{\partial x}\right)_i = \frac{f_{i+1} - f_i}{x_{i+1} - x_i} + \frac{1}{2}\left(\frac{\partial^2 f}{\partial x^2}\right)_i \Delta x + HOT, \qquad \text{(D3)}$$

or

$$\left(\frac{\partial f}{\partial x}\right)_i = \frac{f_{i+1} - f_i}{x_{i+1} - x_i} + O(\Delta x), \qquad \text{(D4)}$$

where $O(\Delta x)$ refers to terms of order Δx. The finite difference resulting from the forward expansion of the partial derivative is written as

$$\frac{\partial f}{\partial x} \approx \frac{\delta f}{\delta x} = \frac{f_{i+1} - fi}{\Delta x} \qquad \text{(D5)}$$

and has a truncation error of order Δx. A backward expansion around point 'i', following the procedure above,

$$\left(\frac{\partial f}{\partial x}\right)_i = \frac{f_i - f_{i-1}}{x_i - x_{i-1}} + \frac{1}{2}\left(\frac{\partial^2 f}{\partial x^2}\right)_i \Delta x + HOT \qquad \text{(D6)}$$

gives another finite difference

$$\frac{\partial f}{\partial x} \approx \frac{\delta f}{\delta x} = \frac{f_i - f_{i-1}}{\Delta x}. \qquad \text{(D7)}$$

An analogous procedure can be followed for the temporal discretization. It can be shown that the forward differencing scheme is numerically unstable for all grid spacings, $\Delta x > 0$, and for all time steps, $t_n > 0$, and can, therefore, not be used to discretize the partial derivative. The backward, or more commonly referred to as first-order upwind, differencing on the other hand is stable for all $\Delta x > 0$ and for all time steps, $t_n > 0$. This upwind differencing scheme is frequently used because it is inherently numerically stable. However, the stability is achieved through the truncation error, which has the same effect as diffusion, and is hence referred to as numerical diffusion. An initial step change in a variable would soon be diffused, or smeared out.

D3. Second-Order Discretization Schemes

D3.1. Central Differencing Scheme

Higher order discretization schemes should nominally be more accurate as the truncation error will be of order Δx^2. However, there are other issues to consider, such as whether the discretization scheme is stable. A second order accurate differencing scheme can be obtained by subtracting eqn. D7 from eqn. D5

$$\frac{\partial f}{\partial x} \approx \frac{\delta f}{\delta x} = \frac{f_{i+1} - f_{i-1}}{2\Delta x}. \qquad \text{(D8)}$$

This formulation is often referred to as the central differencing scheme. The expression is stable for $\mathrm{Re}_{cell} < 2$, where the cell Reynolds number is based on the cell width as the characteristic length. The scheme exhibits an unphysical, oscillatory behaviour for cases where $\mathrm{Re}_{cell} \geq 2$. This makes the central differencing scheme unsuitable unless the mesh is sufficiently fine so that the cell Reynolds number is below 2.

A solution to the problem of too much diffusion, when using the first-order upwind scheme, and unphysical wiggles, when using the central differencing scheme, is to use the more accurate central differencing method, where the scheme is stable, and use the upwind scheme everywhere else. It is often referred to as hybrid differencing. Considerable effort has gone into devising blending functions so that central differencing scheme is used to as large an extent as possible.

D3.2. Total Variation Diminishing Schemes

The discretisation schemes, discussed above, are not well suited to compressible flows. A number of different discretisation methods were devised, where sensors which would detect an incipient build up of a shock wave and then locally apply a weighted first order method in the vicinity of the shock wave, in order to avoid overshoots, Roache (1998). Total Variation Diminishing (TVD) schemes were shown, Lax (1973), to have a functional to the solution, called total variation, which will not increase with time for (linear and non-linear) scalar conservation laws. TVD schemes are always first order near the shock but can be higher order

accurate away from the shock. Please see Roache (1998) and references therein for a more detailed discussion of the TVD methods.

D4. References

Hirsch, C. (1988)
Numerical Computation of Internal and External Flows. Volume 1 : Fundamentals of Numerical Discretization
John Wiley & Sons, Guildford, U.K.

Lax, P. D. (1973)
Hyperbolic Systems of Conservation Laws and the Mathematical Theory of Shock Waves
SIAM, Philadelphia, U.S.A.

Roache, P.J. (1998)
Fundamentals of Computational Fluid Dynamics
Third Edition, Hermosa Publishers, New Mexico, U.S.A.

APPENDIX E - COMMUNICATIONS WITH CHRISTIAN MICHELSEN RESEARCH

E1. Introduction

The comments in Sections E2 and E3 are taken verbatim from communications with Christian Michelsen Research in Norway. Lines beginning with '**HSL**' in Section E3 are the questions posed by HSL to the code developers, while lines beginning with '**CMR**' are the answers (verbatim) from CMR. All the views expressed in Appendix E are those of CMR; HSE' s comments and views can be found in Section 2.3.3.

E2. Comments from J. R. Bakke on 20 June 2001

When simulations of dispersion and explosions in large areas like chemical plants or offshore installations are performed the geometry is meshed with a grid of cells of one cubic metre in volume. This is done for practical reasons (acceptable runtimes). FLACS can also be used for other simpler applications, in which case the gridding procedure may be very different.

It is true that for explosion simulations the code can be said to be calibrated for cells of the order one metre cubed. However, grid size sensitivity simulations are performed - not to ensure that the solution is grid independent but rather to see if the grid dependence is acceptable. It is not expected for these kinds of problems that full grid independence can be achieved.

E3. Reply from O.R. Hansen on 9 July 2001

HSL : What control does the user have when it comes to meshing? (Cell size and distribution)

CMR : The user of FLACS will choose the grid embedding himself. The FLACS manual and FLACS-I and FLACS-II course handouts give relatively rigid guidelines on how the gridding should be performed, in order to avoid mistakes. Essential is close to cubical grid cells in combustion regions, and also outside the geometry if far field blast is considered. Stretching of grid towards boundaries is OK, and there are some demands wrt grid resolution relative to geometry and gas cloud size.

1m x 1m x 1m grids was required up to 1993, as FLACS-89 combustion models were calibrated for this. FLACS-93, -94, -95, -96, -97, -98 and FLACS-99 have no requirements on grid size, but rather that the grid resolution is a certain number of grid cells across the room or gas cloud (if less then (sic) the room). In a typical offshore module, we would still use 1m x 1m x 1m, but also 0.5m or less. For large offshore modules, and onshore plants, 2m x 2m x 2m is also sometimes used. For other situations, like explosions inside pipes or equipment, much smaller control volumes than this will be used.

HSL : Dr Bakke said that FLACS has been used to carry out blind predictions with acceptable results. Have any of these calculations been published in the open literature so that I can read it and reference the work?

CMR : Generally most of the work done is confidential in one way or the other. Usually experiments are not shared outside the sponsorgroup of the experiments. A range of different blind tests have been performed (but the degree of blindness vary).

A) During the MERGE and EMERGE projects, some tests were simulated prior to performance of the tests. Some of the tests with initial turbulence were published (see chapter 6 in the EMERGE final report for reference to paper). These were blind, but a range of tests carried out prior to the tests made it not so hard to guess the outcome of the blind tests, and the value is thus questionable.

B) During the Blast and Fire Campaign blind tests were carried out. The first round lost most of its value as the project did a poor job describing the geometry, so that the blind tests and experiments were carried out at quite different geometries. The test 24, 25, 26 and 27 were simulated blind with FLACS. The project did not report test 24 in the final report from SCI, as the rig was destroyed. The SCI final report from the Blast and Fire project (1998) you will easily find at HSE or order from the SCI.

C) 1996 we carried out some simulations in a 20m and a 200m tunnel in South Africa. One year later the experiments were performed by CSIR, and FLACS predicted with good accuracy the outcome of the tests. One of these comparisons from the report from South Africa (CSIR AERO 97/299) is published at a paper from a conference held in Poland 1999:

Hansen, O.R., Storvik, I., and Wingerden, K. van, "*Validation of CFD-models for gas explosions, FLACS is used as example. Model description, experiences and recommendations for model evaluation*", **European Meeting on Chemical Industry and Environment III** pp 365-382, Krakow, Poland September 1999.

D) In a lot of experimental projects we are involved in, we carry out simulations prior to or during experiments. This is also the case for the Blast and Fire Phase 3B project, where we have performed a range of simulations before getting knowledge about the results. In general the results are quite good.

HSL : What criteria do you use to deem the results to be acceptable?

CMR : It is very difficult to set up criteria that makes comparisons acceptable or not. In our validation work, hundreds of simulations are carried out and compared, using different grids, and doing a range of parameter variations (experimentally as in simulations). For pressures we are typically happy if the pressures are predicted within +/-30%, and still find it acceptable with a factor of two deviation in pressure. But this vary with the tests. Some tests sponsored by the HSE showed local pressures to vary with more than a factor of 10 in identical experiments, whereas the average pressures varied by almost a factor of 2. Under these circumstances it is difficult to demand +/-30% from the simulator. In a closed vessel explosion, higher precision is expected.

In one of our studies where 30-40 full scale explosion experiments were simulated and compared with experiments (more than 1000 monitor point comparisons) we find a good trend in general, but still find tests where the deviation is larger than we would like. HSE sponsored this work (report CMR-98-F30058).

With FLACS guidelines and pre-settings of choices are quite strict, so that the user have limited opportunities to influence the results by choosing non-physical parameters. Very often BP or Norsk Hydro perform validation simulation at the same time as ourselves, and get similar answers.

Other CFD-simulators may have strength parametres as input when starting the simulation. A validation work by such a simulator will have limited value.

Harpur Hill, Buxton, SK17 9JN
Telephone: +44 (0)114 289 2000
Facsimile: +44 (0)114 289 2050

A Review of the State-of-the-Art in Gas Explosion Modelling

HSL/2002/02

Project Leader: C. J. Lea

H. S. Ledin MSc PhD DIC

Fire and Explosion Group

Summary

Objectives

1. To identify organisations involved in gas explosion research in the U.K. and Europe.
2. To survey these organisations, to determine their areas of current and proposed work.
3. To collate their responses in a report, which also provides an up to date literature review of gas explosion modelling.
4. To critically assess the strengths and weaknesses of available gas explosion models.
5. To recommend areas where further work is needed to improve the accuracy of the gas explosion models.

Main Findings

1. There are a wide range of class of models available - from empirical and phenomenological, through to those which are Computational Fluid Dynamics (CFD) based. The latter category falls into two areas: 'simple' - many obstacles not resolved and 'advanced' - all obstacles resolved by the 3-D CFD grid.
2. Generally as one moves from empirical to advanced CFD, models become based on more fundamental physics, are able to more accurately represent the real geometry, but require increasing resource to set-up, run and interpret the results.
3. Models in each class embody a number of simplifications and assumptions, limiting their ability to be used as reliable predictive tools outside their range of validation against test data. It appears that only those models falling into 'advanced' CFD class could in principle be capable of being truly predictive tools outside their immediate range of validation. However, even here the existing models have limitations and require further development and testing before this capability is fully realised - which even then will currently be limited to relatively simple geometries by the required computer resources.
4. Many of the CFD-based explosion models in current use employ relatively crude approximations of the modelled geometry, relying on calibrated sub-grid models.
5. Most of the 'simple' CFD codes and some of the 'advanced' CFD codes most commonly used for explosion prediction use simple, dated numerical schemes for both the computational grid and the finite differencing, which could lead to substantial numerical errors.
6. The combustion model used in CFD-based approaches to predict the reaction rates are also subject to a considerable degree of uncertainty. Models, which

employ prescribed reaction rate, could be more sound than those relying on an Eddy Break-Up model, because the latter requires a resolution of the flame front unlikely to be achieved in practice. Work is currently under way on the incorporation of detailed chemical kinetics into a gas explosion model, but it will not be feasible to use such a model on a real complex plant geometry in the foreseeable future.

7. The simple eddy-viscosity concept is ubiquitous amongst the explosion codes for modelling turbulent transport, but this model of turbulent transport is not strictly applicable in high speed, combusting flows, leading to further possible errors. There is a move to full Reynolds stress turbulence models, these have either been implemented in research type codes - currently not available on general release, or have not been tested for explosions. There are numerical stability problems associated with Reynolds stress transport models which need to be addressed.

8. The accuracy expected from, say phenomenological and 'simple' CFD models, is generally fairly good (to within a factor of two), e.g. the models yield solutions which are approximately correct, but, importantly, only for a scenario for which the model parameters have been tuned. This limits the applicability of these models as truly predictive tools.

Main Recommendations

1. There is a range of modelling approaches available, each with their own strengths and weaknesses. In order to establish greater confidence in model predictions, it is clear that, for the future, improvements in the physics and the numerics are required, particularly for the CFD-based approaches. However, predictive approaches are needed now. It is thus important that the user be aware of the uncertainties associated with the different models. The following recommendations are essentially those needed to be taken on board by model developers and their funders. They primarily relate to CFD models, which, in principle, should offer the best hope of becoming truly predictive models of gas explosions, with wide applicability.

2. Ideally one would replace the Cartesian grid / PDR (Porosity / Distributed Resistance) based CFD models by models that are capable of representing a given geometry more accurately. However, the likely time scale for the necessary advances in computing power and code efficiency which will possibly allow geometries to be fully grid resolved is large, possibly of the order of ten years or more. Until this is possible a hybrid approach has to be adopted, whereby body-fitted grids are used to represent the larger objects within the explosion domain, with the PDR approach reserved for the regions that may not be resolved by the grid. It is therefore recommended that methodologies are developed to allow a seamless transition between resolved and PDR-represented solutions as grids are refined. There should be a move away from fixed grid cell size, because such models will require constant re-calibration for new scenarios due to physical and numerical errors associated with the large grid cell size always needing to be

compensated. This situation cannot improve until there is a move to a more soundly based methodology.

3. More work is needed to establish the reliability of the combustion models used. Presently, the majority of the explosion models investigated prescribe the reaction rate according to empirical correlations of the burning velocity. However, it should be recognised that these correlations are subject to a large uncertainty. The eddy break-up combustion model should ideally not be used if the flame front cannot be properly resolved or, the resulting errors should be recognised and quantified.

4. The sensitivity of model predictions to the turbulence model used should be investigated. Turbulence modelling has not yet received much attention in the field of explosion modelling. The commonly used two-equation, k-ε model has a number of known failings i.e. does not predict counter-gradient diffusion, but remains in use due to its economy and robustness. Large improvements in over-pressure prediction have been noted by including simple terms into the k-e model, to account for compressibility effects. However, inclusion of these terms is by no means universal. There is a wide range of advanced, non-linear k-e models now available. Ideally Reynolds stress transport modelling should be used but the models require much work to ensure that improvements are not offset by lack of numerical stability.

5. Model development should now be driven by repeatable, well defined, detailed experiments, focusing on key aspects of the physics of explosions. This tends to imply small or medium-scale experiments. Large-scale experiments are suitable as benchmark tests, but code calibration on the basis of macroscopic property measurements should be treated with caution, since it is quite possible to obtain approximately correct answers but for the wrong reasons due to gross features swamping finer details. Detailed comparisons of flame speeds, species concentrations, etc., should allow deficiencies in explosion model physics and numerics to be identified, and solutions developed and tested.

6. There are no, or few, technical barriers to implementation of the above model improvements, beyond a willingness and need to do so.

7. Perhaps the safest that can be advised at this point is that it would be unwise to rely on the predictions of one model only, i.e. better to use a judicious combination of models of different types, especially if a model is being used outside its range of validation.

Contents

1. INTRODUCTION 1
1.1. Background 1
1.2. A Description of Gas Explosions 1
1.3. Why Model Explosions? 2
1.4. Model Requirements 3
1.5. Review Methodology 4

2. DESCRIPTION AND DISCUSSION OF CURRENT MODELS 7
2.1. Empirical Models 7
2.1.1. Introduction 7
2.1.2. TNT Equivalency Method 7
2.1.3. TNO Method 8
2.1.4. Multi-Energy Concept 8
2.1.5. Baker-Strehlow Method 9
2.1.6. Congestion Assessment Method 10
2.1.7. Sedgwick Loss Assessment Method 11
2.2. Phenomenological Models 12
2.2.1. Introduction 12
2.2.2. SCOPE 12
2.2.3. CLICHE 14
2.3. CFD Models 17
2.3.1. Introduction 17
2.3.2. EXSIM 18
2.3.3. FLACS 20
2.3.4. AutoReaGas 22
2.4. Advanced CFD Models 24
2.4.1. Introduction 24
2.4.2. CFX-4 24
2.4.3. COBRA 26
2.4.4. NEWT 27
2.4.5. REACFLOW 29
2.4.6. Imperial College Research Code 31

3. DISCUSSION 34
3.1. Overview of Model Constraints 34
3.2. Empirical Models - Main Capabilities and Limitations 36
3.3. Phenomenological Models - Main Capabilities and Limitations 37
3.4. Simple CFD Models - Main Capabilities and Limitations 37
3.5. Advanced CFD Models - Main Capabilities and Limitations . . . 39
3.6. Model Accuracy 39
3.7. Recommendations for Future Work 42
3.7.1. Grid Improvements 42
3.7.2. Combustion Model Improvements 42
3.7.3. Turbulence Model Improvements 43
3.7.4. Experimental Input to Model Development 43

3.7.5. Miscellaneous Issues 43

4. CONCLUSION 44

5. REFERENCES 46
5.1. References Cited in the Report 46
5.2. References Used but not Cited 53

APPENDIX A - THEORETICAL DESCRIPTION OF GAS EXPLOSIONS 54
A1. Conservation Equations 54
A2. Turbulence Modelling 56
A3. Reaction Rate Modelling 57
A3.1. Turbulent Flame Speed 58
A3.2. Turbulent Reaction Rate 59
A4. Numerical Modelling 61

APPENDIX B - COMBUSTION MODEL IN SCOPE CODE 66

APPENDIX C - COMBUSTION MODELS IN CFD CODES 68
C1. Exsim 68
C2. FLACS 69
C3. CFX-4 70
C4. COBRA 73
C5. NEWT 74

APPENDIX D - DISCRETISATION OF PARTIAL DIFFERENTIAL EQUATIONS 77
D1. Introduction 77
D2. First-Order Discretisation Schemes 77
D3. Second-Order Discretisation Schemes 78
D3.1. Central Differencing Scheme 78
D3.2. Total Variation Diminishing Schemes 78
D4. References 79

APPENDIX E - COMMUNICATIONS WITH CHRISTIAN MICHELSEN RESEARCH 80
E1. Introduction 80
E2. Comments from J. R. Bakke on 20 June 2001 80
E3. Reply from O. R. Hansen on 9 July 2001 80

List of Figures

Figure 1 - Example of a congested geometry 40

Figure 2 - Comparison of calculated and measured maximum over-pressures for MERGE medium-scale experiments, (×) - COBRA predictions and (◇) - EXSIM predictions; a) all experiments and b) experiments with maximum over-pressures below 1.5 bar, see also Popat *et al.* (1996) 40

Figure 3 - Comparison of calculated and measured maximum over-pressures for MERGE large-scale experiments, (×) - COBRA predictions, (◇) - EXSIM predictions, (●) - FLACS predictions and (○) AutoReaGas predictions; a) all experiments and b) experiments with maximum over-pessures below 1 bar, see also Popat *et al.* (1996) 41

Figure A1 - Schematic description of the flame reaction zone 58

Figure A2 - A non-orthogonal structured grid 62

Figure A3 - A multi-block, non-orthogonal structured grid 62

Figure A4 - An unstructured grid with prismatic grid in the boundary layer 63

Figure A5 - Control volume in one dimension 64

List of Tables

Table 1 - Numerical Model Summary 5

1. INTRODUCTION

1.1. Background

The aim of this review is to inform the Hazardous Installations Directorate about the current status and future direction of gas explosion numerical models presently in use. Gas explosions are a major hazard in both the on-shore and off-shore environments.

The 1974 explosion at the Nypro plant at Flixborough is one of the most serious accidents to afflict the chemical processing industry. The explosion at Flixborough was caused by the ignition of a flammable cloud containing about 50 tons of cyclohexane, the cyclohexane release was probably due to the failure of a temporary pipe. The blast has been estimated to be equivalent to about 16 tons of TNT, with the result that 28 people were killed, 89 injured, the plant was totally destroyed, and damage was caused to nearly 2000 properties external to the site.

In 1988 on the offshore platform Piper Alpha a small explosion in a compressor module caused fires which resulted in the rupture of a riser. Most of the platform was subsequently destroyed by fire, causing the death of 167 people. The over-pressure generated by the initial explosion has been estimated to be only 0.3 bar, Cullen (1990).
This report describes empirical models, phenomenological models and Computational Fluid Dynamics (CFD) based models. Empirical models are the simplest way of estimating deflagration over-pressures. These models contain correlations and contain little or no physics. Phenomenological models are simplified models which represent the major physical processes in the explosion. CFD models involve numerical evaluation of the partial differential equations governing the explosion process and yield a great deal of information about the flow field.

The report is further restricted to numerical models of deflagrations. Detonations are not included. A deflagration is the name given to the process of a flame travelling through a combustible mixture where the reaction zone progresses through the medium by the processes of molecular (and / or turbulent) diffusion of heat and mass. The burning velocity - i.e. the velocity of the combustion front relative to the unburnt gas is sub-sonic relative to the speed of sound in the unburnt gas. A detonation is a self-driven shock wave where the reaction zone and the shock are coincident. The combustion wave is propagating at super-sonic velocity relative to the speed of sound in the unburnt gas. The chemical reaction is initiated by the compressive heating caused by the shock, the energy released serving to drive the compression wave. Propagation velocities of the combustion wave for a detonation can be up to 2000 m s^{-1} with a pressure ratio across the detonation front of up to 20.

This is a update and extension of the gas explosion model review by Brookes (1997).

1.2. A Description of Gas Explosions

An explosion is the sudden generation and expansion of gases associated with an increase in temperature and an increase in pressure capable of causing structural damage. If there is only a negligible increase in pressure then the combustion phenomena is termed a flash-fire.

Gas explosions are generally defined as either confined or unconfined. An explosion in a process vessel or building would be termed as confined. If the explosion is fully confined - i.e. if there is no venting and there is no heat loss, then the over-pressure will be high, up to about eight times higher than the starting pressure. The pressure increase is determined mainly by the ratio of the temperatures of the burnt and unburnt gases. Explosions in confined but un-congested regions are generally characterised by low initial turbulence levels and hence low flame speeds. If the region contains obstacles, the turbulence level in the flow will increase as the fluid flows past the objects, resulting in a flame acceleration. If the confining chamber is vented, as is usually the case, then the rate of pressure rise and the vent area become factors that will influence the peak pressure. The rate of pressure rise is linked to the flame speed, which in turn is a function of the turbulence present in the gas.

The over-pressure generated by an unconfined explosion is a function of the flame speed, which in turn is linked to the level of turbulence in the medium through which the flame progresses. As the flame accelerates the pressure waves generated by the flame front begin to coalesce into a shock front of increasing strength. If the explosion occurs in a medium of low initial turbulence, is fully unconfined, and there are no obstacles present then the generated over-pressure is very low. If obstacles are present then expansion-generated flow, created by the combustion, of the unburnt gas passing through the obstacles will generate turbulence. This will increase the burning velocity by increasing the flame area and enhancing the processes of molecular diffusion and conduction, and this will in turn increase the expansion flow which will further enhance the turbulence. This cycle, so called Schelkchkin mechanism, continues generating higher burning velocities and increasing over-pressures.

1.3. Why Model Explosions?

Deflagrations are unwanted events. Models containing physical descriptions of deflagrations are a complement to experiments in risk assessments and/or when designing or assessing mitigating features. The more complex models have the wherewithal to be applied to diverse situations, but must not therefore be assumed to be more accurate.

The effects of an explosion depends on a number of factors, such as maximum pressure, duration of shock wave interaction with structures, etc. These factors in turn depend on a number of variables:

- Fuel type
- Stoichiometry of fuel
- Ignition source type and location
- Confinement and venting (location and size)
- Initial turbulence level in the plant
- Blockage ratios
- Size, shape and location of obstacles

- Number of obstacles (for a given blockage ratio)
- Scale of experiment/plant

The reactivity of fuel has a profound effect on the overpressures generated in a given geometry. The least reactive gas is methane, while acetylene and especially hydrogen give rise to very high pressures.

The stoichiometry of the gas cloud is also important. Lean mixtures produce lower overpressures than rich or stoichiometric mixtures, while slightly rich mixtures yield the highest over-pressures for a given plant layout.

Ignition source type also affects the strength of the explosion; jet-type, or bang-box-type, ignition sources give rise to higher over-pressures than a planar or point source. The location of the ignition is also important, but must be viewed in conjunction with information about the plant geometry, e.g. how confined and/or congested is the plant. Confinement leads to pressure build-up and influences the way the flame front advances through the geometry. Venting is one way of reducing the over-pressure generated by the combustion. Strategically placed vents can greatly reduce the impact of a deflagration.

Explosions situated in a quiescent environment will generally lead to lower over-pressures than those occuring in turbulent flow environments. This is due to the enhanced burning rate experienced by the flow.

One can define a blockage ratio, which is measure of how congested the plant is. Explosions in plants with large blockage ratios usually yield higher over-pressures than small blockage ratios. However, the size and shape of the obstacles are also important factors to take into account. In general, for a given blockage ratio, many small objects results in higher pressures than larger objects. Furthermore, the location of the obstacles also affects the pressure. The more tortuous route the flame has to travel through the domain, the higher pressure is likely to be produced, due to turbulence enhancement of the burning velocity.

Finally, the scale of experiment/plant is also an important factor. Large-scale experiments generally yield higher pressures than small-scale ones. This makes it difficult to predict, from a small-scale experiment, what the pressures are likely to be in real plants.

Ideally, explosion risks should be considered at the plant design stage, but for various reasons this might not be possible. Unfortunately accidents do happen, but research programmes consisting of experiments and modelling should hopefully result in a better understanding of why the accident happened and how the impact can be minimised or the risk of explosion be mitigated or eliminated completely. In most cases, a great number of scenarios needs to be investigated, which is one justification for developing and using models of varying degrees of complexity.

1.4. Model Requirements

A number of factors influencing the strength of the deflagration were identified in the previous section. A model should ideally take all these variables into account. In addition to

this, the model should contain appropriate physics, be able to deal with different fuels and ambient conditions without special tuning of constants, and be easy to use. Furthermore, the computer code in which the model is implemented should be numerically accurate, allow for an accurate representation of the geometry, be easy to use and the run times should be short.

Some of these requirements are contradictory. Complex models are unlikely to run very quickly. In some cases the understanding of the underlying physics is sketchy, at best. Turbulent premixed combustion is an active area of research and new findings may find their way into the models currently in use. However, there are limitations in terms of computer resources. A real world plant is very complex, with a large number of pipes, tanks and other equipment of various shapes and sizes, and it is not possible today to resolve all the features of the geometry - due to the demands on computer memory and processor speed. The flame acceleration due to turbulence generated when the flow has to make its way past obstacles is partly down to a more intense combustion, but also an increase in flame area. Most of the CFD codes do not allow for flame front tracking, neither would these codes be able to properly resolve the flame front.

However, the models currently in use do contain some physics and chemistry. In many situations, the results of the simulations are in good agreement with experiments, but it is important to remember that the models have their limitations. The choice of model depends on the level of detail required, on the level of accuracy required, and time available for the calculations.

The turbulence models implemented in the CFD codes can perform well for some types of flows, mainly high Reynolds number, isothermal, isotropic, incompressible flows. These models have no mechanism for modelling transition from laminar to turbulent flow. Deflagrations in confined spaces might start in a quiescent environment. A transition from laminar to turbulent flow is a distinct possibility, which can contribute to inaccurate solutions.

1.5. Review Methodology

This review was conducted by following three approaches. The HSL Sheffield Information Centre was asked to carry out an on-line search seeking information on gas explosion modelling. A number of key words and phrases, as well as a large number of possible authors, were provided

A paper based literature survey was conducted. Relevant reports and papers were collected, the reference lists of which were used to discover further useful sources of information. The survey continued to 'fan out' in this manner, generating a large quantity of useful material. This search has been mainly used to provide the background to this report, but some recent information on certain models was also discovered in the open literature.

Finally, the most recent information on each of the models has been obtained directly from the model developers. This was achieved by sending a standard letter to a number of organisations, inviting comment on the current status and future development of their gas explosion modelling. Further letters were sent to organisations that failed to respond to the original request. Letters were sent to around twenty organisations, over half of which eventually responded to the request for information. Generally, however, the organisations

that did reply showed some reluctance to divulge full technical details of their models, most probably due to the increasing commerciality of their operations - either through consultancy or code sales. The numerical models reviewed in the present report are listed in Table 1.

Table 1 - Numerical Model Summary

Name	Type	Grid	Accuracy	Reaction Model
TNT Equivalency	Empirical	N/A	N/A	None
TNO	Empirical	N/A	N/A	None
Multi Energy	Empirical	N/A	N/A	None
Baker-Strehlow	Empirical	N/A	N/A	None
Congestion Assessment Method	Empirical	N/A	N/A	None
Sedgwick Loss Assessment Method	Empirical	N/A	N/A	None
SCOPE	Phenomeno-logical	N/A	N/A	Empirical Correlation
CLICHE	Phenomeno-logical	N/A	N/A	Empirical Correlation
EXSIM	3D CFD Finite Volume	Structured, Cartesian, PDR Treatment of Sub-Grid Scale Objects	First Order Temporal Second Order Spatial	Eddy Break-Up
FLACS	3D CFD Finite Volume	Structured, Cartesian, PDR Treatment of Sub-Grid Scale Objects	First Order Reaction Progress Variable Second Order	Empirical Correlation
AutoReaGas	3D CFD Finite Volume	Structured, Cartesian, PDR Treatment of Sub-Grid Scale Objects	First Order Temporal and Spatial	Empirical Correlation
CFX-4	2D and 3D CFD Finite Volume	Structured, Body-fitted	Higher Order Temporal and Spatial	Eddy Break-Up and Thin Flame

COBRA	2D and 3D CFD Finite Volume	Unstructured, Cartesian, Cylindrical Polar or Hexahedral, Adaptive, PDR Treatment of Sub-Grid Scale Objects	Second Order Temporal and Spatial	Empirical Correlation
Imperial College Research Code	2D CFD Finite Volume	Unstructured, Adaptive	Implict Temporal, Second order (TVD) Spatial	Laminar Flamelet and PDF Transport
NEWT	3D CFD Finite Volume	Unstructured, Adaptive	Higher Order Temporal and Second Order Spatial	Eddy Break-Up and Laminar Flamelet
REACFLOW	2D and 3D CFD Finite Volume	Unstructured, Adaptive	First or Second Order Temporal and Spatial	Eddy Break-Up

2. DESCRIPTION AND DISCUSSION OF CURRENT MODELS

2.1. Empirical Models

2.1.1. Introduction

Empirical models are based on correlations obtained from analysis of experimental data. The models described below constitute a selection of methods commonly used in industry for risk assessment, etc. It does not purport to be an exhaustive selection.

2.1.2. TNT Equivalency Method

The TNT equivalency method is based on the assumption that gas explosions in some way resemble those of high charge explosives, such as TNT. However, there are substantial differences between gas explosions and TNT. In the former the local pressure is much less than for TNT detonations. Furthermore, the pressure decay from a TNT detonation is much more rapid than the acoustic wave from a vapour cloud explosion. Nevertheless the model has been used extensively to predict peak pressures from gas explosions. The TNT equivalency model uses pressure-distance curves to yield the peak pressure. One must use a relationship, see below, to find the mass of TNT equivalent to the mass of hydrocarbon in the cloud.

$$W_{TNT} \approx 10\ \eta\ W_{HC}\ , \qquad \text{[kg]} \tag{1}$$

Where W_{TNT} is the mass of TNT, W_{HC} is the actual mass of hydrocarbons in the cloud, and η is a yield factor ($\eta \approx 0.03$-0.05) based on experience. The factor 10 represents the fact that most hydrocarbons have ten times higher heat of combustion than TNT. In the original TNT equivalency model no consideration was taken of the geometry and therefore it is recommended that this model should not be used, Bjerketvedt, Bakke and van Wingerden (1997).

A TNT equivalency model which does take geometry effects into account has been proposed, Harris and Wickens (1989). Results from experiments formed the basis for the new formulation. The yield factor was increased to 0.2 and the mass of hydrocarbon in stoichiometric proportions was to correspond to the mass of gas in the severely congested region of the plant. For natural gas the mass of TNT can be arrived at using

$$W_{TNT} = 0.16\ W_{eff}\ , \qquad \text{[kg]} \tag{2}$$

where $V_{eff} = \min(V_{con}, V_{cloud})$ is the total volume of the congested region and $_{Vcloud}$ is the total volume of the gas cloud. The equation will hold for most hydrocarbons. It is recommended that the TNT equivalency model should not be used.

Weaknesses:

- Non-unique yield factor is needed
- Weak gas explosions not well represented
- Information only of the positive phase duration

- Not suited for gas explosions, since the physical behaviour of gas explosions differs substantially from that of solid explosives

- Difficult to define a sensible charge centre

2.1.3. TNO Method

The TNO method, Wiekema (1980), resembles the multi-energy method described in Sect. 2.1.4 below. The main difference between the two methods is that the TNO method assumes that the whole vapour cloud contributes to the over-pressure, rather than just the portion which happens to be in a confined and/or congested area. The TNO model and TNT equivalency model were used in the Dutch CPR14E handbook of methods for calculation of physical effects of the escape of dangerous materials, CPR14E (1979). The multi-energy method has replaced the TNO model in the revised CPR14E handbook, Mercx and van den Berg (1997). The TNO method will not be discussed further, but see Sect. 2.1.4 for details and comments.

2.1.4. Multi-Energy Concept

The multi-energy concept, van den Berg (1985), can be used to estimate the blast from gas explosions with variable strength. The method assumes that only that part of the gas cloud which is confined or obstructed will contribute to the blast. The rationale being that unconfined vapour clouds give rise to only small over-pressures if ignited. The over-pressure increases with increasing confinement. In essence, the method is based on numerical simulations of a blast wave from a centrally ignited spherical cloud with constant velocity flames.

There are two parameters feeding into the model. Firstly, a combustion-energy scaled distance, R_{ce} , related to the distance to the explosion centre can be defined as

$$R_{ce} = R_0 / (E/P_0)^{1/3}, \quad [\text{m}] \tag{3}$$

where R_0 is the distance to the explosion centre, E is the total amount of combustion energy, e.g. the combustion energy per volume times V_{cloud}, where V_{cloud} is the volume of vapour cloud in the congested area, and P_0 is the atmospheric pressure. The total amount of energy for a stoichiometric hydrocarbon-air mixture does not vary significantly with the type of hydrocarbon. Thus for a hydrocarbon-air mixture, the total combustion energy an be estimated from

$$E \approx 3.5\ V_{cloud}, \quad [\text{MJ}] \tag{4}$$

Where V_{cloud} is measured in m^3. It is important to note that only the confined and/or congested areas contribute to the blast. Secondly, the strength of the explosion can be estimated by taking into account the layout of the explosion source. The charge strength is given a number between one and 10, where 10 represents a detonation.

The two parameters can then be used to read a non-dimensional maximum "side-on" over-pressure and a non-dimensional positive phase duration from diagrams, where the source strength is represented by a set of curves.

Strengths:

- Fast method
- Conservative approximation can be made

Weaknesses:

- Setting a sensible value for the charge strength is difficult.
- Setting a sensible value for the total combustion energy, e.g. charge size is difficult.
- Not ideally suited to weak explosions, i.e. partly confined clouds.
- Difficult to accurately represent complicated geometries
- Not clear how to deal with several congested regions
- Not clear how to deal with multiple blast waves

In light of the weaknesses listed above, the choice of charge size and strength must ideally be based on other simulations, experimental data or by making a conservative assumption. Van den Berg (1991) suggested that V_{cloud} should be chosen to encompass the total volume of gas, that is both the confined and the unconfined part. This will in many cases lead to an overestimation of the over-pressure caused by the blast.

2.1.5. Baker-Strehlow Method

The Baker-Strehlow method, Baker, Tang, Scheier and Silva (1994), was developed to provide estimations of blast pressures from vapour cloud explosions. The model was further extended by Baker, Doolittle, Fitzgerald and Tang (1998). The methodology consists of a number of steps, assessing flame speed, fuel reactivity, confinement, etc.

- Walk through plant identifying potential explosion sites
- Decide on the dimensionality of the confined areas to work out flame speed
- Calculate burning velocity for fuel mixtures

The blast pressure and impulse are the read from a series of graphs. The revisions proposed by Baker *et al.* (1998) were the results of experience gained from plant walk throughs and hazard assessments.

Strengths:

- Easy to use
- Fast
- Takes into account some geometrical details, with regards to confinement
- Can handle multi-ignition points

Weaknesses:

- Can be over conservative

2.1.6. Congestion Assessment Method

The Congestion Assessment Method (CAM) was developed at Shell Thornton Research Centre, Cates and Samuels (1991). The model has been enhanced and further extended by Puttock, (1995, 1999).

Cates and Samuels (1991) devised a decision tree procedure as guidance for estimating the source pressure, taking into account the layout of the plant, e.g. degree of confinement and congestion and the type of fuel involved. The accuracy of the estimations was variable, but the method was designed to yield conservative pressures.

The method comprises three steps:

1) An assessment of the congested region is carried out to assign a reference pressure, P_{ref}, which is an estimation of the maximum over-pressure generated by a deflagration of a vapour cloud of propane.

2) The type of fuel is taken into account through a fuel factor, which is then multiplied by the reference pressure worked out in step i) to determine the maximum source pressure.

3) It is now possible to estimate the pressure experienced at various distances from the ignition point. Cates and Samuels (1991) assumed a simple decay law inversely proportional to the distance. Puttock (1995) generated pressure decay curves by fitting polynomials to detailed computations, which in turn had been validated by experimental data.

Puttock (1999,2000b) further improved the model when the results from the MERGE (Modelling and Experimental Research into Gas Explosions) project, which involved small scale, medium scale and large scale experiments were published, Mercx (1993). Development of CAM 2, Puttock (1999,2000b) also addressed the problems of i) non-symmetric plants, ii) plants which are much longer in one spatial direction than the other two, iii) making allowance for partial fill, e.g. where the gas cloud size is smaller than the

congested volume, and iv) how to deal with sharp-edged rather than rounded objects. The congestion assessment method is the most advanced empirical model reviewed in the present report. However, it is not known how well the model would perform for a new scenario for which the model has not been calibrated.

The user must assess the level of congestion and the level of confinement in the plant. This is not a problem for simple geometries, but many plant installations are highly complex in nature. There are guidelines for how to assess the congestion and the confinement of the plant. Nevertheless, it is quite possible that two people could independently make sufficiently different assessments of the plant which could lead to potentially significantly different predicted explosion generated over-pressures.

Strengths:

- Easy to use
- Short run times
- Calibrated against a large number of experiments
- Approaches sensible maximum over-pressure as severity index goes to infinity
- Can deal with non-symmetrical congestion and long, narrow plant

Weaknesses:

- Allows only a relatively crude representation of the geometry
- No uniqueness in the specification of level of congestion and level of confinement

2.1.7. Sedgwick Loss Assessment Method

Thyer (1997) tested the vapour cloud explosion model developed by Sedgwick Energy Ltd. The Sedgwick model is based on Puttock's CAM model, see Section 2.1.6, with some refinements. Thyer (1997) noted that the degree of resemblance with the CAM method was not easy to assess, in part due to scarce amount of details in their promotional leaflets. The package allows the user to set up a simple computer representation of the plant, using a graphical interface.

2.2. Phenomenological Models

2.2.1. Introduction

Phenomenological models are simplified physical models, which seek to represent only the essential physics of explosions. The greatest simplification made is with respect to the modelled geometry. Generally, no attempt is made to model the actual scenario geometry, which is instead represented by an idealised system - e.g. a single vented chamber containing a number of turbulence generating grids. This is a reasonable approximation for certain types of geometry (an offshore module for example), but may not be adequate for more complex situations. The physics of the explosion process may be described either empirically or theoretically. Phenomenological models fall somewhere between empirical correlations and CFD models, in terms of complexity. CFD models may in fact share some of the embedded physics with phenomenological models, but of course are in principle better able to model complex, arbitrary geometries. The run times for phenomenological models are short, of the order of a few seconds. This type of model is well suited to running through large number of different scenarios and can be used to pick out particular situations which can then be investigated using a CFD code to obtain further details.

2.2.2. SCOPE

The SCOPE (**S**hell **C**ode for **O**ver-pressure **P**rediction in gas **E**xplosions) model is under continuing development at Shell's Thornton Research Centre. The SCOPE model was initially designed for modelling explosions in offshore modules. However, the model may be applied to any geometry where a single flame path may be identified. SCOPE 2 was released in March 1994. It is based on the original version of SCOPE described by Cates and Samuels (1991). The present incarnation of SCOPE is SCOPE 3 which went live in early 1997, Puttock, Yardley and Cresswell (2000). This section will describe the SCOPE 2 code and then highlight the revisions which have been incorporated in SCOPE 3. Appendix B contains the differential equations solved in SCOPE.

SCOPE 2

The SCOPE code seeks to model gas explosions by representing the essential physics in a simplified form. Models of this type are to be distinguished from empirical models that are nothing more than 'fits' to existing experimental data and are of limited applicability. The model is one-dimensional and is based on the idealised geometry of a vented vessel containing a series of obstacle grids. The flow through each of these grids determines the turbulence and hence the rate of turbulent combustion downstream from the grid.

The flows from the vents are modelled using standard compressible vent flow relations. Vent opening may also be modelled using SCOPE 2. The vent area is taken to be zero until the vent opening pressure is reached, at which point the vent area is increased linearly with time until the vent is fully open at a pre-set value of the vent opening time.

The external explosion, generated by combustion in the unburnt gas pushed from the box, may exert a large influence on the internal pressure felt by the box. The vented gas forms a mushroom-shaped jet and the highest external pressure is generated when the flame burns in

the vortex at the mushroom head. The last of the gas to be vented from the box forms the stem of the mushroom. Therefore, the gas vented in the last stages of the explosion event contributes little to the external over-pressure. The external over-pressure calculated by the model is related to the vent flow (which in turn is related to the box internal pressure) when the flame has traversed 70 % of the box length. The ratio of the external pressure to the internal pressure also depends on the vent area, this ratio is taken as

$$\frac{P_{ext}}{P_{0.7}} = 3.75 \left(\frac{A_v}{V^{2/3}} \right)^{0.85}, \qquad (5)$$

where V is the box volume, P_{ext} is the external explosion over-pressure, and $P_{0.7}$ is the maximum internal pressure for $X/L \leqslant 0.7$. Finally, the maximum internal pressure is determined by

$$P_{max} = P_{emerg} + 0.7\, P_{ext}, \qquad (6)$$

where P_{emerg} is the internal pressure at the time that the flame emerges from the box.

SCOPE 2 has received extensive experimental calibration by comparison with experiments in idealised geometries similar to that modelled by SCOPE 2. The experiments have been conducted at various scales and include a 2.5 m^3 box, a 35 m^3 box, and the 550 m^3 SOLVEX experiments, Puttock *et al.* (1996).

SCOPE 3

One of the most significant changes from SCOPE 2 is the ability to handle mixed scale objects. Generally objects will be of mixed scale and in characterising these objects in terms of a blockage ratio and a shape (round or sharp edged) information has been lost. The main effect of obstacles of various sizes is on the flame surface area which increases as it passes between the objects; the flame area affects the consumption rate of the unburnt gas (cf. eqn. B1). This is referred to as 'obstacle complexity' in SCOPE. SCOPE 3 will allow rear venting, in addition to the side and main vents allowed by SCOPE 2. Venting behind the ignition point can have a large effect on the development of the explosion over-pressure. Rear venting allows some of the initial combustion generated expansion flow to leave the box, decreasing the flow of unburnt gas through the obstacles. This reduces the turbulence level in the unburnt gas, which reduces the turbulent burning velocity and hence the over-pressure. Improvements have also been made to the basic combustion model which now has a better treatment for variations in stoichiometry as well as allowing mixtures of fuel gases. A pressure dependency has been implemented for the expansion ratio and the laminar burning velocity. SCOPE 3 has been validated against more than 300 experiments, Puttock *et al.* (2000). Further developments of SCOPE 3 involves modelling of un-confined but congested plant, with central ignition, and modelling the effect of water deluge on explosion development, Puttock *et al.* (2000).

Strengths:

- Can handle venting and external explosions
- Imposed limits to flame self-acceleration yield sensible flame speeds
- Validated against a large number of small-, medium- to large-scale experiments involving different gases and various degrees of congestion
- Contains less geometrical detail than CFD models
- A fast tool for evaluating different scenarios during plant design phase

Weaknesses:

- Does not provide the same wealth of information about the flow field as do CFD models
- Contains less geometrical detail than CFD models
- Can deal with single enclosures only

2.2.3. CLICHE

The CLICHE (**C**onfined **LI**nked **CH**amber **E**xplosion) code has been developed by Advantica Technologies Ltd. The status of its present development is unknown. CLICHE was developed to study confined explosions in buildings but its use has been extended to modelling explosions in off- and on-shore plant. The basis of CLICHE is well established in applications to vented vessels explosions, Fairweather and Vasey (1982) and Chippett (1984), however, the CLICHE code represents a generalisation of this concept to a sequence of interlinked explosion chambers. Typically process plant consist of semi-confined areas congested with pipework and process vessels. The expansion induced flow in an explosion will be subject to a large pressure gradient caused by the drag from these obstacles. Regions are represented in the CLICHE code by a series of linked chambers, the pressure gradients are modelled by applying appropriate resistance terms at the inter-chamber vents. The necessary parameters to model the drag and flame / obstacle interaction are determined from a numerical database containing a detailed description of the plant geometry. A combustion sub-model based on the local flow properties is used to determine both laminar and turbulent burning velocities. Any external burning, caused by vented gases, is treated by a separate external combustion model.

The explosion model formulation used in CLICHE was developed by applying the conservation laws to the unburnt and burnt gas volumes in each chamber, assuming that the properties within each chamber are uniform and that any momentum changes occur only at the perimeter of these volumes. This latter assumption does not allow the prediction of the flow distribution within the volume, and hence the flame distortion. Consequently a flame shape is empirically prescribed, based on the geometry and the volume of burnt gas. The equation set describing the series of chambers forms a system of coupled ordinary differential

equations which are solved numerically. Equilibrium properties are assumed for the burnt gas and these properties are calculated during the CLICHE simulation, taking into account the pressure and temperature dependence. CLICHE uses a numerically generated flame area, which enables the model to simulate ignition from any position, with the initial flame assuming a spherical shape. Flame distortion effects are treated by empirical correlations. When the flame interacts with obstacles it develops 'folds' or 'fingers', which grow as the flame passes the obstacles and within which the burning rates are locally higher due to the turbulence generated in the obstacle wakes. CLICHE calculates the rate of growth of flame folds from the mean velocity of unburnt gas past the obstacles.

The burning velocity is assigned the value of the maximum of the laminar and turbulent burning velocities, calculated from the known flame radius, root mean square turbulence velocity and turbulence integral length scale. Ignition in an initially quiescent medium results in laminar flame propagation, until the flame intersects an obstacle at which point the flame downstream of the obstacle becomes turbulent. Turbulence parameters are based upon the mean flow velocities and the characteristics of the wake turbulence shed by the obstacles. The model also allows an initial non-zero turbulence field to be present.

The laminar burning velocity is based upon empirical correlations of the flame speed as a function of flame radius. The turbulent burning velocity is based upon a Kolmogorov, Petrovsky and Piskounov analysis of the combustion model of Bray (1987) which has been calibrated against measurements made by Abdel-Gayed, Bradley and Lawes (1987). The model is based upon the assumption that the turbulent flame is an ensemble of laminar flamelets and takes account of the quenching of the flamelets by the turbulence strain field.

Combustion in the semi-confined region causes unburnt gas ahead of the flame to be expelled through perimeter vents. When the flame propagates through a vent an external explosion is triggered, which as well as providing an external source of pressure generation may increase the pressure inside the semi-confined region by impeding the escape of further gas. The external explosion and the propagation of the pressure wave towards the vent are described by an acoustic model, Strehlow, Luckritz, Adamczyk and Shimpi (1979) and Catlin (1985) for peak over-pressures below 300 mbar. This assumes a spherical flame and an empirically derived peak over-pressure and flame speed.

Strengths:

- Allows ignition location anywhere within a cuboidal volume
- Simple combustion model, based on a mixture of some fundamental physics and empirical correlations
- Flame distortion effects due to vents, etc., are included
- Can handle external explosions
- Can generate its own input parameters from an obstacle database
- Short run times

Weaknesses:

- Simplified representation of the geometry, through a series of inter-linked chambers
- Does not provide the same wealth of information about the flow field as do CFD models

2.3. CFD Models

2.3.1. Introduction

Computational Fluid Dynamics (CFD) models find numerical solutions to the partial differential equations governing the explosion process. Appendix A describes the Navier-Stokes equations, which govern the fluid flow, and the sub-models used to represent the terms which are not modelled exactly. The numerical solutions are generated by discretizing the solution domain (in both space and time). The conservation equations are applied to each of the sub-domains formed by the discretization process, generating a number of coupled algebraic equations that are normally solved by an iterative procedure.

Solutions obtained with CFD codes contain a great wealth of information about the flow field, i.e. velocities, pressure, density, species concentrations, etc. Surface pressure data can be used for structural analysis. CFD is widely applicable and can be used in many different disciplines - from designing aeroplanes, cars or artificial heart valves, to weather forecasting and environmental modelling. CFD simulations can offer insight into the flow behaviour in situations where it is impractical or impossible to carry out experiments. In principle, it is possible to try out many different scenarios, with little extra effort. CFD and experiments should be viewed as complementary means of investigating flow situations. It is vitally important that the sub-models used are properly validated against well-controlled, well-defined and repeatable experiments. If the models have not been validated, confidence in the results obtained from calculations with CFD codes must be low, and the results used with prudence, if at all. The importance of solving the right problem, i.e. using the correct geometry, correct initial and boundary conditions, can not be over emphasised. CFD codes are immensely powerful and useful tools, if applied correctly.

The main drawbacks associated with the use of CFD are caused by the limitations imposed by the available computing hardware, for example it is currently impractical (if not impossible) to simulate exactly a turbulent combusting flow. Hence, sub-models of combustion and turbulent transport have been developed that simplify the calculation process. Small-scale (relative to the explosion domain) objects may cause significant over-pressure generation in a gas explosion, due to the turbulence generated. Explicit representation of small-scale features is demanding in terms of computer memory and computing speed, hence an alternative method of modelling turbulence generation caused by small-scale objects has been developed, the so-called Porosity/Distributed Resistance, or PDR, method. The CFD models presented in this section rely heavily on sub-models for the representation of small-scale objects, coupled with relatively simple numerical schemes for the solution of the governing flow equations.

The rate of progress in model development in the field has been relatively slow. Turbulence remains a highly active topic of research. The mathematical understanding of the subject is improving, but there are still a number of issues which have not been fully resolved, i.e. transition from laminar to turbulent flow. Furthermore, the process of incorporating the new findings into the existing turbulence models has been slow. This is to some extent due to the fact that most of these models are relatively crude approximations of reality and can therefore not easily accommodate the mechanisms involved. The first papers discussing second moment closure modelling appeared in the early 1970's. In principle, second moment closures should be more general that the simpler turbulence models, Models of that

complexity should able to better represent many different types of flows. But thirty years on, Reynolds stress transport models are still not applied routinely. The implementations of Reynolds stress models in the currently available commercial CFD codes lack one of the most important properties to industry, namely robustness.

In fairness, some of the outstanding issues are to do with numerical aspects, i.e. discretisation of the transport equations, etc., rather than to do with the numerical modelling. It seems unlikely that fully simulating a turbulent combusting flow in a real plant - with all its associated time and length scales, and involving a great number of obstacles and other configurational complexities, will be possible for several decades, judging by the current rate of progress. However the rapid development of faster processors with more random access memory, and parallel processing - but which might require rewriting of parts of the CFD codes to take full advantage of massively parallel architecture, may go some way to alleviate matters.

2.3.2. EXSIM

The EXSIM code is under continuing development at the Telemark Technological R&D Centre (Tel-Tek) in Norway and Shell Global Solutions in United Kingdom. The current version of the EXSIM code is version 3.3. EXSIM is a structured Cartesian grid, semi-implicit, finite volume code that relies on the Porosity / Distributed Resistance method for the representation of small-scale objects. The main effect of these obstacles is to obstruct the flow and generate additional turbulence. Using the PDR approach, small scale objects are represented by a volume porosity, an area porosity, and a drag coefficient. The drag generated by the obstacles feeds into the k-ε turbulence model, via a modified generation rate of turbulence term, and subsequently into the Navier-Stokes equations. Sect. C1 of Appendix C describes how the PDR method is implemented in the code and gives details on the implemented combustion model. EXSIM, version 3.3, is using AUTOCAD 14 as pre-processor with an additional LISP program called EXCAD.

The scalar variables are stored at positions within the control volumes, whereas the velocity components and the area porosities are stored at the control volume boundaries. First or second order accurate upwind differencing schemes may be used to generate the numerical approximations to the governing equations. The second order upwind scheme is bounded by the van Leer limiter. Time integration is performed using the implicit Euler scheme, which is first order accurate. The resulting system of non-linear algebraic equations is solved by applying the tri-diagonal matrix algorithm in the three co-ordinate directions. A version of the SIMPLE, (Patankar and Spalding (1972), algorithm, modified for compressible flows, Hjertager (1982), is used to solve the pressure/velocity/density coupling of the momentum equations and the mass balance. The method introduces a pressure correction, which makes the necessary corrections to the velocity components, pressure and density to ensure that mass is conserved at the new time step.

The pre-processor in older versions, pre 3.3, of EXSIM only allowed geometry specification with standard obstacles. A box shaped domain is specified, the subsequent geometry being built up by the addition of variations of eight basic objects. These objects are:

1) Large box, resolved by the grid.

2) Cylinder aligned with one of the co-ordinate directions.

3) Pipe bundle in the form of a box.

4) General porous box.

5) Louvered wall

6) Box beam or box that is not resolved by the grid.

7) Sharp edged beam.

8) Grating.

The pre-processor in version 3.3 of EXSIM makes it possible to convert data from a number of different CAD formats, extracted from CAD databases, to EXSIM format which allows for a quicker setting up of the geometry, Chynoweth (2000).

Version 3.3 of Exsim, Chynoweth and Ungut (2000) has been extensively validated against the experimental data from Phase 2 of the Flast and Fire Engineering for Topside Structures, experiments carried out by DNV, Shell Solvex full and 1/6-th scale tests, tests carried out by CMR on their M24 and M25 modules, further tests carried out by Shell at their Buxton site, etc. The code can also be applied to congested configurations with varying degrees of confinement, including a completely unconfined geometry.

Current developments include implementation of an adaptive mesh algorithm to improve the resolution of areas of interest, i.e. flame fronts, and inclusion of a gas dispersion model so that the shape of a vapour cloud and the gas concentration, i.e. from a pipe rupture, can be estimated.

Strengths:

- Allows the user to specify (arbitrary?) spatial resolution of obstacles
- Has been compared against small-scale, medium-scale and large-scale experiments
- Can be applied to congested but unconfined geometries
- Can be applied to external explosions
- Can read in CAD data

Weaknesses:

- Using standard k-ε model
- Does not have a local grid refinement / de-refinement facility yet

2.3.3. FLACS

The FLACS (**FL**ame **AC**celeration **S**imulator) code has been developed at the Christian Michelsen Research Institute in Norway, now CMR-GEXCON. FLACS is a finite volume code based on a structured Cartesian grid. The Porosity / Distributed Resistance approach is used to model sub-grid scale obstacles. Transport of scalars and momentum through turbulent processes is modelled using the k-ε turbulence model. The discretisation of the governing equations follows a weighted upwind / central differencing scheme, which is first order accurate. However, for the reaction progress variable the second order accurate van Leer scheme is used - van Leer (1974) - to prevent artificial flame thickening, caused by numerical diffusion.

The combustion model originally employed in FLACS was a version of the eddy break-up model. This has recently been replaced by a model, called β flame model, based on correlations of turbulent burning velocities with turbulence parameters - Arntzen (1995,1998). The β flame model assumes that the flame propagates at a constant burning velocity and has a specified constant flame thickness, e.g. three grid cells, Arntzen (1998). Furthermore, the flame model uses correction functions to account for flame thickness, due to numerical diffusion, flame curvature and burning towards walls, Arntzen (1998). The reaction rate and the turbulent viscosity are set in the transport equation for the reaction progress variable so as to ensure that the burning velocity matches that given by a correlation - this is similar to the method employed in COBRA.

An advanced user interface to FLACS has been developed. This consists of Computer Aided Scenario Design (CASD) and Flowvis. CASD is used to generate the scenario definition for FLACS and Flowvis presents the results from the FLACS simulations. The scenario is defined by simplifying the geometry - for example pipes are represented by long cylinders, beams which are not vertical or horizontal are represented by horizontal or vertical beams with a blockage similar to the original beams. In general all objects with a dimension greater than 0.03 m are included, although areas which contain a high density of smaller obstacles will have to be represented as well. Obstacles which are not resolved by this grid are represented as an area blockage and a volume blockage. Walls and decks may be modelled in four different ways: solid unyielding surface, porous surface, blow out / explosion relief panel, or open.

Earlier versions of FLACS - up to 1993, required that the geometry be meshed with a grid of cells of 1 m^3 volume (1 m sides), as the code was calibrated for cells of this size. This is contrary to generally accepted CFD practice, in which it should - at least in principle, be possible to perform a grid dependency study to ensure that the solution does not contain gross numerical errors due to grid coarseness. In FLACS-93 and later versions the grid resolution is based on a certain number of cells across the gas cloud. This means that the cells can be smaller than 1 m cube, see Appendix E. However for a 'typical' offshore module a cell size of 1 m would still be used, with 2 m x 2 m x 2 m cells employed for large offshore modules and onshore plants, see Appendix E.

FLACS does not have adaptive meshing capabilities. However, the user can, a priori, refine the grid in the region where it is deemed to be needed, i.e. the grid cells could be of the order of 2 to 5 cm near a jet leak, Hansen (2001) - Appendix E. FLACS does not have multi-grid

capability per se. However, for blast waves in the far field FLACS has a multi-block concept, allowing turbulence and combustion equations to be solved in the explosion block and the Euler equations in the blocks where the flow is essentially inviscid, Hansen (2001) - Appendix E.

CMR state that FLACS has been validated against a wide range of experiments. Unfortunately many of these results are confidential. However, comparisons of FLACS predictions with measurements were undertaken and published as part of the MERGE, Mercx (1993), EMERGE and BFETS, Selby and Burgan (1998), projects.

CMR state that they are content if the accuracy with which the code predicts explosion over-pressures is of the order of ± 30 %, see Section E3 of Appendix E. They also note that in some cases the discrepancy can be a factor of two. Hansen (2001), in Section E3 of Appendix E, states that, since average over-pressure measurements can vary by a factor of two between tests which are essentially identical, it is difficult to see how accuracies can be substantially improved. The need for accurate measurements and high repeatability has been discussed elsewhere, see Section 3.6, in the present report.

There have apparently been further developments in the FLACS code, van Wingerden (2001), i.e. to the laminar and turbulent combustion modelling, to the modelling of turbulence generation at walls and implementation of a subgrid model describing turbulence length scale as a function of obstacle size. Unfortunately, these developments are not published in the open literature - being kept confidential to clients and sponsors. It is therefore not possible to comment on the impact of these developments.

Strengths:

- Have been compared against a range of small-scale, medium-scale and large-scale experiments
- Uses second order accurate discretisation scheme, a van Leer Upwind scheme, but for the reaction progress variable only
- Can be applied to congested, but unconfined geometries
- Can be applied to external explosions
- Can read in CAD data
- Incorporates a water deluge model

Weaknesses

- Uses k-ε model, but with modifications to deal with near-wall flows, etc.
- Uses a first-order accurate, weighted upwind/central differencing scheme for all variables except for the reaction progress variable

- Versions of the code up to 1993 were calibrated for 1 m cube grid cell size - thus not allowing grid dependency to be examined.

- Recent developments not in the open literature, hence not possible to comment on present theoretical basis.

2.3.4. AutoReaGas

AutoReaGas is the result of a joint venture, between Century Dynamics Ltd. and TNO, that began in 1993. The code integrates features of the REAGAS and BLAST codes developed by TNO and have been incorporated into an interactive environment based on the AUTODYN-3D code developed by Century Dynamics Ltd. REAGAS is a gas explosion simulator whereas BLAST simulates the propagation of blast waves. The REAGAS and BLAST software were implemented in AutoReaGas as the gas explosion solver and blast solver, respectively. AutoReaGas can be used on most computer platforms running under either UNIX, Windows 95 or later versions or Windows NT operating systems.

The gas explosion solver is a three dimensional finite volume CFD code based on a structured, Cartesian grid. Discretization is achieved by use of the first order accurate Power Law scheme, with the SIMPLE algorithm implemented for pressure correction. Turbulent transport is modelled by use of the standard two equation k-ε model. Large objects may be resolved by the grid, but sub-grid scale obstacles are modelled as a source of turbulence and drag (a Porosity / Distributed Resistance approach). The code also allows blow-out panels to be included in a simulation. The combustion model assumes that the combustion reaction takes place as a single step process. Transport equations are solved for the fuel mass fraction and the mixture fraction, which is a conserved quantity (i.e. a quantity that is unaffected by chemical reactions). The addition of the mixture fraction transport equation allows the modelling of explosions in non-uniform gas mixtures. The reaction rate is determined from an empirical correlation for flame speed (Bray (1990) and see also section 2.2.3), where the transition from laminar to turbulent combustion is based upon the local flow conditions.

The blast solver solves the three dimensional Euler equations for blast wave propagation using the Flux Corrected Transport technique. An automatic 'remapping' facility is available to take the output from a gas explosion simulation into a larger domain for a study of the far-field blast effects.

Scenario geometry may be supplied to the code by defining a combination of object primitives, such as boxes, cylinders and planes (cf. EXSIM, section 2.3.2), or alternatively may be imported from a CAD package.

Present development work is concerned with improving important aspects of the solver; in particular a higher order numerical discretization scheme will be implemented in the near future. A new improved combustion model will also be implemented. In addition, a wall friction model will be incorporated for modelling gas explosions in geometries with no sub-grid scale obstacles. In the longer term a number of developments are planned; these include:

- A dynamic structural response capability coupled with the explosion and blast processor

- Gas dispersion modelling

- Multi-block mesh, which allows a more efficient grid structure to be used

The latest release, version 3.0, contain a number of new features: the pre- and post-processing has been improved and a new flow solution and geometry visualizer has been implemented. The objects database uses dynamic memory allocation, e.g. there is no restriction on the number of objects. Furthermore, object modelling has been enhanced, i.e. non-orthogonal objects can now be used. Pressure surfaces (when specifying blow out panels), cold front quenching and a water deluge model have been implemented.

Considerable effort has gone and continues to go into model validation against the medium-scale and large-scale experiments carried out within the MERGE/EMERGE projects and the Joint Industry Project Blast and Fire Engineering for Topside Structures (phases 2 and 3), respectively.

Significantly, a validation manual is supplied with the latest release of AutoReaGas, version 3.0.

Strengths:

- Has been compared against small-scale, medium-scale and large-scale experiments

- Incorporates a water deluge model

- Can read in CAD data

- Can accept a large number of objects through dynamic memory allocation of the objects database

Weaknesses:

- Currently uses a first-order accurate discretization scheme for all variables

- Uses standard k-ε turbulence model

2.4. Advanced CFD Models

2.4.1. Introduction

The CFD models presented in this section attempt a more complete description of the explosion process. The differences between these models and those presented in the previous section mainly lie with the representation of the geometry and the accuracy of the numerical schemes used. The CFD codes presented in this section (with the exception of the COBRA code) allow an exact geometric representation of the explosion scenario, limited by the available computer memory. The memory limitations can limit the applicability of the code to less complex configurations or might force the user to omit objects to stay within the available memory. All of the codes detailed in this section use numerical schemes of increased accuracy, when compared with the CFD codes described in the previous section.

2.4.2. CFX-4

CFX-4 is a general purpose, commercially available CFD code, under development at AEA Technology Engineering Software at Harwell. An explosion module has been developed for this code by the code vendors, funded by the HSE. This module was initially available to the HSE, but has now been released commercially in release 3, December 1999. CFX-4 is a finite-volume, structured grid code. To facilitate the modelling of complex geometries the code allows multi-block, non-orthogonal grids. A variety of equation solvers may be used along with a wide selection of first order and bounded second order accurate differencing schemes. As well as the commonly used k-ε turbulence model, the code also includes a full Reynolds stress turbulence model, which has not been tested for explosion modelling. Further information on the basic code may be obtained from the solver manual. A CFD code using unstructured grids, called CFX-5, is also under development at AEA Technology Engineering Software. However, at present CFX-5 does not contain the physical models necessary to model an explosion.

Before release 3, the standard CFX-4 software included many options for spatial differencing, but only two for temporal differencing. These are the first order accurate implicit Euler and the second order Crank-Nicolson schemes. The Crank-Nicolson scheme is not bounded for positive definite variables and therefore very small time steps must be used when a turbulence model is included (turbulence kinetic energy and its dissipation rate are strictly positive quantities). Therefore, a new higher order backward differencing scheme has been included in release 3, that guarantees positivity. The temporal differencing scheme is also adaptive, failure to meet the convergence criteria at a particular time step results in the time step being reduced for another attempt at convergence. Successful convergence at five successive time steps results in the time step being increased.

Mesh generation for CFX-4 may be accomplished by using either of two codes written for this purpose, CFX-MESHBUILD and CFX-BUILD. To allow further flexibility the CFX-BUILD code allows the user to import geometry files from a wide range of CAD packages.

The code has been used for prediction of explosion over-pressure in a series of small-scale baffled and vented enclosures - Pritchard, Freeman and Guilbert (1996). The agreement reported by Pritchard *et al.* (1996), between the CFD predictions and the experimentally

determined over-pressures for these enclosures, is very good. Pritchard, Lewis, Hedley and Lea (1999) stressed that great care must be taken when applying models to other gases than the one for which the model has been "tuned", or calibrated. Pritchard *et al.* (1999) found that the agreement between calculations and experiments was poor when changing gas from methane, the gas for which the model was calibrated, to propane. A recent paper, Rehm and Jahn (2000), presented good agreement between over-pressures calculated by CFX-4 and measured over-pressures in hydrogen explosion experiments.

Pritchard *et al.* (1999) contains a detailed discussion on the deficiencies with the ignition model and the thin flame model implemented in CFX-4. The ignition model gives physically implausible results. One would expect the gas velocity ahead of the approaching flame to increase with time until the flame reaches the observer. The ignition model implemented in CFX-4 predicts that the gas velocity reaches a peak and then decreases before flame arrival. Moreover the flame is not fully developed by the end of the ignition period. Thus the model does not provide a suitable precursor to the thin flame model. There is also an exponential growth in numerical error in all conservation equations due to the steep gradient in volume expansion at the boundary of the ignition region. The thin flame model will give rise to unwanted oscillations which are caused by the abrupt initiation of reaction in each new cell entering the reaction zone. Furthermore, the steep gradient in volume expansion between neighbouring reacting and non-reacting cells at the cold front is a source of exponential growth in numerical error.

Strengths:

- Offers multi-block capability for greater control over the meshing
- Wide selection of discretization schemes
- A number of turbulence models, including Reynolds stress transport models, are implemented
- Can read in CAD data
- Has an integrated geometry building front-end
- Performs adequately for CH_4 and H_2 deflagrations

Weaknesses:

- Yields poor agreement with experiments for gases other than methane and hydrogen, to which the model appears to have been tuned.
- Uses a thin flame model which is not well suited to explosion modelling
- Uses an ignition model with deficiencies
- The explosion model and ignition model are not thoroughly validated

2.4.3. COBRA

The COBRA CFD code has been developed by Mantis Numerics Ltd. in conjunction with Advantica Technologies Ltd. It appears that there has been no development of the code since 1997, although its Advantica Technologies Ltd application continues.

COBRA uses an explicit or implicit, second order accurate (spatial and temporal), finite-volume integration scheme coupled to an adaptive grid algorithm. The grid is effectively unstructured and may be refined and de-refined automatically locally within the flow, in principle allowing features such as flame fronts and shear layers to be resolved accurately. The grid is updated after each time-marching cycle, ensuring that a fine grid resolution follows moving flow features, Catlin, Fairweather and Ibrahim (1995). Despite this adaptive grid capability COBRA employs the PDR approach for modelling sub-grid scale obstacles - see the discussion of EXSIM (section 2.3.2) for a description of this approach. The PDR approach has its deficiencies, but if there is a need for practical simulations for real complex geometries, then PDR is, in many cases, the only viable approach. The turbulent reaction rate is prescribed using burning velocity correlations.

In addition to the conventional ensemble averaged, density-weighted equations for continuity and momentum, COBRA also solves transport equations for a reaction progress variable and the total mixture energy. Closure of this equation set in the turbulent flow is achieved through use of the k-ε turbulence model, which is modified to include compressibility effects, Jones (1980), or a Reynolds stress transport model.

COBRA is a finite volume code, with the cell average values of the dependent variables stored in the computational cells. To second order, these cell averages correspond to values at the centroids of computational cells. Diffusion and source terms are approximated using central differencing and the convective and pressure fluxes are obtained using a second order accurate variant of Godunov's method - Godunov (1959) - derived from a conventional first order Godunov scheme by introducing gradients within the computational cells. The mesh employed within COBRA is Cartesian, cylindrical polar or curvilinear and may be refined, where necessary, by successively overlaying layers of refined mesh. Each layer is generated from the previous layer by doubling the number of cells in each co-ordinate direction. The mesh can also be de-refined, but only to its original fineness.

Mantis Numerics has supplied a simple visualisation program called MUVI, which is command line driven. It is possible to dump out data from the solution by means of adding a lines of code to a user subroutine.

Results with the COBRA code has been compared to experimental data from Phase II of the BFETS project, Popat et al. (1996), to experiments carried out by Advantica in 1 m long tubes of 1m length, and to experiments carried out by CMR in a 10 m long tube, Catlin, Fairweather and Ibrahim (1995), Fairweather, Ibrahim, Jaggers and Walker (1996), and Fairweather, Hargrave, Ibrahim and Walker (1999). Catlin, Fairweather and Ibrahim (1995) showed good agreement, to within 50 %, between the calculations and the experiments for the over-pressure at two different locations in the explosion tube; however, at two other locations the calculated maximum over-pressure was twice the measured over-pressure. The calculations underpredicted time of arrival of the pressure wave, at the four pressure transducers, by about

20 ms, equivalent to an error of the order of 20 %. Moreover, the pressure decay was much more rapid in the experiments than in the COBRA calculations.

Strengths:

- Second order accurate spatial and temporal discretization
- Cartesian mesh, which makes meshing particularly easy, but can also handle cylindrical polar or arbitrary hexahedral meshes
- Advanced grid refinement/de-refinement facility enabling flame front tracking and shock wave capturing.
- Can read in CAD generated geometries

Weaknesses:

- Uses the standard k-ε model, but offers Wolfshtein's two-layer k-ε turbulence model, which uses an algebraic expression for the energy dissipation rate, ε, in the near-wall region and the standard k-ε model elsewhere
- Setting up complex geometries can be time-consuming and difficult
- Does not have a model for transition from laminar to turbulent flow, which might affect the initial growth of the flame
- Visualisation of flow fields with the MUVI program is slow and laborious, being command line driven, compared to commercially available visualisation tools, i.e. EnSight and Fieldview

The underlying numerical methods available within COBRA have recently been updated to improve computer run times, particularly for complex three-dimensional geometries, by Mantis Numerics Ltd. This new code, called PICA, is currently being developed as an explosion model by Mantis Numerics Ltd. and the University of Leeds independently of Advantica Technologies Ltd.

2.4.4. NEWT

NEWT is an unstructured adaptive mesh, three dimensional, finite volume (tetrahedral volumes), computational fluid dynamics code. The unstructured mesh makes it amenable to the modelling of very complex geometries. NEWT was originally developed for non-combusting, turbomachinery applications but is now being adapted for explosion prediction at the Engineering Department of Cambridge University, the work being part-funded by the Offshore Safety Division of the Health & Safety Executive.

Due to its adaptive grid capabilities, the NEWT code should allow explosion prediction in very congested environments containing, of the order, one hundred obstacles. Current objectives of the work on NEWT are to refine the code and also to use the model to help

refine current PDR methods. The first phase of the OSD, HSE sponsored work has concentrated on implementing into NEWT models developed for the CFX-4 code by AEA Technology Engineering Software, Harwell in collaboration with the Health & Safety Laboratory, Buxton.

A second-order accurate discretisation scheme is used for the convective fluxes. Artificial dissipation - a combination of second-order and fourth-order derivatives - is added to control shock capture and solution decoupling. The fourth-order smoothing takes place throughout the domain, while the second-order smoothing is only used in regions of large pressure gradients. A fourth-stage Runge-Kutta time integration approach is used for the time dependent calculations. Maximum local time steps can be used in order to enhance convergence, when a steady state solution is sought.

The NEWT code uses a modified Lam and Bremhorst variant of the k-ε turbulence model where the near wall damping function is dependent on the turbulence Reynolds number and not the wall normal distance, Watterson, Connell, Savill and Dawes (1998).

The combustion is modelled using the eddy break-up model or a laminar flamelet model, Bray *et al.* (1985). The eddy break-up model can give rise to spurious ignition ahead of the flame. This is countered by suppressing the flame leading edge at each time step, Watterson *et al.* (1998). Ignition of the gas mixture is achieved through a ramping of the reaction progress variable, from zero to unity, in the specified ignition region during the specified ignition period. The laminar flamelet model does not requires fixes, like the leading edge suppression described above, and yields better agreement between the predicted and experimentally observed flame shapes for baffled channel test cases, Birkby, Cant and Savill (1997), while incurring slightly higher computational overheads than the EBU model.

Special treatment was needed for low Mach number flows ($Ma \leqslant 0.3$), due to convergence problems with density based flow solvers. This was a particular problem for the laminar flame propagation phase, Watterson *et al.* (1998).

Also currently in progress at Cambridge University is a research project that will lead to the development of a CAD interface to NEWT. This interface will automatically mesh the CAD generated geometry, allowing the modelling of more complex scenarios. The first implementation of the adaptive grid only allowed a single level of refinement (and de-refinement), whereby one parent cell may split into up to eight child cells. However, to increase the accuracy of the code, and to reduce the memory requirements, a multi-level refinement algorithm has been implemented, Watterson *et al.* (1998).

Watterson *et al.* (1998) presented calculations where they claimed to achieved qualitative agreement in terms of flame brush propagation and flame brush shape with small-scale experiments in the HSE baffled channel, Freeman (1994), and with large-scale experiments in Shell SOLVEX box, Puttock, Cresswell, Marks, Samules and Prothero (1996). However, the calculated maximum over-pressure was overpredicted by between 2 and 15 times. The maximum flames speed was also overpredicted, by about 50 % or more, while time to maximum overpressure in the SOLVEX test case was substantially underpredicted by NEWT. These discrepancies can perhaps be explained by a number of factors: an inaccurate ignition

model, inaccurate modelling of the initial development of the laminar flame and a crude approximation of the transition from laminar to turbulent flow.

Strengths:

- Incorporates an adaptive mesh algorithm
- Uses unstructured meshes which reduces the amount of effort required to generate a mesh, even for complex geometries
- Any 3D tetrahedral mesh generator can be used, provided that the output from the generator is converted to the format expected by NEWT

Weaknesses:

- Uses the standard k-ε model, but with a better near-wall damping
- Uses a crude ignition model
- Uses a crude transition model

2.4.5. REACFLOW

REACFLOW is a CFD code developed over the last nine years at the Joint Research Centre of the European Union in Ispra, Italy. The code is designed to simulate gas flows with chemical reactions. REACFLOW is a finite-volume, unstructured mesh code, which may be used to model two or three dimensional geometries. An advantage of the unstructured mesh approach is that the code is more easily able to handle geometries of arbitrary complexity. The code is still under development. Hence, the following code description contains features that are still in the process of being implemented. The present status of the code is given at the end of this description.

REACFLOW initially divides the flow domain into elements which are triangular in 2-D and tetrahedral in 3-D. The control volumes are defined by the medians of these elements. Within each control volume only the averages of the flow variables are known. These averages may be interpreted as constants or as linearly varying functions through the control volume. The first interpretation results in a discretization method that is first order accurate in space, whereas the second interpretation yields a method that is second order accurate. Given the variation through the control volumes the fluxes across the control volume boundaries are calculated as an approximation to a Riemann problem on each interface. REACFLOW incorporates two methods, Roe's approximate Riemann solver, Roe (1981), and van Leer's flux vector splitting, van Leer (1982). The discretization of the transient term is performed by a simple finite difference formulation, which may be either explicit or implicit.

To be better able to calculate slow-flow phenomena, REACFLOW contains a module for simulating incompressible, variable density flows. The incompressible flow solver takes as its control volumes the basic elements (triangles in 2-D). The fluxes are calculated at the boundaries of each triangular element. The flux calculation is done in a fully upwind manner,

which means that the flux calculation is not necessarily conservative. The incompressible solver exists in versions that are first order accurate in space (variables assumed to be constant within the elements) or second order (variables assumed to vary linearly through each element). Time discretization may be first order (Euler) or second order (Lax-Wendroff correction).

Presently, only two types of source terms are present in REACFLOW. These are body forces due to gravity and chemical reaction source terms. REACFLOW employs two methods for the calculation of the chemical source terms, the first is based on finite rate chemistry and the other is based on the eddy dissipation concept (eddy break-up model). The use of finite rate chemistry is more applicable when the influence of the turbulence on the chemical reactions is negligible, such as in the case of a laminar flame. For flames that are turbulent, a different approach is necessary. The eddy dissipation concept may be used to model this turbulent combustion rate. The eddy dissipation concept, leading to the eddy break-up model of turbulent combustion, is discussed in appendix A3.2. The implementation in REACFLOW is very similar to that in the EXSIM code (section 2.3.2). The disappearance rate of fuel is given by

$$\overline{\omega}_f = -A\,\overline{\rho}\,\frac{\varepsilon}{k}\,\widetilde{Y}_{\min}. \qquad (7)$$

A cut-off criterion based on the Damköhler number is applied to set the reaction rate to zero if the temperature becomes too low (this is the same cut-off criterion as applied in EXSIM).

The effect of the turbulence on the flowfield is modelled using the standard k-ε turbulence model, incorporating a correction for variable density / compressible flows.

In studies of explosions the regions of interest are generally much smaller than the total flow domain. It is therefore advantageous to be able to concentrate the computational effort in these regions. REACFLOW has an adaptive grid capability, which allows regions of the grid to be refined or coarsened locally, depending on the local conditions. For example a steep gradient in the reaction progress variable indicates the reaction zone, and this may be resolved with more cells for greater accuracy. Grid adaptation in REACFLOW is dynamic and fully reversible. However, to avoid excessive refinement a minimum grid size is specified.

The present status of REACFLOW may be summarised as:

2-D Solvers. This module of the code is nearly complete. There are 2-D solvers for compressible and incompressible flows, including convective and diffusive processes, as well as the models for turbulence and chemistry. The compressible solver exists in both explicit and implicit versions. The implementation of adaptive gridding has been completed. Arienti, Huld and Wilkening (1998) describe the grid adaptation methodology implemented in REACFLOW. Arienti et al. (1998) showed comparisons between 2D calculations and experiments for shock tube tests; the advantage of using grid adaptation was highlighted by the better representation of the shock wave.

2-D Axisymmetric solver. An axisymmetric version of the 2-D solver is presently under development.

3-D Solver. The three dimensional solver is presently under development. The geometry has been implemented and an explicit compressible solver is under development. So far this solver includes diffusion and chemistry, but not yet the turbulence model. Grid adaptation is under development. Wilkening and Huld (1999) present results from calculations of large scale Hydrogen explosions. The grid adaptation was used to good effect, keeping the number of elements down and thus minimising the runtime. Wilkening and Huld (1999) found good agreement between the simulations and experiments in terms of generated overpressure, pressure time history and detonation velocity.

Future plans for REACFLOW:

The plans for the near future are to finish the development work outlined above under the heading 3-D Solver. In the longer term there is the possibility that some form of joint Probability Density function (PDF) combustion model will be implemented (see appendix A3.2). This combustion model is highly parallelizable (i.e. the calculation may be split into smaller parts running simultaneously on different processors) and its computationally intensive nature will demand a parallel implementation of the code. A graphical user interface (GUI) will developed to make it easier for the user to define and create a mesh for plant configuration.

Strengths:

- Unstructured mesh capability for easier meshing
- Adaptive meshing for better obstacle representation and flame front resolution
- Accurate solver and second-order, van Leer discretisation scheme has been used

Weaknesses:

- Standard k-ε turbulence model
- Simple combustion models

2.4.6. Imperial College Research Code

Professor Lindstedt, in the Mechanical Engineering Department, has studied premixed flames, including explosions, for a number of years. He and his group have developed a 2D computer code, for research purposes, which incorporates all the latest findings with respect to the combustion model, a sophisticated gradient/flame front tracking refinement and de-refinement mesh algorithm, as well as using an accurate time (implicit Euler) and spatial discretisation (Total Variation Diminishing - TVD) schemes. A parallelized version the code, for greater speed, exists.

The k-ε model is the turbulence model being used in most explosion calculations, though shortcomings of the model are well known. Lindstedt and Váos (1998, 1999) have used second order moment closures to calculate premixed turbulent flames with prescribed PDF to good effect. In the two papers Lindstedt and Váos have improved the modelling of the terms,

focusing on the pressure redistribution/scrambling in the scalar flux equation. Previously the terms in the scalar flux equation have been treated analogously to those of an isothermal constant density flow, but combusting flows, with reacting scalars and large heat release, are of the variable density variety and behaves differently to constant density flows. The Reynolds stress/scalar flux model performs appreciably better than the k-ε model, Lindstedt and Váos (1998, 1999), but more work is still needed on the second order moment closure methods. However, the present closure does provide, arguably for the first time, the ability to model the dynamics of turbulent flames, e.g. burning velocity and flame thickness, with good accuracy.

In non-premixed combustion, quantities like density and species mass fractions, etc., have traditionally been obtained from flamelets and a prescribed probability density function (PDF), often a β−PDF, whose form is dependent on, say, the mixture fraction and the mixture fraction variance. The flamelets are effectively tables of data relating density and species mass fractions to some variable for which a transport equation is solved, i.e. mixture fraction. The data can be obtained from laminar flame calculations with detailed or reduced kinetics or from equilibrium calculations. For premixed combustion the use of laminar flamelets with a prescribed PDF was proposed by Bray and Moss (1981) and has been further extended by, amongst others, Bray *et al.* (1985). The model is often referred to as the Bray-Moss-Libby model. The Bray-Moss-Libby model has not been used extensively, the eddy break-up model being the preferred choice, despite its shortcomings.

A very promising approach is the PDF-transport combustion model, which allows detailed chemical kinetics to be used, Hulek and Lindstedt (1996). Solving a transport equation for the PDF should lead to more accurate combustion predictions. There are experimental uncertainties in the kinetics data, but those are modest in this context and sensitivity studies can reveal whether these uncertainties will greatly affect the predictions. The results of the research will filter into existing combustion models, but it is currently not tractable to use the PDF-transport technique for large industrial problems. The disadvantages with the PDF transport approach is that a large number of "particles" must be used to obtain sensible statistics if using a Monte Carlo approach (commonly used), which leads to long run times, calculations of reaction rates, which feed into the source terms in species transport equations, can be done at run time (leading to long run times) or the data can be tabulated which for detailed kinetics necessitates access to computers with large memory. Development of other ways of obtaining reaction rate data is likely, but probably on a three to five year time scale. However, the advent of faster computers with large memory and running jobs in parallel on multi-processor machines might make it feasible, though unlikely within the next ten years, to use PDF transport models to simulate explosions in large-scale installations on- and off-shore. However, it should be pointed out that the method currently is the only way to account for direct kinetic effects in the context of high Reynolds number flows. The latter are typical of gaseous explosions and finite Damköhler effects have a direct influence on heat release and turbulent burning velocities. The latter property clearly control the severity of gaseous explosions.

Strengths:

- Higher order spatial and temporal discretization techniques are used

- Has adaptive meshing capability
- Use of second-order moment closures, with more accurate modelling of variable ensity flows
- Incorporates detailed chemical kinetics
- Realistic method of obtaining the PDF (through a transport equation)
- Is available in a parallelized form

Weaknesses:

- Long run times with transported PDF method for large-scale problems of interest to industry
- Great requirements for computer memory, if using tabulated rate data
- Not readily available as it is, strictly, a research code

3. DISCUSSION

3.1. Overview of Model Constraints

The empirical model constraints are twofold. Firstly the geometrical representation is quite crude, and secondly, the relative lack of physics incorporated in these models means that they have to be calibrated for every fuel. One of the models, the TNT equivalency model, even assumes that gas explosions behave like TNT explosions, which is not the case. It is necessary to make assumptions about the explosion source strength and degree of confinement, etc., when using some of the models, leading to a range of possible answers, i.e. uncertainties. There are guidelines for how to estimate source strength and confinement, but it is inevitably a much simplified approach. These approaches are open to abuse by inexperienced users or extrapolation beyond bounds of applicability, but many of constraints forced by use of a simple method designed to generate answers with the minimum of effort.

The phenomenological models contains more physics than the empirical models. Moreover, it is still necessary to carry out calibrations for all fuels of interest. The geometry is not represented in as a great detail as in the CFD codes reviewed in the present report, though one of the codes, CLICHE, calculates its input parameters from an obstacle database, which in principle allows a more accurate representation. There is also uncertainty introduced by non-unique obstacle representation - the choice of obstacle representation dependent on the experience of the user.

There are several fundamental constraints imposed on the CFD models discussed in this report.

The first constraint applies to the representation of the modelled geometry. (This is not applicable to the empirical and the phenomenological model type, as these attempt no detailed representation of the actual geometry.) Desktop computers presently have only a limited amount of memory, the maximum capacity being of the order 10^9 bytes. However, the latest desktop PC's, even with more than 1 Gb of random access memory, are becoming very affordable, and offer fast processor speeds, compared to many (more expensive) workstations. It is also possible to reduce the amount of memory required (per processor) by partitioning the mesh into a number of smaller parts, e.g. use a parallelized version of the CFD code. Clusters of PC's, i.e. Beowulf clusters, running the Linux operating system, are now making parallel computing affordable. In light of this, memory constraints might become less of an issue in the next decade.

Experience has shown that each finite volume used by a CFD code requires around 10^3 bytes of computer memory. Hence, the maximum number of finite volumes available to represent a geometry on a poweful desktop PC is around 10^6. In three dimensions this would allow approximately 100 volumes in each co-ordinate direction, equating to equal sized cells of around 0.1 to 1.0 m per side for typical process plant. Many of the objects within a process plant that are important for turbulence production in an explosion will be this size or smaller. Fitting the grid around these objects would clearly require an even larger number of grid cells. This has resulted in the development of various techniques, in particular the Porosity / Distributed Resistance (PDR) approach, to allow some form of geometric representation for

large-scale scenarios, but there are uncertainties in the PDR approach as to how drag induced by the obstacles feeds into the source terms in the turbulence transport equations. However, smaller domains (e.g. flame proof enclosures) can be fully grid-resolved using current computers.

There are also the effects of the grid size on the flow calculation to be considered. Numerical studies have shown that, if the eddy break-up description is used to represent the turbulent reaction rate, then for the flame speed to be grid independent the reaction zone must be resolved by at least four cells, Catlin and Lindstedt (1991). The turbulent reaction zone thickness is around the same size as the turbulence integral length scale, which amongst obstacles may be taken as being equal to a characteristic obstacle dimension. Thus the obstacles would have to be few and large in relation to the overall geometry for the eddy break-up model to be a fundamentally sound practical approach.

The transport equations are discretized using finite differences. An idealised general requirement for the solution to a given problem, generated by a CFD code, is that the solution is grid independent - i.e. that the solution no longer varies as the grid is progressively refined. This may be impractical to demonstrate rigorously. Nevertheless, a grid dependency investigation should ideally form an integral part of CFD studies, certainly at the validation stage. The problem of obtaining a grid independent burning velocity, using the eddy break-up combustion model, is only one of the problems that may occur due to a lack of grid resolution. For example, lack of grid resolution around grid resolved obstacles could smooth the velocity profile in the shear layer caused by these obstacles, reducing the predicted turbulence generation - lowering the predicted flame speed and hence lowering the predicted explosion over-pressure. The simple CFD models do not allow grid independent solutions to be found, as these codes are generally calibrated for a fixed cell size (which is usually very large).

All of the CFD models presented in this report, without exception, model turbulent transport processes by applying the gradient transport assumption and using the two-equation, k-ε turbulence model to generate an effective turbulent viscosity. However, this model was developed over twenty-five years ago and not surprisingly there are several deficiencies associated with this turbulence model. First, it is important to remember that this is only a model of turbulent transport, one that has been validated / calibrated against only a limited number of fundamental flow types - e.g. planar shear layer, axisymmetric jet, etc. The model constants used for prediction of the turbulent mixing in a planar shear layer are actually different to those needed for an axisymmetric jet. Such a model is not expected, therefore, to accurately represent the turbulent processes in an arbitrary three dimensional geometry. Also, this turbulence model was developed for non-reacting, constant density flows. Hence, there is the basic question of whether or not such a model may be applied to a combusting flow without modification. Evidence suggests - Libby and Bray (1980) - that the conventional gradient transport expression (equations A13 and A14, appendix A) may not even correctly predict the sign of the turbulent flux in premixed flames - i.e. that there may be counter-gradient diffusion. Lindstedt *et al.* (1997) have conducted a numerical modelling study of flame propagation in a simple geometry (a long rectangular section tube containing a single flat plate obstacle, aligned perpendicularly to the flow) using the k-ε turbulence model and a form of the eddy break-up combustion model. Lindstedt *et al.* (1997) find that although the large-scale features of the flow are well predicted, such as the over-pressure and mean

flow velocities, the turbulence intensities are not at all well predicted. Such good agreement for the macroscopic parameters may then be merely fortuitous, but further work is needed.

The eddy break-up combustion model, used by some of the 'simple' and 'advanced' CFD codes, requires a high grid resolution to yield a grid independent value of the burning velocity. The model also requires corrections to prevent unphysical behaviour near to surfaces and also at the flame leading edge to prevent numerical detonation. This has led most CFD explosion model developers to use empirical correlations for the flame speed which are grid independent and implicitly include strain rate effects. Implementation of detailed chemical kinetics through the use of a PDF transport equation holds great promise for the future, but due to the heavy demand on computer resources in terms of both processor speed and computer memory, it is unlikely that this approach will be feasible for calculations of real complex geometries for perhaps another ten or more years. Furthermore, there are large uncertainties with regards to rate data for many combustion related reactions; the combustion chemistry is extremely complex and may involve many tens of reactants and intermediate species in over one hundred reactions. It is possible to reduce the detailed kinetics schemes to a smaller number of species (maybe only five or six species), but the resulting set of species conservation equations can become mathematically stiff, with the associated sensitivity to small changes in the dependent variables. Generally, explosion models represent the combustion reactions by a single reaction step involving fuel and oxidant species only. This simplification is necessary due to present constraints in terms of both computer memory and computer speed (cf. appendix A3.2).

The models investigated fall naturally into four basic categories, empirical models, phenomenological models, Computational Fluid Dynamics (CFD) models, and 'advanced' CFD models. The differences between the three groups lie in the simplifications introduced to ease the problem solution. The phenomenological model types compromise geometric accuracy, by approximating a given geometry with an idealised model geometry, but do include reasonably advanced models for the underlying physics. The simple CFD models rely heavily on sub-grid models, such as the Porosity / Distributed Resistance model, to represent objects and, in some cases, the reaction zone. The 'advanced' CFD models allow a more realistic representation of the modelled geometry, through the use of body-fitted or unstructured grids. Grid efficiency for these latter models may be further enhanced by the use of adaptive grids, where a high grid resolution is generated only in those regions that require it. This feature also allows the reaction zone to be fully grid resolved, even for large-scale scenarios.

3.2. Empirical Models - Main Capabilities and Limitations

The main focus will be on the limitations of the empirical models, while the capabilities are described in Sect. 2.1.1 to Sect. 2.1.7. Empirical models are based on correlations of experimental data. The main effort involved in their use is spent deciding on source strengths, degree of confinement, etc. Once the different parameters have been given sensible values, calculations of overpressures, pulse duration and shape are fast. Another advantage is, in some cases, that as long as the representation is good and one is working within the bound of the empiricism, then answers may be adequate. Non-uniqueness in how the parameter values are chosen means that different risk assessors can arrive at very different answers. Also, many empirical models tend to be over conservative.

The models are limited in their applicability and give only a few details of the flow conditions and pressure. The TNT equivalency model does not incorporate the correct physics, since gas explosions behave very differently from TNT detonations.

For all their shortcomings, empirical models have a role to play. The run times are short, of the order of seconds, which means that a number of different scenarios can be quickly tested. Scenarios of particular interest can then be singled out for further analysis with a CFD code or a phenomenological model. The required degree of accuracy and the required level of flow detail may well be such that these simple models will suffice. Extensive calibration against, predominantly, large-scale experiments ensures that the accuracy is, in many situations, acceptable.

3.3. Phenomenological Models - Main Capabilities and Limitations

The main focus will be on the limitations of the phenomenological models, while the capabilities are described in Sect. 2.2.1 to Sect. 2.2.3. The phenomenological models have been extensively calibrated against medium-scale and large-scale experiments . They should be suitable for calculations of geometrical scenarios similar to the ones for which the models have been calibrated. These model may be used in conjunction with both empirical and CFD models

The phenomenological models are subject to a number of uncertainties arising mainly from the simplified geometrical descriptions employed. For example, an accurate representation of plant layouts by a sequence of obstacle grids relies on the judgement of the code operator. This applies to a far lesser extent to the CLICHE code which calculates its input parameters from an obstacle database. The modelling approach taken by these phenomenological models disregards the presence of shock waves. Hence, the pressure distribution within a volume may be incorrectly predicted if shock waves are present.

The over-pressure predicted by the phenomenological codes is generated for the worst case scenario, that of the explosion volume being filled with a uniform gas mixture corresponding to stoichiometric proportions. The more general case, of a non-uniform cloud of fuel and oxidant, may not be modelled. One advantage of CFD codes is that gas explosions in non-uniform clouds can be modelled. In principle, CFD codes are also capable of performing a dispersion calculation prior to ignition.

3.4. Simple CFD Models - Main Capabilities and Limitations

The main focus will be on the limitations of the 'simple' CFD models, while the capabilities are described in Sect. 2.3.1 to Sect. 2.3.4. The 'simple' CFD models have been extensively calibrated against medium-scale and large-scale experiments. They should be suitable for calculations of geometrical scenarios similar to the ones for which the models have been calibrated. These model may be used in conjunction with both 'simple' models and 'advanced' CFD models to yield an insight into the flow. These models benefit from relatively short run times, compared to the 'advanced' CFD models, but which may still be several hours or overnight.

The main limitation of the 'simple' CFD models lies with the simple grids used for discretising the computational domain. All of the 'simple' CFD models presented in this report use Cartesian grids, with sub-grid scale objects represented by the PDR approach. Cartesian meshes are easy to generate and do not incur large computational overheads. However, even objects that are similar in size to the grid cells, or larger, can then only be crudely represented. A sphere, for example, when represented by a Cartesian grid, can be represented only as either an equivalent cube or as a volume / area porosity and resistance. Obviously, neither of these descriptions is an accurate representation of the sphere and the effect of such a simplification on the flowfield and flame development is uncertain.

The other point to consider is the effect of grid resolution on the predicted reaction rate. The FLACS and AutoReaGas codes employ a prescribed burning velocity, obtained from an empirical correlation, whereas the EXSIM code uses the eddy break-up expression to model the turbulent reaction rate. However, it has been shown that a grid independent value of the burning velocity is not obtained for the eddy break-up expression unless the reaction zone is resolved by at least four cells. In practice the developers of the majority of PDR based CFD codes recommend a single cell size. The codes are then compared and developed against experimental data for this size of cell. This effective calibration introduces an element of uncertainty: The codes may work well for scenarios that are similar to the calibration situation but in other instances the performance would be uncertain. Such a strategy does not guarantee grid independence of the final solution and, given the large recommended cell size, grid independence is unlikely. The end result is that these codes may be concealing large numerically generated errors.

The 'simple' CFD codes tend to use first order accurate numerical schemes, see Appendix D for a brief introduction. These schemes cause 'numerical diffusion', which may be greater than the real turbulent diffusion, leading to flame front thickening, increased flame spread and the smoothing of velocity profiles. Numerical diffusion is entirely artificial and may be largely eliminated by the use of numerical schemes of higher order accuracy. The EXSIM code is the only 'simple' CFD code which uses second order accurate schemes for all spatial differencing. The AutoReaGas code is currently first order accurate only, although a version incorporating higher order spatial differencing schemes is under development.

There are other problems associated with this approach. Code validation exercises have tended to concentrate on the measurement of macroscopic explosion properties - i.e. explosion over-pressure and time of flame / over-pressure arrival. The recent Joint Industry Project on Blast and Fire Engineering for Topside Structures Phase II, Selby and Burgan (1998), is an example of this type of exercise. One of the problems with this type of benchmarking is that the code may be forced to give the right result for the wrong reasons. At the microscopic level, the processes of turbulence generation, combustion, flame area enhancement, etc. may not be represented correctly at all. Small scale experiments, concentrating on key areas of the explosion process, coupled with detailed measurements of microscopic properties would provide a more useful tool for code development - cf. Lindstedt and Sakthitharan (1993), as well as another source of data for code evaluation.

3.5. Advanced CFD Models - Main Capabilities and Limitations

The main focus will be on the limitations of the 'simple' CFD models, while the capabilities are described in Sect. 2.4.1 to Sect. 2.4.6. The 'advanced' CFD models use more complicated numerical schemes to improve the representation of the geometry and / or the reaction zone. The COBRA code, for example, uses the PDR approach to represent the explosion geometry, but the code's adaptive grid capability allows the reaction zone to be fully resolved. The NEWT and REACFLOW codes use an adaptive, unstructured mesh, which (in principle at least) allows a full representation of the modelled geometry and of the reaction zone. However, both of these codes are under development and it will be some time, perhaps another ten years, before such a fully resolved approach can take over from the PDR based codes, further developments in both computing power and the codes being required. NEWT was used to calculate two experiments with reasonable success within a factor of 2, after some adjustments for laminar burning, for flame arrival time, flame speed and time to maximum over-pressure, but significantly overpredicted the maximum over-pressure, Watterson *et al.* (1998).

The CFX-4 code uses a structured grid that may be fitted to a given geometry, this allows a much better representation of a given geometry than any of the PDR based codes, but is not as memory efficient as the unstructured, adaptive grid approach. The CFX-4 code also allows regions to be modelled using the PDR approach, although this has not yet been proven in application to an explosion.

3.6. Model Accuracy

Many of the code developers claim extensive model 'validation' for their codes, by making comparison with many experiments. In practice much of what is termed validation is in fact calibration. Most of the models contain a certain degree of empiricism that must be calibrated by making comparisons with experimental measurement. However, there have been some studies to independently determine the accuracy of commonly used explosion models. These studies include the EU co-funded projects MERGE and EMERGE, as well as the more recent Joint Industry Project on Blast and Fire Engineering for Topside Structures Phase 2 (JIP-2). The CFD component of the MERGE project was split into three phases. The first phase was concerned with the evaluation of the various sub-models incorporated into the CFD codes. The second phase involved verification of the CFD explosion models against small and medium scale geometries. For the third phase the code developers submitted 'blind' (i.e. before the experiments were carried out) predictions of the explosion over-pressures in the large scale MERGE geometry. The MERGE geometry consisted of a regular cuboidal pipe array, that was filled with the combustible gas mixture - see Figure 1.

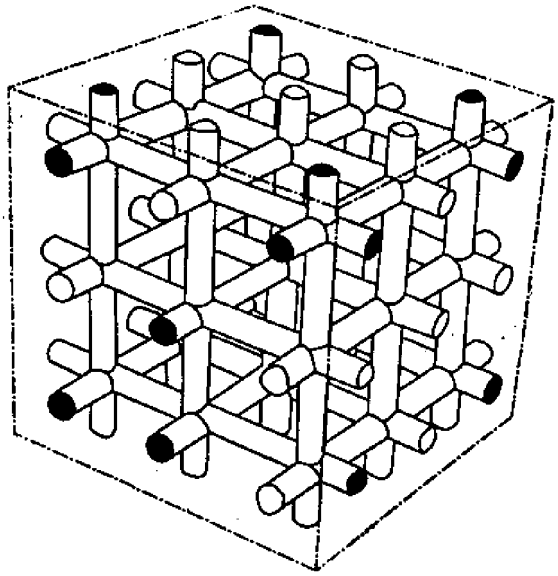

Figure 1 - Example of a congested geometry

The ignition point was at floor level, in the centre of this array, resulting in an expanding hemispherical flame front moving through the obstacles. Predictions generated by four of the codes detailed in this report were submitted for this geometry. Figure 2 shows comparisons between calculated and measured over-pressures for MERGE medium-scale experiments, see also Popat, Catlin, Arntzen, Lindstedt, Hjertager, Solberg, Sæter, van den Berg (1996). Figure 3 shows the calculated and measured maximum over-pressures for MERGE large-scale experiments, see also Popat *et al.* (1996). The results presented in Figures 2 and 3 are representative of the accuracy that may be generally expected from simple CFD explosion models in blind predictions. There is considerable scatter in the results.

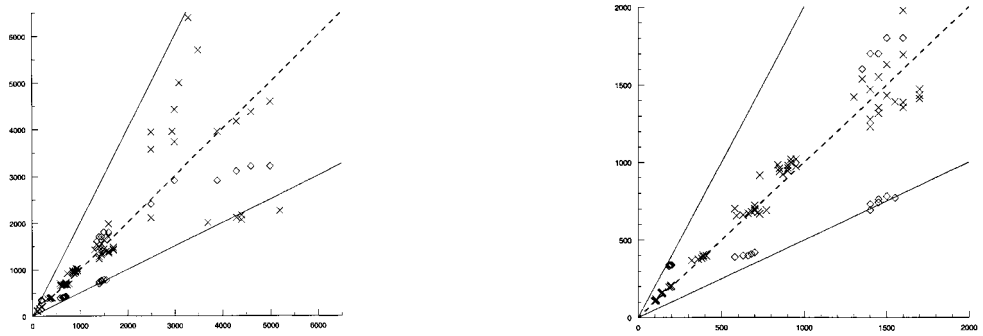

Figure 2 - Comparison of calculated and measured maximum over-pressures for MERGE medium-scale experiments, (×) - COBRA predictions and (◇) - EXSIM predictions; a) all experiments and b) experiments with maximum over-pressures below 1.5 bar, see also Popat *et al.* (1996)

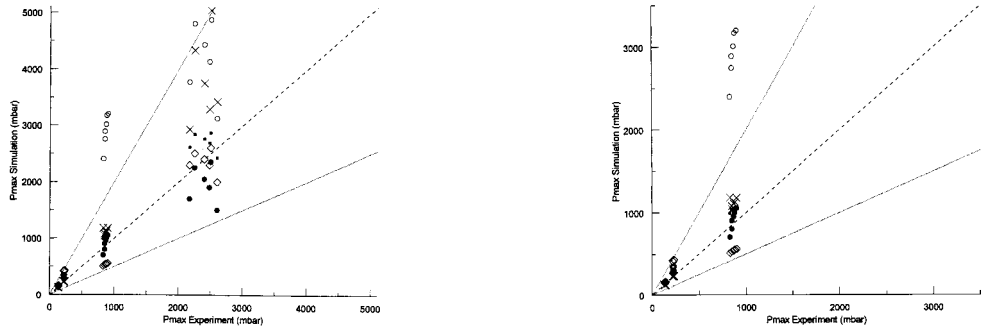

Figure 3 - Comparison of calculated and measured maximum over-pressures for MERGE large-scale experiments, (×) - COBRA predictions, (◇) - EXSIM predictions, (●) - FLACS predictions and (○) AutoReaGas predictions; a) all experiments and b) experiments with maximum over-pressures below 1 bar, see also Popat *et al.* (1996)

The JIP-2 programme was sponsored by 10 offshore operators and the Health & Safety Executive, Selby and Burgan (1998). The programme consisted of an experimental part and a modelling part. The experimental phase consisted of 27 large-scale experiments in an offshore module with varying 'equipment density'. One of the important findings of the experiments was the profound effect water deluge has on the mitigation of explosion overpressures. There is now a database of large-scale experiments against which CFD models can be calibrated. The modelling part consisted of three phases, A) blind predictions on an 8 m wide geometry, which unfortunately did not correspond exactly to the actual experimental geometry, B) predictions of the same geometry as in Phase A but after the tests had been carried out and the models developed / re-tuned and C) blind predictions of a 12 m wide geometry using the correct experimental geometry.

The results of calculations carried out as part of JIP-2, Selby and Burgan (1998), suggest that small changes, or inaccuracies in the representation of the geometry, can lead to over predictions in one case and under predictions (or vice versa) when the geometry changes have been implemented. The findings of the modelling phase were:

- Large scatter in the predictions from the models evaluated in Phase A
- Better agreement between the predictions and the experiments after the models had been re-tuned in Phase B
- Slightly reduced scatter in the predictions from the models, with their re-tuned parameters from Phase B, evaluated in Phase C
- Some models were sensitive to small changes in the geometry
- Some models were very sensitive to small changes in the input conditions
- All models have associated uncertainties, which vary widely between models

JIP-2 did not enhance fundamental understanding of the underlying physics of explosions. Instead of being a true blind predictive test of models, it could perhaps be said that Parts A and B became refocused as a model calibration exercise. In Part A, the maximum over-pressure was, in general, underpredicted and the rise time and duration overpredicted. In Part C as many models underpredicted each parameter as overpredicted. This observation that the models exhibited a completely opposite behaviour for two different geometries, even development and re-tuning in Part B, raises the question whether it would not also have been useful to carry out an experimental investigation into the fundamental physical aspects of explosions as well. My interpretation of the outcome of JIP-2 is that confidence can be attached to the model predictions only if the new geometry strongly resembles one of the two geometries in the database.

It must be emphasised that even with the use of what appears to be in principle a more advanced model, i.e. CFD-based, outside its area of validation/calibration it may in fact give little overall reduction in uncertainties over the use of simpler modelling approaches.

3.7. Recommendations for Future Work

There is a range of modelling approaches available, each with their own strengths and weaknesses. In order to establish confidence in model predictions, it is clear that, for the future, improvements in the physics and the numerics are required, particularly for the CFD-based approaches. However, predictive approaches are needed now. It is thus important that the user be aware of the uncertainties associated with the different models. The following recommendations are essentially those needed to be taken on board by model developers and their funders. They primarily relate to CFD models, which, in principle, should offer the best hope of becoming truly predictive models of gas explosions, with wide applicability.

3.7.1. Grid Improvements

Ideally one would replace the Cartesian grid / PDR based CFD approach by models that are capable of representing a given geometry more accurately. However, the likely time scale for the necessary advances in computing power and code efficiency which will possibly allow geometries to be fully grid resolved is large, possibly of the order of ten years or more. Until this is possible, a hybrid approach could be adopted, whereby body-fitted grids are used to represent the larger objects within the explosion domain, with the PDR approach reserved for the regions that may not be resolved by the grid. It is therefore recommended that methodologies are developed to allow a seamless transition between resolved and PDR-represented solutions as grids are refined. There should be a move away from fixed grid cell size, because such models will require constant re-calibration for new scenarios due to physical and numerical errors associated with the large grid cell size always needing to be compensated. This situation cannot improve until there is a move to a more soundly based methodology.

3.7.2. Combustion Model Improvements

More work is needed to establish the reliability of the combustion models used. Presently, the majority of the explosion models investigated prescribe the reaction rate according to

empirical correlations of the burning velocity. However, it should be recognised that these correlations are subject to a large uncertainty.

The eddy break-up combustion model should ideally not be used if the flame front cannot be properly resolved or, the resulting errors should be recognised and quantified.

Incorporation of detailed or reduced chemical kinetics with a PDF transport approach is appealing, but it is unlikely that this will be feasible for real complex configurations in the foreseeable future - due to the heavy demand placed by this approach on computer resources, in terms of processor time and memory.

3.7.3. Turbulence Model Improvements

The sensitivity of model predictions to the turbulence model used should be investigated. Turbulence modelling has not yet received much attention in the field of explosion modelling. The commonly used two-equation, k-ε model has a number of known failings (i.e. does not predict counter-gradient diffusion), but remains in use due to its economy. Large improvements in over-pressure prediction have been noted by including simple terms into the k-ε model, to account for compressibility effects. However, inclusion of these terms is by no means universal. There is a wide range of advanced k-ε models now available. Ideally Reynolds stress transport modelling should be used but the models require much work to ensure that improvements are not offset by lack of stability.

3.7.4. Experimental Input to Model Development

Model development should now be driven by repeatable, well defined, small-scale, detailed experiments, focusing on key aspects of the physics of explosions. This tends to imply small or medium-scale experiments. Large-scale experiments are suitable for benchmarking, but code calibration on the basis of macroscopic property measurements should be treated with caution, since it is quite possible to obtain approximately correct answers but for the wrong reasons due to gross features swamping finer details. Detailed comparisons of microscopic properties, i.e. initial flame growth, should allow deficiencies in explosion model physics and numerics to be identified, and solutions developed and tested.

3.7.5. Miscellaneous Issues

There are no or few technical barriers to implementation of the above model improvements, beyond a willingness and need to do so.

Perhaps the safest that can be advised at this point is that it would be unwise to rely on the predictions of one model only, i.e. better to use a judicious combination of models of different types, especially if a model is being used outside its range of validation.

4. CONCLUSION

A wide ranging review of numerical models for explosion over-pressure prediction has been conducted and a number of numerical models have been outlined in this report. The models are of varying degrees of complexity, but naturally fall into four distinct groups - i.e. empirical models, phenomenological models, 'simple' CFD models and 'advanced' CFD models.

The limitations associated with the empirical and phenomenological models. i.e. simplified physics and relatively crude representations of the geometry, can only be overcome through additional calibration. This limits the scope for improvements.

The codes comprising the group 'simple' CFD models (EXSIM, FLACS, and AutoReaGas) are in widespread use, as is the phenomenological model SCOPE.

The main limitation of codes in the 'simple' CFD group lies with the crude representation of the explosion geometry. In the long term, ten years hence perhaps, unstructured, adaptive mesh codes may replace the PDR based approaches as the codes and computer hardware develop. In the short term constraints imposed by computing hardware necessitate the use of the PDR approach. However, in the near future the PDR approach could be enhanced by the use of codes employing body-fitted grids, allowing large-scale objects to be fully resolved by the grid, with the PDR description reserved for regions containing very small-scale objects. However, there are uncertainties in how the PDR based approaches feed drag induced by the obstacles into the turbulence transport equations.

It is widely accepted CFD practice that a grid dependency study should ideally be carried out for CFD applications. This is not possible with all 'simple' CFD models as some of these models appear to have been essentially calibrated for a single cell size, with the model developers recommending that this cell size is used throughout. This procedure is likely to lead to large numerically generated errors, which the use of first order accurate numerical schemes is likely to exacerbate. This situation seems, to the author, to lead to the conclusion that 'simple' CFD models will require continual calibration for new scenarios.

The eddy break-up combustion model, used in some 'simple' and 'advanced' CFD codes, has been found to have a number of shortcomings. This combustion model requires a high grid resolution to yield a grid independent value of the burning velocity. The model also requires corrections to prevent unphysical behaviour near to surfaces and also at the flame leading edge to prevent numerical detonation. Most of the explosion model developers have therefore opted to use combustion models based on empirical correlations for the flame speed. Such models have the major advantage that they are grid independent and implicitly include the effects of turbulent strain. However, the experiments upon which the correlations are based show considerable scatter around the correlation function (typically a factor of 2). Hence, even this model should not be thought of as yielding totally reliable values of the reaction rate. A laminar flamelet combustion model has been implemented in the NEWT code. Qualitatively this model shows much better agreement with experiment than the previously used eddy break-up model. Overall, considerable uncertainty still exists in the specification of the reaction rate.

All of the CFD-based explosion models presented use the well known k-ε turbulence model. This model of turbulent transport is known to be deficient even for some aspects of non-combusting flows. In reacting and/or compressible flows, such as those occurring in an explosion, the use of this model is even less well founded. The effects of these model deficiencies, on explosion predictions, are uncertain. Further work is needed to quantify the limitations of this model and to determine whether or not, for example, a full Reynolds stress turbulence model would improve the agreement between CFD model results and experiments. Early indications from the work carried out at Imperial College by Prof. Lindstedt and co-workers suggest that full Reynolds stress/scalar flux transport calculations lead to much better results when applied to deflagrations than the traditional eddy viscosity models. Preliminary results also show that more work is needed, especially for the modelling of the terms in the scalar flux equations for variable density flows, and to improve numerical stability.

Experimental measurements for gas explosions have tended to concentrate on macroscopic properties, such as peak over-pressure. Model development would now be better served by more detailed experimental measurements, such as measurements of turbulence parameters in an explosion and the detailed interaction of a propagating flame front with obstacles. Such measurements would aid the calibration of the PDR approach to explosion modelling as well as providing a sound experimental basis for the development of more advanced physical sub-models. It would be of benefit to both 'simple' and 'advanced' CFD models. This should not in any way be seen as taking a defeatist view, but rather a pragmatic one, as CFD models using the PDR approach are unlikely to be replaced by the next generation of CFD codes, which will be able to resolve all important obstacles, until perhaps the next decade.

In light of the fact that gas explosion predictions are needed now, but that it will probably be ten or more years before the CFD-based models will incorporate fully realistic combustion models, be able to more adequately model turbulence and turbulence-combustion interaction as well as being able to accurately represent all important obstacles in real, complex geometries, one must make the best use of the currently available models. However, it may be unwise to rely on the predictions of one model only, given the uncertainties which remain - especially if the model is used outside its range of validation. One must also be aware of the uncertainties associated with whatever modelling approach is used.

5. REFERENCES

5.1. References Cited in the Report

Abdel-Gayed, R.G., and Bradley, D. (1976)
16th Symposium (International) on Combustion, The Combustion Institute, Pittsburgh, Pennsylvania, U.S.A., pp. 1725-1735

Abdel-Gayed, R. G., and Bradley, D. (1989)
Combustion and Flame **76**:213

Abdel-Gayed, R. G., Al-Khishali, K. J., and Bradley, D. (1984)
Turbulent burning velocity and flame straining in explosions
Proceedings of the Royal Society of London **A391**:393-414

Abdel-Gayed, R. G., Bradley, D., and Lawes, M. (1987)
Turbulent burning velocities: a general correlation in terms of straining rates
Proceedings of the Royal Society of London **A414**:389-413

Abu-Orf, G. M. (1996)
Laminar Flamelet Reaction Rate Modelling for Spark-Ignition Engines
PhD Thesis, University of Manchester Institute of Science and Technology, Manchester, U.K.

Andrews, G. E., Bradley, D., and Lwakabamba, S. B. (1975)
15th Symposium (International) on Combustion, The Combustion Institute, Pittsburgh, Pennsylvania, U.S.A., pp. 655-664

Arienti, M., Huld, T., and Wilkening, H. (1998)
An adaptive 3-D CFD solver for simulating large scale chemical explosions
Proceedings of the 4th ECCOMAS Computational Fluid Dynamics conference, 7-11 September, 1998, Athens, Greece

Arntzen, B. J. (1995)
Combustion Modelling in FLACS 93
HSE Offshore Technology Report, **OTN 95 220**

Arntzen, B. J. (1998)
Modelling of turbulence and combustion for simulation of gas explosions in complex geometries
Dr. Ing. Thesis, Norges Tekniske-Naturvitenskapelige Universitet, Trondheim, Norway

Baker, Q. A., Tang, M. J., Scheier, E. A., and Silva, G. J. (1994)
Vapor Cloud Explosion Analysis
AIChE Loss Prevention Symposium, Atlanta, Georgia, U.S.A.

Baker, Q. A., Doolittle, C. M., Fitzgerald, G. A., and Tang, M. J. (1998)
Recent developments in the Baker-Strehlow VCE Analysis Methodology
Process Safety Progress **17**(4):297-301.

Bakke, J. R. (1986)
Numerical Simulations of Gas Explosions in Two-dimensional Geometries
Christian Michelsen Institute, **CMI 865403-8**.

Berg, A. C. van den (1985)
The Multi-Energy Method - A Framework for Vapour Cloud Explosion Blast Prediction
Journal Hazardous Materials **12**:1-10.

Birkby, P., Cant, R. S., and Savill, A. M. (1997)
Initial HSE Baffled Channel Test Case Results with Refined Combustion and Turbulence Modelling
1st Milestone Report on the HSE Research Contract Research at Cambridge University under Agreement No. **HSE/8685/3278**

Bjerketvedt, D, Bakke, J. R., and Wingerden, K. van (1997)
Gas Explosion Handbook
Journal Hazardous Materials **52**:1-150

Bradley, D., Kwa, L. K., Lau, A. K. C., and Missaghi, M. (1988)
Laminar Flamelet Modelling of Recirculating Premixed Methane and Propane-Air Combustion
Combustion and Flame **71**:109-122.

Bradley, D., Lau, A. K. C., and Lawes, M. (1992)
Flame Stretch Rate as a Determinant of Turbulent Burning Velocity
Philosophical Transactions of the Royal Society of London **A338**:359

Bray, K. N. C. (1987)
9th Australasian Fluid Mechanics Conference, Auckland, New Zealand

Bray, K. N. C., Champion, M., and Libby, P. A. (1989)
The Interaction Between Turbulence and Chemistry in Premixed Turbulent Flames
Turbulent Reactive Flows, Lecture Notes in Engineering No. 40, Springer Verlag, pp. 541-563

Bray, K. N. C. (1990)
Studies of the turbulent burning velocity
Proceedings of the Royal Society of London **A431**:315-325

Bray, K. N. C. and Moss, J. B. (1977)
A Unified Statistical Model of the Turbulent Premixed Flame
Acta Astronautica **4**:291-320

Bray, K. N. C., Libby, P. A., and Moss, J. B. (1985)
Unified Modelling Approach for Premixed Turbulent Combustion - Part 1: General Formulation
Combustion and Flame, **61**:87-102

Brookes, S. J. (1997)
A Review of Gas Explosion Models
HSL Report No. **FS/97/12 - GE/97/05**

Cates, A. T., and Samuels, B. (1991)
A Simple Assessment Methodology for Vented Explosions
Journal of Loss Prevention in the Process Industries **4**:287-296

Catlin, C. A. (1985)
IChemE Symp. Series No. **93**

Catlin, C. A., and Lindstedt, R. P. (1991)
Premixed Turbulent Burning Velocities Derived from Mixing Controlled Reaction Models with Cold Front Quenching
Combustion and Flame **85**:427-439

Catlin, C. A., Fairweather, M., and Ibrahim, S. S. (1995)
Predictions of Turbulent, Premixed Flame Propagation in Explosion Tubes
Combustion and Flame **102**:115-128

Chippett, S. (1984)
Modeling of Vented Deflagrations
Combustion and Flame **55**:127-140

Chynoweth, S. (2000)
Private communication.

Chynoweth, S., and Ungut, A. (2000)
Private communication.

Connell, I. J., Watterson, J. K., Savill, A. M., Dawes, W. N., and Bray, K. N. C. (1996a)
An Unstructured Adaptive Mesh CFD Approach to Predicting Confined Premixed Methane-Air Explosions
Proceedings of the 2nd International Specialists Meeting in Fuel-Air Explosions

Connell, I. J., Watterson, J. K., Savill, A. M., and Dawes, W. N. (1996b)
An Unstructured Adaptive Mesh Navier Stokes Solution Procedure for Predicting Confined Explosions
19th IUTAM Congress of Theoretical and Applied Mechanics, Kyoto, Japan

CPR14E (1979)
Methods for Calculation of the Physical Effects of the Escape of Dangerous Materials
Commission for the Prevention of Disasters, Dutch Ministry of Social Affairs, Directorate-General of Labour, Voorburg, the Netherlands.

Cullen, Hon. Lord (1990)
The Public Inquiry into the Piper Alpha Disaster
The Department of Energy, HMSO, London, UK

Damköhler, G. (1940)
Zeitschrift für Elektrochemie **46**:601-626

Fairweather, M., Hargrave, G. K., Ibrahim, S. S., and Walker, D. G. (1999)
Studies of Premixed Flame Propagation in Explosion Tubes
Combustion and Flame **116**(4):504-518

Fairweather, M., and Vasey, M. W. (1982)
A Mathematical Model for the Prediction of Overpressures Generated in Totally Confined and Vented Explosions
19th Symposium (International) on Combustion, The Combustion Institute, Pittsburgh, Pennsylvania, U.S.A., pp. 645-653

Fairweather, M., Ibrahim, S. S., Jaggers, H. and Walker, D.G. (1996)
Turbulent Premixed Flame Propagation in a Cylindrical Vessel
26th Symposium (International) on Combustion, The Combustion Institute, Pittsburgh, Pennsylvania, U.S.A., pp. 365-371

Freeman, D. J. (1994)
Visualisation of explosions in a baffled plate, vented enclosure
HSL Report **IR/L/GE/94/08**

Godunov, S. K. (1959)
A Finite Difference Method for the Computation of Discontinuous Solutions of the Equations of Fluid Dynamics
Mat. Sb. **47**:271-290

Gouldin, F. C. (1987)
An Application of Fractals to Modelling Premixed Turbulent Flames
Combustion and Flame **68**:249-266

Guilbert, P. W., and Jones, I. P. (1996)
Modelling of Explosions and Deflagrations
HSE Contract Research Report No. **93/1996**

Gülder, O. L. (1990a)
23rd Symposium (International) on Combustion, The Combustion Institute, Pittsburgh, Pennsylvania, U.S.A., pp. 743-750

Gülder, O. L. (1990b)
Turbulent Premixed Combustion Modelling Using Fractal Geometry
23rd Symposium (International) on Combustion, The Combustion Institute, Pittsburgh, Pennsylvania, U.S.A., pp. 835-842

Hansen, O. R. (2001)
Private communication

Hjertager, B. H. (1982)
Numerical Simulation of Flame and Pressure Development in Gas Explosions
SM study no. 16, University of Waterloo Press, Ontario, Canada, pp. 407-426

Hjertager, B. H. (1982)
Simulation of Transient Compressible Turbulent Reactive Flows
Combustion Science and Technology **41**:159-170

Hulek, T., and Lindstedt, R. P. (1996)
Computations of Steady-State and Transient Premixed Turbulent Flames Using pdf Methods
Combustion and Flame **104**:481-506

Jones, W. P. (1980)
Models for turbulent flows with variable density and combustion
in *Prediction Methods for Turbulent Flows* (Ed.: Kollmann W.), Hemisphere, Washington D.C., U.S.A., pp. 423-458

Leer, B. van (1974)
Towards the Ultimate Conservative Difference Scheme. II. Monotonicity and Conservation Combined in a Second-Order Scheme
Journal of Computational Physics **14**:361-370

Leer, B. van (1982)
Flux Vector Splitting for the Euler Equations
Lecture Notes in Physics, Springer-Verlag, **170**:507-512

Leuckel, W., Nastoll, W., and Zarzalis, N. (1990)
Experimental Investigation of the Influence of Turbulence on the Transient Premixed Flame Propagation Inside Closed Vessels
23rd Symposium (International) on Combustion, The Combustion Institute, Pittsburgh, Pennsylvania, U.S.A., pp. 729-734

Libby, P. A., and Bray, K. N. C. (1980)
Counter-Gradient Diffusion in Premixed Turbulent Flames
AIAA 18th Aerospace Sciences Meeting, Pasadena, California

Lindstedt, R. P., and Sakthitharan, V. (1993)
Transient Flame Growth in a Developing Shear Layer
9th Symposium on Turbulent Shear Flows, Kyoto, Japan

Lindstedt, R. P., Hulek, T., and Váos, E. M. (1997)
Further Development of Numerical Sub-models and Theoretical Support
EMERGE Project Report, Task 10

Lindstedt, R. P., and Váos, E. M. (1998)
Second Moment Modeling of Premixed Turbulent Flames Stabilized in Impinging Jet Geometries

27th Symposium (International) on Combustion, The Combustion Institute, Pittsburgh, Pennsylvania, U.S.A., pp. 957-962.

Lindstedt, R. P., and Váos, E. M. (1999)
Modeling of Premixed Turbulent Flames with Second Moment Methods
Combustion and Flame **116**:461-485

Magnussen, B. F., and Hjertager, B. H. (1976)
On Mathematical Modelling of Turbulent Combustion with Special Emphasis on Soot Formation and Combustion
16th Symposium (International) on Combustion, The Combustion Institute, Pittsburgh, Pennsylvania, U.S.A., pp. 719-729

Mandelbrot, B. B. (1975)
On the Geometry of Homogeneous Turbulence, with Stress on the Fractal Dimension of the Iso-surfaces of Scalars
Journal of Fluid Mechanics **72**:401-416

Mercx, W. P. M. (1993)
Modelling and experimental research into gas explosions: overall final report on the MERGE project
Commission of the European Communities Report, Contract **STEP-CT-011** (SSMA)

Mercx, W. P. M., and Berg, A. C. van den (1997)
The Explosion Blast Prediction Model in the Revised CPR 14E (Yellow Book)
Process Safety Progress **16**(3):152-159

Patankar, S. V., and Spalding, D. B. (1972)
A Calculation Procedure for Heat, Mass and Momentum Transfer in Three-dimensional Parabolic Flows
International Journal of Heat and Mass Transfer **15**:1787-1806

Popat, N. R., Catlin, C. A., Arntzen, B. J., Lindstedt, R. P., Hjertager, B. H., Solberg, T., Sæter, O., and Berg, A. C. van den (1996)
Investigations to Improve and Assess the Accuracy of Computational Fluid Dynamic Based Explosion Models
Journal of Hazardous Materials **45**:1-25

Prandtl, L. (1925)
Bericht über Untersuchungen zur ausgebildete Turbulenz
Zeitschrift für Angewandte Mathematik und Mechanik **3**:136-139

Pritchard, D. K., Freeman, D. J., and Guilbert, P. W. (1996)
Prediction of Explosion Pressures in Confined Spaces
Journal of Loss Prevention in the Process Industries **9**:205-215

Pritchard, D. K., Lewis, M. J., Hedley, D., and Lea, C. J. (1999)
Predicting the effect of obstacles on explosion development
HSL Report No. **EC/99/41 - CM/99/11**

Puttock, J. S. (1995)
Fuel Gas Explosion Guidelines - the Congestion Assessment Method
2nd European Conference on Major Hazards On- and Off-shore, Manchester, UK, 24-26 September 1995.

Puttock, J. S. (1999)
Improvements in Guidelines for Prediction of Vapour-cloud Explosions
International Conference and Workshop on Modeling the Consequences of Accidental Releases of Hazardous Materials, San Francisco, Sept-Oct, 1999

Puttock, J. S. (2000a)
Private communication

Puttock, J. S. (2000b)
Private communication

Puttock, J. S., Cresswell, T. M., Marks, P. R., Samuels, B., and Prothero, A. (1996)
Explosion Assessment in Confined Vented Geometries. SOLVEX Large-Scale Explosion Tests and SCOPE Model Development
HSE Offshore Technology Report, **OTO 96 004**

Puttock, J. S., Yardley, M. R., and Cresswell, T. M. (2000)
Prediction of Vapour Cloud Explosions Using the SCOPE Model
Journal of Loss Prevention in the Process Industries **13**:419-430

Rehm, W., and Jahn, W. (2000)
CFX German User Conference

Roe, P. L. (1981)
Approximate Riemann Solvers, Parameter Vectors, and Difference Schemes
Journal of Computational Physics **43**:357-372

Sæter, O. (1994)
Implementation of New Laminar Model in EXSIM
Shell UK and EMERGE Progress Report, Tel-Tek

Selby, C. A., and Burgan, B. A. (1998)
Blast and Fire Engineering for Topside Structures - Phase 2 (Final Summary Report)
SCI Publication No. **253**, The Steel Construction Institute, Ascot, U.K.

Smith, K. O., and Gouldin, F. C. (1978)
Experimental Investigation of Flow Turbulence Effects on Premixed Methane-Air Flames in Turbulent Combustion
Progress in Astronautics and Aeronautics, Vol. 58, ed. by Kennedy L. A.

Spalding, D. B. (1971)
Concentration Fluctuations in a Round Turbulent Free Jet
Chemical Engineering Science **26**:95-107

Strehlow, R. A., Luckritz, R. T., Adamczyk, A. A., and Shimpi, S. A. (1979)
The Blast Wave Generated by Spherical Flames
Combustion and Flame **35**:297-310

Thyer, A. M. (1997)
Updates to VCE Modelling for Flammable Riskat: Part 1
HSL Report No. **RAS/97/04 - FS/97/01**

Watterson, J. K., Savill, A. M, Dawes, W. N., and Bray, K. N. C. (1996)
Predicting Confined Explosions with an Unstructured Adaptive Mesh Code
Joint Meeting of the Portuguese, British and Spanish Sections of the Combustion Institute

Watterson, J. K., Connell, I. J., Savill A. M., and Dawes, W. N. (1998)
A Solution-Adaptive Mesh Procedure for Predicting confined Explosions
International Journal for Numerical Methods in Fluids **26**:235-247

Wiekema, B. J. (1980)
Vapour Cloud Explosion Model
Journal of Hazardous Materials **3**:221-232

Wilkening, H., and Huld, T. (1999)
An adaptive 3-D CFD solver for explosion modelling on large scales
17th International Colloquium on the Dynamics of Explosions and Reactive Systems,
25-30 July, 1999, Heidelberg, Germany

Wingerden, K. van (2001)
Developments in Gas Explosion Safety in the 1990's in Norway
FABIG Newsletter, Article R397, Issue no. **28** (April 2001), pp. 17-20

5.2. References Used but not Cited

Bray, K. N. C. (1980)
Turbulent Flows with Premixed Reactants
in *Turbulent Reacting Flows*, Topics in Applied Physics, Vol. **44**, Springer-Verlag

British Gas Plc (1989)
Review of the Applicability of Predictive Methods to Gas Explosions in Offshore Modules
Department of Energy Offshore Technology Report **OTH 89 312**

Gardner, D. J. and Hulme, G. (1994)
A Survey of Current Predictive Methods for Explosion Hazard Assessments in the UK Offshore Industry
HSE Offshore Technology Report **OTH 94 449**

APPENDIX A - THEORETICAL DESCRIPTION OF GAS EXPLOSIONS

A1. Conservation Equations

The basic equations describing the instantaneous state of a reacting flow are, for mass continuity

$$\frac{\partial \rho}{\partial t} + \nabla \bullet (\rho \boldsymbol{u}) = 0, \tag{A1}$$

for momentum conservation

$$\rho \frac{\partial \boldsymbol{u}}{\partial t} + \rho \boldsymbol{u} \bullet \nabla \boldsymbol{u} = \rho \boldsymbol{g} - \nabla P + \nabla \bullet \boldsymbol{\tau}, \tag{A2}$$

for species conservation

$$\rho \frac{\partial Y_n}{\partial t} + \rho \boldsymbol{u} \bullet \nabla Y_n + \nabla \bullet (\rho Y_n \boldsymbol{U}_n) = \omega_n, \tag{A3}$$

and for energy conservation

$$\rho \frac{\partial h}{\partial t} + \rho \boldsymbol{u} \bullet \nabla h = \frac{\partial P}{\partial t} + \boldsymbol{u} \bullet \nabla P - \nabla \bullet \boldsymbol{q} + \Phi + \dot{Q} + \rho \Sigma_{n=1}^{N} Y_n \boldsymbol{f}_n \bullet \boldsymbol{U}_n, \tag{A4}$$

where $\boldsymbol{\tau}$ is the deviatoric stress tensor, $\boldsymbol{q}$ is the heat flux vector, Φ is the dissipation of energy by viscous stresses, $\dot{Q}$ is the external heat input, $\boldsymbol{f}_n$ is the body force vector, and $\boldsymbol{U}_n$ is the diffusion velocity of species n relative to the mean mixture velocity. The enthalpy (h) is defined by

$$h = \Sigma_{n=1}^{N} h_n, \text{ where } h_n = \Delta h_{f,n}^{\circ} + \int_{T^{\circ}}^{T} C_{P,n} dT', \tag{A5}$$

$\Delta h_{f,n}^{\circ}$ is the heat of formation of species n at the reference temperature T° and $C_{P,n}$ is the specific heat capacity of species n. The heat flux vector is obtained from the summation of three components, conduction, diffusion, and the Dufour effect - a heat flux that arises from a concentration gradient. The Dufour effect is generally negligible. Hence, the heat flux vector is given by

$$\boldsymbol{q} = -\lambda \nabla T + \rho \Sigma_{n=1}^{N} h_n Y_n \boldsymbol{U}_n \tag{A6}$$

For closure of this system of equations relationships are needed for the equation of state for the gas and the rates of production of the chemical species. The equation of state for the gas is most easily approximated by the perfect gas law

$$\rho = \frac{MP}{RT}, \tag{A7}$$

where M is the molecular weight of the gas, P is the pressure and R is the universal gas constant. The production rate of each species may be approximated using the Arrhenius expression.

The complexity of this system of equations renders their solution intractable for all but the very simplest of situations. The chemical reaction time scales are generally smaller than the turbulence time scales, which in turn are smaller than the time scales characterising the mean flow. Explosions are transient phenomena, but to resolve the time scales of all the processes occurring within the explosion is beyond the capabilities of present computers and will remain so for the foreseeable future. Hence, the equations are averaged over a time period that is short in comparison with the macroscopic features of the explosion, but is long compared to the time scales of the chemical and turbulent processes. This averaging process results in additional correlations that need to be modelled. Also, closure of the mean chemical source terms presents a problem because of the non-linear dependence of these terms on temperature and species concentrations. The number of correlations introduced by the averaging process may be reduced by employing Favre (density weighted) averaging. The Favre mean of a variable is defined by $\tilde{x} = \overline{\rho x} / \overline{\rho}$. By replacing the instantaneous variables with their Favre mean plus a fluctuating component - i.e. $x = \tilde{x} + x''$ - and averaging over a suitable time period the conservation equations may be recast in the following form, for continuity and momentum conservation

$$\frac{\partial \overline{\rho}}{\partial t} + \nabla \bullet (\overline{\rho}\tilde{\boldsymbol{u}}) = 0 \qquad \text{(A8)}$$

$$\overline{\rho}\frac{\partial \tilde{\boldsymbol{u}}}{\partial t} + \overline{\rho}\tilde{\boldsymbol{u}} \bullet \nabla\tilde{\boldsymbol{u}} + \nabla \bullet \overline{\rho \boldsymbol{u}'' \otimes \boldsymbol{u}''} = \overline{\rho}\boldsymbol{g} - \nabla\overline{P} + \nabla \bullet \overline{\boldsymbol{\tau}}. \qquad \text{(A9)}$$

The third term on the left hand side represents the Reynolds stresses, these are additional stress terms that arise due to the turbulent transport of momentum. The last term on the right hand side, the molecular stress term, is generally small in comparison to the Reynolds stress term and may generally be neglected. Approaches for dealing with the Reynolds stress term are discussed in the next section.

For species and energy conservation the equations become

$$\overline{\rho}\frac{\partial \tilde{Y}_n}{\partial t} + \overline{\rho}\tilde{\boldsymbol{u}} \bullet \nabla\tilde{Y}_n + \nabla \bullet \overline{\rho \boldsymbol{u}'' Y_n''} = \bar{\omega}_n - \nabla \bullet (\overline{\rho}\tilde{Y}_n \boldsymbol{U}_n) \qquad \text{(A10)}$$

$$\overline{\rho}\frac{\partial \tilde{h}}{\partial t} + \overline{\rho}\tilde{\boldsymbol{u}} \bullet \nabla\tilde{h} + \nabla \bullet \overline{\rho \boldsymbol{u}'' h''} = \frac{\partial \overline{P}}{\partial t} + \tilde{\boldsymbol{u}} \bullet \nabla\overline{P} + \overline{\boldsymbol{u}'' \bullet \nabla P} - \nabla \bullet \overline{\boldsymbol{q}} + \overline{\Phi} + \overline{\dot{Q}} + \overline{\rho}\,\Sigma_{n=1}^{N}\, \tilde{Y}_n \boldsymbol{f}_n \bullet \boldsymbol{U}_n. \qquad \text{(A11)}$$

The third terms on the left hand side of these equations are the turbulent scalar fluxes of species and energy respectively. These terms arise from the transport of species and energy by turbulent motions in fluid. These terms will be discussed further in the next section.

It should be noted that all of the conservation equations have a similar form, i.e.

$$\overline{\rho}\frac{\partial \tilde{\phi}}{\partial t} + \overline{\rho}\tilde{\boldsymbol{u}} \bullet \nabla\tilde{\phi} + \nabla \bullet \overline{\rho \boldsymbol{u}'' \phi''} = \bar{S}_\phi + \bar{M}_\phi, \qquad \text{(A12)}$$

where ϕ represents the general variable, $\bar{S}_\phi$ the mean production rate of ϕ, and $\bar{M}_\phi$ is a term representing all the processes that occur at the molecular level. In a turbulent flow the molecular transport processes are usually negligible and the transport of momentum, species, and energy through turbulent action is dominant. The next section discusses the modelling of

turbulent transport processes and introduces the important models used for capturing turbulent transport.

A2. Turbulence Modelling

The Reynolds stresses and the turbulent scalar fluxes that appear in the averaged form of the transport equations for momentum, species, and energy require modelling for closure of this equation set. One of the simplest closure's models turbulent transport by making an analogy with molecular motion. Molecular momentum or scalar transport takes place by the random motion of molecules, turbulent transport may therefore be thought of as transport occurring through the random motion of macroscopic turbulent eddies - Prandtl (1925). Hence, the turbulent transport of a fluid property may be related to the gradient of its mean. The Reynolds stresses are given by

$$\overline{\rho u_i'' u_j''} = \tfrac{2}{3}\delta_{ij}(\bar{\rho}k + \mu_T \nabla \bullet \tilde{\boldsymbol{u}}) - \mu_T\left(\frac{\partial \tilde{u}_i}{\partial x_j} + \frac{\partial \tilde{u}_j}{\partial x_i}\right), \tag{A13}$$

where δ_{ij} is the Kronecker delta function ($\delta_{ij} = 1$ if $i = j$, $\delta_{ij} = 0$ if $i \neq j$) and k is the turbulence kinetic energy given by $k = \tfrac{1}{2}\overline{\rho \boldsymbol{u}'' \bullet \boldsymbol{u}''}/\bar{\rho}$. The turbulent scalar fluxes are given by

$$\overline{\rho u_j'' \phi''} = -\frac{\mu_T}{\sigma_\phi}\frac{\partial \tilde{\phi}}{\partial x_j}. \tag{A14}$$

The first constant introduced in these equations (μ_T) is the effective (or eddy) viscosity. The second constant (σ_ϕ) is the Prandtl / Schmidt number for the variable ϕ. The Prandtl number is defined as

$$\mathrm{Pr} = \frac{\mu}{\rho a}, \tag{A15}$$

where a is the thermal diffusivity. The Prandtl number is the ratio of momentum diffusion to energy diffusion. The Schmidt number is defined similarly

$$\mathrm{Sc} = \frac{\mu}{\rho D_\phi}, \tag{A16}$$

where D_ϕ is the diffusivity of species ϕ in the gas mixture. The Schmidt number is the ratio of momentum diffusion to mass diffusion.

From dimensional analysis the eddy viscosity is shown to be proportional to the product of a characteristic turbulence velocity and a turbulence length scale. Hence, the eddy viscosity may be given by

$$\mu_T = C_\mu \bar{\rho}\frac{k^2}{\varepsilon}, \tag{A17}$$

where ε is the dissipation rate of turbulence kinetic energy and C_μ is a model constant. The turbulence kinetic energy and its dissipation rate may be obtained from their respective balance equations. The transport equation for the turbulence kinetic energy is

$$\bar{\rho}\frac{\partial k}{\partial t} + \bar{\rho}\tilde{\boldsymbol{u}} \bullet \nabla k = -\overline{\rho \boldsymbol{u}'' \otimes \boldsymbol{u}''} : \nabla \tilde{\boldsymbol{u}} + \nabla \bullet (\frac{\mu_T}{\sigma_k}\nabla k) + \nabla \bullet \overline{\boldsymbol{u}'' \bullet \boldsymbol{\tau}} - \overline{\boldsymbol{u}'' \bullet \nabla \bullet \boldsymbol{\tau}^T} - \overline{\boldsymbol{u}'' \bullet \nabla P}, \tag{A18}$$

where the meanings of the terms on the right hand side are: i) production of turbulence kinetic energy due to the work done against the Reynolds stresses (which are generally modelled using the gradient transport assumption given above), ii) turbulent diffusion of turbulence kinetic energy (modelled by the eddy viscosity assumption), iii) molecular diffusion which is generally negligible, iv) removal of turbulence kinetic energy due to viscous effects, this term must be modelled and is often represented as $\overline{\boldsymbol{u}'' \bullet \nabla \bullet \boldsymbol{\tau}^T} = \bar{\rho}\varepsilon$, v) the pressure velocity correlation term, this represents a second source of turbulence kinetic energy. The velocity fluctuation-pressure gradient correlation term is generally ignored in most applications of the k-ε turbulence model. The equation for the dissipation rate of the turbulence kinetic energy may be modelled as

$$\bar{\rho}\frac{\partial \varepsilon}{\partial t} + \bar{\rho}\tilde{\boldsymbol{u}}\nabla \bullet \varepsilon = -C_{\varepsilon_1}\overline{\rho \boldsymbol{u}'' \otimes \boldsymbol{u}''} : \nabla \tilde{\boldsymbol{u}}\frac{\varepsilon}{k} - \bar{\rho}\, C_{\varepsilon_2}\frac{\varepsilon^2}{k} + \nabla \bullet (\frac{\mu_T}{\sigma_\varepsilon}\nabla \varepsilon), \qquad \text{(A19)}$$

where gradient diffusion has been assumed for the turbulent transport of the dissipation rate and C_{ε_1} and C_{ε_2} are model constants. The model constants for this turbulence model are normally given as $C_\mu = 0.09$, $C_{\varepsilon_1} = 1.44$, and $C_{\varepsilon_2} = 1.92$. In addition the turbulent Prandtl / Schmidt numbers for k and ε are normally given as 1.0 and 1.3 respectively.

Two-equations models of turbulence, such as the k-ε model outlined above, are commonly used due to their simplicity. However, eddy viscosity models have some serious deficiencies, partly in consequence of equations A13 and A14 not being strictly valid. In a three-dimensional flow the Reynolds stress and the strain rate are usually not related in a simple manner. This means that the eddy viscosity may no longer be a scalar but will in fact become a tensor. Models that account for the anisotropy are new and have not yet been applied to explosion modelling, so will not be further discussed here.

A more complicated, but potentially more accurate, approach is to model the transport of the Reynolds stresses and the turbulent scalar fluxes. These transport equations contain further triple correlations, which need to be modelled. In three dimensions an additional seven transport equations are required to model the Reynolds stresses, with another three additional equations for each scalar - there is one turbulent scalar flux in each co-ordinate direction. Reynolds stress modelling is being used in the field of combustion modelling, but has yet to make an impact on the more specialised application of explosion modelling.

A3. Reaction Rate Modelling

CFD models of explosions do not track the flame front directly. Instead the position of the flame front is inferred from a characteristic value for a certain scalar variable - e.g.. the reaction progress variable. The effect of the passage of a flame front through the gaseous medium is conveyed through the reaction rate source terms appearing in the equations for the species mass fractions and energy. Although the flame is not tracked directly, some CFD models (for example COBRA) infer the reaction rate from a locally fitted flame speed that is obtained from an empirical correlation. Hence, this section will begin by discussing ways of determining the turbulent flame speed.

A3.1. Turbulent Flame Speed

This sub-section will begin by explaining the relationship between the flame speed and the burning velocity. The burning velocity is defined as the mass consumption of unburnt gas divided by its density per unit area of flame. The flame speed is the speed of the flame relative to a stationary observer. Consider a planar combustion wave propagating through a premixed fuel / air mixture - fig. A1.

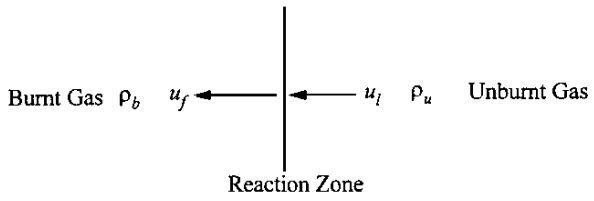

Figure A1 - Schematic description of the flame reaction zone

The mass consumption of reactant mixture must equal the mass production of product mixture. Hence, the speed of the flame is given by

$$u_f = \frac{\rho_u}{\rho_b} u_l, \qquad \text{(A20)}$$

where u_f is the flame speed, u_l is the burning velocity, and ρ_u and ρ_b are the densities of the unburnt and burnt gas mixtures respectively. The flame speed includes the expansion generated flow due to the decrease in density of the product gas mixture. Note that the burning velocity in this case is actually the laminar burning velocity, because an undisturbed combustion wave is considered. In a laminar gas mixture the flame speeds generated are fairly low. A burning velocity of 0.5 m s^{-1} is typical for a hydrocarbon fuel, with a density ratio of around 8. This yields a flame speed of approximately 4 m s^{-1}. Large scale experiments to measure flame speed have been conducted in initially quiescent media. The maximum flame speeds obtained in these experiments were between 7 and 15 m s^{-1} for various hydrocarbon / air mixtures. The increase over the expected value of around 4 m s^{-1} is caused by the formation of a 'cellular' flame surface. Flame front instabilities, of hydrodynamic or diffusional-thermal origin, cause the flame front to wrinkle with a characteristic cellular appearance. This wrinkling increases the surface area of the flame and hence the effective flame speed. The flame speed caused by this self-turbulization mechanism does not in itself generate a significant over-pressure. However, the enhanced expansion flow could potentially increase the turbulence level more in the unburnt gas, if obstacles were present.

An alternative approach to obtaining the turbulent burning velocity has been adopted by Gouldin (1987). The turbulent burning velocity is defined as the mean mass flux of unburnt

gas moving in to the flame divided by the unburnt gas density per unit area of flame. The flame area considered is a mean, smoothed flame area. However, at a small scale the flame front will be highly contorted. At low to moderate turbulence levels the reaction is known to occur in thin flame sheets ('flamelets') which are rough with multiple scales of wrinkling. Moreover, at a small scale the flame will be propagating at the laminar burning velocity, relative to the unburnt gas, in a direction normal to this flamelet surface (ignoring the effects of strain). Hence, the increase in burning velocity may be considered in terms of a flame area enhancement due to the turbulence. From continuity

$$\frac{u_T}{u_l} = \frac{A_l}{A_T} \,, \tag{A21}$$

where A_l is the 'exact' flame area and A_T is the flame area used to define u_T. Gouldin considers the flamelet surface to be a fractal surface - i.e. a surface that displays multiple scales of wrinkling. Consider a volume of dimension L^3 filled uniformly (in a statistical sense) with a wrinkled surface and with the scales of wrinkling being self-similar - Mandelbrot (1975), then if the volume is split into cubes with a length per side of ε, on average the number of cells touched by the surface is proportional to $(L/\varepsilon)^D$. If the surface is smooth the fractal dimension (D) will approach 2 (if it is rough then D will approach 3 and the surface will appear to fill the volume L^3). It follows that the surface area in L^3 as measured with a scale ε^2 is given by

$$A \sim \varepsilon^{2-D} L^D \,. \tag{A22}$$

Mandelbrot (1975) suggests two possible values for D, 8/3 for Gauss-Kolmogorov turbulence or 5/2 for Gauss-Bergers turbulence. More recent results, for the fractal dimension of an iso-surface in a turbulent shear flow, have suggested that the value should lie between 2.35 and 2.6. Eqn. A22 implies that if $D > 2$ then the flame surface area approaches infinity as ε approaches zero. In practice there is a lower limit for ε below which the flame surface area ceases to increase. Such a lower limit would be the Kolmogorov turbulence length scale. Similarly there is an upper limit for ε beyond which eqn. A22 will no longer describe the variation of the flame surface area with ε. This upper limit for ε is taken as the turbulence integral length scale, which may be thought of as the maximum scale of the surface wrinkling. Associating these two limiting values of the surface area with A_l and A_T above, then from eqn.s A21 and A22

$$\frac{u_T}{u_l} = \frac{A_l}{A_T} = \left(\frac{l}{\eta}\right)^{D-2} , \tag{A23}$$

where l is the integral length scale and η is the Kolmogorov length scale. The length scale ratio is given by $l/\eta = A_t^{1/4} R_l^{3/4}$ where A_t is a constant of order unity and $R_l = u'l/\nu$. Gouldin (1987) modifies this basic expression to account for the effects of flame propagation on the flamelet surface and also the effect of the strain on the laminar burning velocity.

A3.2. Turbulent Reaction Rate

The mean reaction rate for species n ($\bar{\omega}_n$) appears in the equation describing the transport of the species mass fraction (eqn. A10) and is a function of the gas mixture composition and its temperature (and pressure, as this will have an effect on the concentrations of the reacting

species). In general, the highly non-linear dependence of the reaction rate on these variables precludes the use of mean properties in generating the mean reaction rate, i.e.

$$\bar{\omega}_n \neq \omega_n(\overline{Y_n}, \overline{T}, \overline{P}), \tag{A24}$$

with the main non-linearity arising from the dependence of the reaction rate on temperature. The exact mean reaction rate may be written as a multiple integral of the instantaneous reaction rate weighted by the joint probability density function (PDF) describing the thermochemical state of the mixture

$$\overline{\omega} = \int_T \int_{Y_1} \ldots \int_{Y_N} \omega_n(Y_1, \ldots, Y_N, T)\, P(Y_1, \ldots, Y_N, T)\, dY_1 \ldots\, dY_N\, dT, \tag{A25}$$

where the effect of pressure has been neglected and $P(Y_1, .., Y_N, T)$ is the joint PDF of composition and temperature. Derivation of joint PDFs is possible, but has so far been limited to small scalar spaces and steady state calculations due to the very high computational overhead. Hence, approximations for the mean reaction rate are required.

Consider the simple reaction scheme

$$F + sO \rightarrow (1 + s)\, P, \tag{A26}$$

where s is the stoichiometric mass requirement of oxidant required to oxidise 1 kg of fuel. Magnussen and Hjertager (1976) propose a model for this reaction rate, based on the Spalding (1971) eddy break up model. Under the assumption of fast chemistry, it is assumed that the reaction rate will be determined by the mixing of the fuel and oxidant eddies at the molecular level. This small scale mixing is described by the dissipation rate of the eddies. The mean disappearance rate of the fuel is given by

$$\bar{\omega}_F = -A \tfrac{\varepsilon}{k} \bar{\rho}\, \tilde{Y}_{\min}, \text{ where } \tilde{Y}_{\min} = \min\left(\tilde{Y}_F,\ B \tfrac{\tilde{Y}_P}{1+s}\right), \tag{A27}$$

where A and B are constants. The function min indicates that the smallest of the terms within the brackets is to be used to determine the reaction rate. The presence of the product mass fraction within the brackets ensures that the flame propagation is determined by the turbulent diffusion of the product species into the reactants. This form of the reaction rate is widely used (in a modified form) in codes such as EXSIM and CFX-4.

The preceding sub-section introduced the laminar burning velocity, which is defined as the mass consumption of unburnt gas divided by its density per unit area of flame. It was also shown that the turbulent burning velocity may be determined from the laminar flame burning velocity if the instantaneous surface area of the flame is known. A knowledge of the flame surface area per unit volume may also be used to define a reaction rate, which is the product of the laminar burning velocity, the flame surface area, and the unburnt gas density

$$\bar{\omega}_F = -\rho_u\, Y_{F,u}\, u_l\, f \Sigma, \tag{A28}$$

where Σ is the mean flame surface area per unit volume, ρ_u is the density of the unburnt gas, $Y_{F,u}$ is the fuel mass fraction in the unburnt gas, and f is a correction factor for the effects of

strain on the laminar burning velocity. A transport equation may be derived for the flame surface area, which may be modelled and solved. However, the modelling process introduces uncertainties and an increase in computational effort. A simpler method is to obtain the flame surface area algebraically. An expression for Σ may be obtained by treating the passage of flame surfaces past a point in space as a stochastic process analogous to a random telegraph signal - Bray *et al.* (1989)

$$\Sigma = \frac{g\bar{c}(1-\bar{c})}{|\bar{\sigma}_y|\hat{L}_y}, \tag{A29}$$

where g and $\bar{\sigma}_y$ are model constants (assuming the values of 1.5 and 0.5 respectively), $\hat{L}_y$ is the integral length scale of the telegraph signal process, and the reaction progress variable c may be defined as

$$c = \frac{Y_{F,u}-Y_F}{Y_{F,u}-Y_{F,b}}, \tag{A30}$$

where $Y_{F,b}$ is the fuel mass fraction in the fully combusted mixture. One of the more recent codes, NEWT, uses this combustion model.

A4. Numerical Modelling

A brief description of the numerical methods applicable to CFD codes will be given in this section. The equations describing the explosion process have been given in the preceding sections. An analytical solution of this system of equations is not possible and one must resort to numerical methods. To obtain a numerical solution a discretization method is used. The solution domain (in both space and time) is discretized and the final solution yields values of the dependent variables at these discrete points. Three discretization approaches are commonly used in CFD. The first, the finite difference method, covers the solution domain by a grid. At each grid point the differential equations describing the explosion flow are represented by replacing the partial derivatives with values derived using the discrete grid point values. This results in one algebraic equation per variable for each grid node. The disadvantage of the finite difference method is that conservation is not automatically enforced. The most widely used approach is the finite volume method, which uses an integral form of the conservation equations. The spatial solution domain is divided into a number of control volumes to which the conservation equations are applied. At the centroid of each control volume is a computational node at which the variable values are calculated / stored. Variable values at the control volume faces are obtained by interpolation between neighbouring control volume centroid values. Advantages of the finite volume method include the ability to model complex geometries and conservation of the flow variables. Finally, the finite element method is similar to the finite volume method in that the spatial domain is split into a set of discrete volumes (finite elements). A simple piece-wise function, valid on each of the elements, is used to describe the local variations of the flow variables.

The discrete positions at which the variables are to be calculated are defined by a grid, which is a discrete representation of the flow geometry. Different types of grid may be used and these are described below. The first type of grid is the structured grid, which consists of families of grid lines with the property that grid lines belonging to the same family do not cross each other and only cross each member of the other families once. A simple example of

a Cartesian structured grid (in two dimensions) would be a series of lines crossing each other at right angles, forming a pattern of squares. It is not generally a requirement, however, that the grid lines are regularly spaced. Non-orthogonal (or body-fitted) grids do not have their grid lines crossing at right angles and are capable of modelling more complex geometries. An example of a non-orthogonal structured grid is shown in fig. A2.

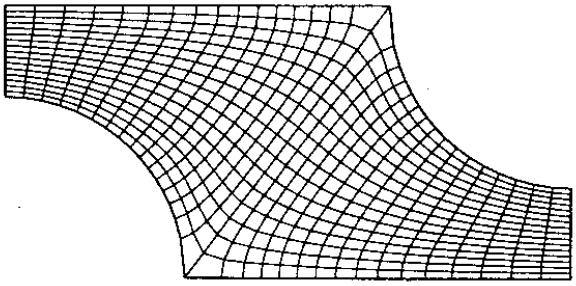

Figure A2 - A non-orthogonal structured grid

An increase in functionality is obtained by the use of multi-block structured grids. The flow geometry is split into a number of large scale regions, each of which is gridded with a structured mesh - which may or may not match the meshes on the other blocks at the block interfaces. This method is more adaptable than the previous single block method and may be used to model more complex geometries or to provide local grid refinement in regions where it is necessary to resolve the flow more accurately. Fig. A3 shows an example of a matched interface, multi-block, non-orthogonal structured grid.

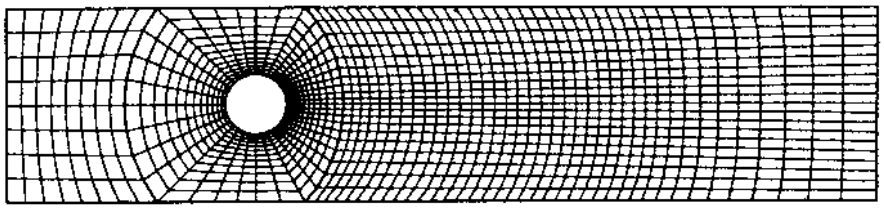

Figure A3 - A multi-block, non-orthogonal structured grid

For very complex geometries an unstructured mesh provides the best representation and works best with the finite volume or finite element approach. The control volumes may assume any shape and there is no limit to the number of neighbouring control volumes. However, a disadvantage of the unstructured grid approach is that the solution is slower than for a structured grid. An example of an hybrid grid with combination of a prismatic part in the boundary layer and an unstructured part is shown in fig. A4.

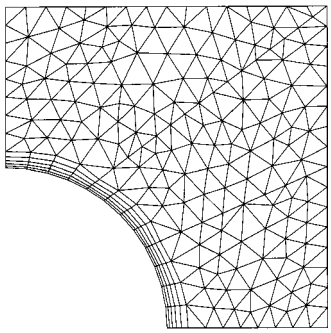

Figure A4 - An unstructured grid with prismatic grid in the boundary layer

The memory efficiency of any gridding technique may be further enhanced by use of adaptive gridding, whereby the grid is initially coarse, but during the calculation locally refines in order to resolve flow features. One advantage of adaptive gridding is that the optimum grid resolution need not be known a priori. Also, the local grid refinement increases memory efficiency, as the grid only refines where necessary. Codes that implement adaptive gridding generally also allow the grid to be de-refined, when there is no longer a need for a high grid resolution. During transient calculations this allows features to be tracked by the grid - e.g.. the flame front may be resolved by a fine mesh in an explosion calculation, whilst maintaining a relatively coarse mesh elsewhere in the solution domain.

Despite the increase in grid efficiency at representing arbitrary flow domains offered by each of these successive gridding techniques, it is not yet possible to represent the most complex geometries. The limit to the geometric complexity that may be modelled is imposed by computer memory and speed. A very high performance PC or workstation might be able to contain a model of one million cells, with the time taken for a solution of around a week. A three-dimensional grid containing one million nodes would only allow, for example, one hundred nodes in each co-ordinate direction. For a typical offshore module or chemical plant this would allow evenly spaced cells of 0.1 to 1.0 m side length. This is clearly too coarse to accurately represent all of the features present. Hence, sub-grid models have been introduced to model the effects of objects that are smaller than the grid spacing. Several of the codes presented in this report (EXSIM, FLACS, etc.) include the Porosity / Distributed Resistance (PDR) formulation of the governing equations. Sub-grid scale obstacles are represented by a volume fraction, an area fraction, and a drag coefficient. These obstacles offer an increased resistance to flow, a decreased flow area, and an increased production rate of turbulence, the effects of which need to be modelled. This modelling introduces additional uncertainty.

The most commonly used method of discretisation used by the explosion codes is the finite volume method. This uses an integral form of the conservation equation as its starting point. Eqn. A12 may be recast in the following form

$$\int_V \frac{\partial}{\partial t}\left(\bar{\rho}\tilde{\phi}\right) dV + \int_S \bar{\rho}\tilde{\phi}\tilde{\mathbf{u}} \bullet \mathbf{n}\, dS - \int_S \frac{\mu_T}{\sigma_\phi}\nabla\tilde{\phi} \bullet \mathbf{n}\, dS = \int_V \bar{S}_\phi\, dV, \qquad \text{(A31)}$$

where the molecular terms have been neglected, gradient transport has been assumed for the turbulent scalar fluxes, and **n** is the unit normal vector at the control volume surface. An approximated form of this integral equation is applied to each of the control volumes yielding a system of simultaneous equations, the solution of which describes the flow. Methods are therefore needed to numerically approximate the surface and volume integrals appearing in eqn. A31. The simplest method of approximating a volume integral is to replace the integral with the product of the cell centre value of the integrand and the cell volume - i.e.

$$\int_V \bar{S}_\phi \, dV \approx \bar{S}_{\phi,Centre} V. \tag{A32}$$

This method is second order accurate - i.e. the error is proportional to the square of the cell size. To evaluate the surface integrals the value of the integrand is required at each position on the surface. The simplest approximation (and one that is also second order accurate) is to replace the integral by the sum over all faces of the products of the integrand values at the cell face centres and the cell face areas - i.e.

$$\int_S \bar{\rho}\tilde{\phi}\tilde{\boldsymbol{u}} \bullet \boldsymbol{n} \, dS \approx \Sigma_i \left(\bar{\rho}\tilde{\phi}\tilde{\boldsymbol{u}} \bullet \boldsymbol{n}\right)_{i,Centre} S_i. \tag{A33}$$

However, the integrand values are not known at the cell faces, but are stored only at the cell centres. Values at the cell faces must be obtained by interpolation. It will be assumed that the velocity field and the fluid properties are known at all positions, the value of ϕ at the cell face centres must be found by interpolation. Consider fig. A5, which shows a one dimensional sequence of cells.

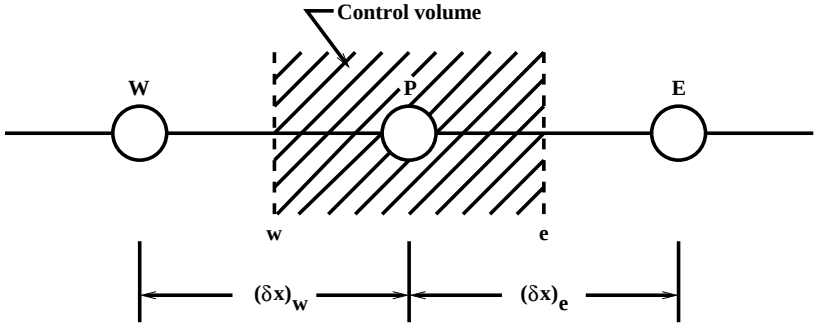

Figure A5 - Control volume in one dimension

The value of ϕ at face 'e' may be found most simply by linearly interpolating between the values at 'P' and 'E':

$$\phi_e \approx a\,\phi_E + (1-a)\,\phi_P, \text{ where } a = \frac{x_e - x_P}{x_E - x_P}, \tag{A34}$$

and the gradient of ϕ at face 'e' is simply given by

$$\left(\frac{d\phi}{dx}\right)_e \approx \frac{\phi_E - \phi_P}{x_E - x_P}. \tag{A35}$$

However, this method is unstable for the convective terms at high Reynolds numbers and is therefore not suitable for explosion flows. A simple scheme that is stable is the first-order

upwind differencing scheme. The value of ϕ at 'e' is taken as the value at the upstream node from 'e' - i.e.

$$\phi_e = \phi_P \text{ if } (\tilde{\boldsymbol{u}} \bullet \boldsymbol{n})_e > 0 \text{ and } \phi_e = \phi_E \text{ if } (\tilde{\boldsymbol{u}} \bullet \boldsymbol{n})_e < 0. \qquad \text{(A36)}$$

However, this method is only first order accurate (the error is proportional to size of the control volume) and may also lead to numerical (false) diffusion. This is a particular problem for multi-dimensional flows, when the direction of flow is oblique to the grid. Numerical diffusion is then produced in directions both normal and aligned with the direction of the flow. Higher order schemes do exist, and are used by the more advanced CFD codes. These schemes use an increased number of nodal points to interpolate the cell-face values using curves. An example of such a higher order scheme is the QUICK scheme, which uses two upstream nodes and one downstream node to fit a local parabola. This scheme is third order accurate but if used with the simple approximation for the surface integral shown above is second order accurate overall.

The discretization process yields a set of algebraic equations that are generally non-linear and hence must be solved by an iterative technique. This technique involves guessing the solution, linearizing the equations about that solution, then improving the solution. The steps of linearization and solution improvement are repeated until the solution reaches (within a certain bound) a steady result - at which point the solution is said to be converged. Transient calculations, such as explosions, march through time in a sequence of time-steps. A converged solution must be obtained at each time-step. Convergence is not trivial, especially for the high speed flows typical of explosions. The choice of time step can be crucial in determining whether or not a converged solution is possible. Hence, adaptive time-stepping may be implemented to aid stability.

APPENDIX B - COMBUSTION MODEL IN SCOPE CODE

The following description of the models used in the SCOPE 2 code is summarised from Puttock *et al.* (1996). The explosion geometry is approximated by a box of length L and cross-sectional area A. At one end of the box is the main vent of area A_v and along the length of the box there is provision to incorporate side vents of total area A_s.

Ignition occurs at the centre of the face opposite the explosion vent, which corresponds to the worst possible case. The flame is assumed to be hemispherical until it reaches the walls of the box, at which point it ceases to increase in size and propagates along the box with a roughly hemispherical shape. The flame position, measured from the ignition point to the flame leading edge, is denoted by the variable X. In order to correctly predict the relationship between pressure generation and vent flow, the code records the evolution of two variables with time; representing the amounts of burnt and unburnt gas inside the box. From the point that the flame reaches the walls, these equations are

$$\frac{dM_u}{dt} = -s A u_T \rho_u - C_D u_v A_v \rho_u \qquad \text{(B1)}$$

and

$$\frac{dB}{dt} = P^{1/\gamma} s A u_T E, \qquad \text{(B2)}$$

where M_u is the mass of unburnt gas inside the box, the flame area is sA, C_D is the vent discharge coefficient, u_v is the velocity of the unburnt gas through the vent, P is the pressure inside the box, and E is the expansion ratio.

The quantity B is given by

$$B = P^{1/\gamma} V_b, \qquad \text{(B3)}$$

where V_b is the volume of burnt gas inside the box. The pressure and flame position is determined by the quantity of burnt and unburnt gas in the box.

The turbulent burning velocity (u_T) is obtained semi-empirically, allowing the model to be adjusted after comparison with experimental data. The basic form follows from Gülder (1990b)

$$\frac{u_T}{u_l} = 1 + \alpha \left(\frac{u'}{u_l}\right)^{1/2} \mathrm{Re}_l^{1/4}, \qquad \text{(B4)}$$

where α is a constant. The laminar burning velocity (u_l) is corrected for the effects of strain using the following expression, cf. Gouldin (1987),

$$\frac{u_l}{u_{l,0}} = 1 - \beta \, \mathrm{Ka}, \qquad \text{(B5)}$$

where $u_{l,0}$ is the unstrained laminar burning velocity, β is a constant which should be proportional to the Markstein number for the gas, and Ka is the Karlowitz stretch factor, which Bradley *et al.* (1984) define as

$$\mathrm{Ka} = 0.157 \left(\frac{u_l}{u_{l,0}}\right)^2 \mathrm{Re}_l^{1/2}, \qquad \text{(B6)}$$

The Markstein number is a physicochemical parameter that expresses the response of a flame to stretching - Bradley *et al.* (1992). The model constants (α and β) are obtained by fitting the model to experimental data provided by Gouldin (1987), Abdel-Gayed *et al.* (1984), and Leuckel *et al.* (1990).

The turbulence in the unburnt gas after each grid is calculated as the sum of the incident turbulence and the flow velocity ahead of the flame as the flame reaches the grid - i.e..

$$u'_{new} = (u'^2 + 0.01\, C_g\, u_u^2)^{1/2}, \qquad \text{(B7)}$$

where u_u is the velocity of the unburnt gas ahead of the flame. C_g is the drag coefficient, which is a function of the obstacle shape and blockage ratio.

APPENDIX C - COMBUSTION MODELS IN CFD CODES

C1. EXSIM

The PDR formulation of the transport equation for the general variable is

$$\frac{\partial}{\partial t}\left(\beta_v \bar{\rho}\tilde{\phi}\right) + \nabla \bullet \left(\boldsymbol{\beta}\bar{\rho}\tilde{u}\tilde{\phi}\right) - \nabla \bullet \left(\boldsymbol{\beta}\frac{\mu_T}{\sigma_\phi}\nabla\tilde{\phi}\right) = \bar{S}_\phi + \bar{R}_\phi, \qquad \text{(C1)}$$

where β_v is the volume porosity, $\boldsymbol{\beta}$ is the area blockage ratio vector, $\bar{S}_\phi$ is the non-obstructed component of the mean source, and $\bar{R}_\phi$ is the additional component of the source term caused by the obstructions. Gradient transport has been assumed for the turbulent diffusion. The effective viscosity (μ_T) is obtained using the two equation k-ε model, which has been modified to include the additional turbulence generation from the sub-grid scale objects. The production rate of turbulent kinetic energy is modelled as

$$\bar{S}_k = -\beta_v \rho \overline{\boldsymbol{u}'' \otimes \boldsymbol{u}''} : \nabla\tilde{\boldsymbol{u}} \text{ and } \bar{R}_k = C_s \mu_T |\tilde{\boldsymbol{u}}|^2 A_w^2 + \Sigma_n \boldsymbol{C}_T \bar{\boldsymbol{R}}_{\boldsymbol{u}} \bullet \tilde{\boldsymbol{u}}, \qquad \text{(C2)}$$

where C_s is a constant, A_w is the wetted area of the obstacles per unit volume, and $\boldsymbol{C}_T$ is a constant vector that gives the fraction of the pressure drop, in each co-ordinate direction, that contributes to the generation of turbulence kinetic energy. $\bar{R}_u$ is the drag force vector, and is given by

$$\bar{R}_{\boldsymbol{u},i} = -C_D \tfrac{1}{2} \bar{\rho} |\tilde{u}_i| \tilde{u}_i, \qquad \text{(C3)}$$

where C_D is the drag coefficient. In regions containing sub-grid scale obstacles the turbulence kinetic energy dissipation rate is not obtained from its transport equation, but is calculated from the following expression

$$\varepsilon = C_\mu^{3/4} \frac{k^{3/2}}{l}, \qquad \text{(C4)}$$

where $l = C_l D_{Ob}$, C_l is a constant and D_{Ob} is a typical obstacle dimension.

The turbulent combustion rate is modelled using the modified eddy break-up combustion model of Magnussen and Hjertager (1976). This is further modified by the inclusion of an ignition / extinction criterion - Hjertager (1982). The turbulent fuel consumption rate is given by

$$\bar{\omega}_f = 0, \text{ when } \frac{\tau_{ch}}{\tau_e} > D_{ie}, \qquad \text{(C5)}$$

or

$$\bar{\omega}_f = -\beta_v E_T A \frac{\varepsilon}{k} \rho Y_{min}, \text{ when } \frac{\tau_{ch}}{\tau_e} \le D_{ie}, \qquad \text{(C6)}$$

where A is a constant (A=20) and E_T is a combustion enhancement factor. The ignition / extinction criterion is based on the turbulent Damköhler number, which is the ratio of the chemical timescale (τ_{ch}) to the turbulent eddy mixing time scale (τ_e). These time scales are defined as

$$\tau_{ch} = A_{ch} \exp\{E_A/RT\} (\bar{\rho}\tilde{Y}_f)^a (\bar{\rho}\tilde{Y}_o)^b \quad \text{(C7)}$$

and

$$\tau_e = \frac{k}{\varepsilon} . \quad \text{(C8)}$$

The critical Damköhler number (D_{ie}) is taken to be 1000. If the turbulence Reynolds number is less than a critical value, the combustion rate is calculated from a quasi-laminar expression

$$\omega_f = -\beta_v E_L A_{lam} \frac{u_l}{\delta_l} \bar{\rho} Y_{\min}, \quad \text{(C9)}$$

where E_L is a flame area enhancement factor related to the instability induced wrinkling of the laminar flame, which varies linearly from 1 at a flame radius of 0 m to 2.5 at a flame radius greater than or equal to 0.5 m. A_{lam} is a constant, and δ_l is the laminar flame thickness.

C2. FLACS

The transport equation for the fuel may be written

$$\bar{\rho}\frac{D\tilde{Y}_F}{Dt} = \nabla \bullet (\bar{\rho} D \nabla \tilde{Y}_F) - Y_{F,0}\,\bar{\omega} \quad \text{(C10)}$$

The diffusion coefficient (D) is modelled as, Arntzen (1995),

$$D = 0.7\, S\, \Delta \quad \text{(C11)}$$

and the reaction rate ($\overline{\omega}$) as

$$\bar{\omega} = 3.5 \frac{S}{\Delta} \min\{c, 9 - 9c\}, \quad \text{(C12)}$$

where S is the burning velocity and Δ is the grid spacing. It is noted that eqn. C12 appears to be deficient by a factor of ρ. The turbulent burning velocity is obtained from one of the two following correlations, Bray (1990) and Abdel-Gayed and Bradley (1989),

$$u_{T_1} = 15\, u_l^{0.784}\, u'^{0.412}\, l^{0.196} \quad \text{(C13)}$$

and

$$u_{T_2} = u_l + 8\, u_l^{0.284}\, u'^{0.912}\, l^{0.196}, \quad \text{(C14)}$$

where $u_T = \min\{u_{T_1}, u_{T_2}\}$. An enhancement factor is applied to this turbulent burning velocity, to account for the flame area change as the flame passes through the sub-grid scale obstacles. This enhancement factor is

$$E_T = \max\{(R/P)^{0.4}, 1\}, \quad \text{(C15)}$$

where R is the radial distance of the flame front from the ignition point and P is a representative obstacle pitch. In some low-turbulence regions, or just after ignition in an

initially quiescent mixture, the flame will propagate in a quasi-laminar fashion. The burning velocity in this quasi-laminar phase is given by

$$u_{l,q} = \max\{1,\ \min\{R/P,\ 2\}.\} \qquad \text{(C16)}$$

The laminar burning velocity in FLACS is obtained from polynomial functions of the equivalence ratio and flammability limits.

C3. CFX-4

The explosion-modified code models the three important stages in the growth of an explosion. First, there is ignition and the establishment of an initial flame kernel. Second, the flame front expands as an initially laminar and then weakly turbulent reaction zone. Finally, if the flame encounters obstacles, or the turbulence level in the unburnt gas ahead of the flame otherwise increases, the flame will accelerate, propagating as a thick, highly turbulent reaction zone. Quenching of a flame is the reduction in reaction rate due to either flame stretch or turbulent time scales. Quenching due to flame stretch has been accounted for in both the thin flame and eddy break-up combustion models by a simple expression based on the Damköhler number.

Initially, the combusting region will be small compared to the volume of grid cells it occupies. A simple model treats this early flame as a laminar fire ball, which allows the fuel consumption rate to be estimated analytically as a function of time. The flame is assumed to be spherical and to burn at the laminar rate. The radius of the ignition region (R_{Ig}) is fixed and it is from this that the ignition time is determined

$$t_{Ig} = \frac{R_{Ig}}{u_f}, \qquad \text{(C17)}$$

where

$$u_f = \frac{\rho_u}{\rho_b} u_l.$$

The fuel mass fraction source term within the ignition region is given by

$$\overline{\omega}_F = \begin{cases} -\bar{\rho}\frac{\tilde{Y}_F}{t_{Ig}}\left(\frac{t}{t_{Ig}}\right)^2 \exp\{-\frac{t}{t_{Ig}}\} & \text{for } t \le t_{Ig} \\ 0 & \text{for } t > t_{Ig} \end{cases}. \qquad \text{(C18)}$$

This form for the ignition source does not give a smooth transition to the quasi-laminar phase, but does ensure that the ignition timescale is accurate. However, the exponential term in Eqn. C18 has not been implemented in CFX-4, release 3. Following ignition the flame propagates as a thin or quasi-laminar reaction zone. The actual physical width of this reaction zone (i.e.. for a real laminar flame) is likely to be smaller than the grid spacing. However, the simulated width of the reaction zone cannot be less than one cell, therefore it is necessary to model the heat release rate. Consider the reaction process to be characterised by a single progress variable (c) where, in this case, $c = 1$ is a property of the unburnt mixture. Now consider a set of values for this progress variable (c_i) at distances along a line normal to the flame front, separated by spacings of Δ_i. The equation describing the development of this progress variable is

$$\frac{dc_i}{dt} = \begin{cases} -\frac{c_i}{t_B} & \text{for } c_{i-1} \le \alpha \\ 0 & \text{for } c_{i-1} > \alpha \end{cases}, \tag{C19}$$

where t_B is the burning time and α is a constant bounded by zero and unity. The burning velocity is given by

$$u_B = \frac{\Delta_i}{t_b \ln\{1/\alpha\}}. \tag{C20}$$

The constant α determines the thickness of the modelled flame. If this constant is too large then the flame will be spread over several cells, whereas a small value will produce a flame that occupies only the thickness of one cell - yielding an undesirably large burning rate. Hence, a moderate value of this constant is used. The purpose of this transformation is to allow the modelled burning rate to be matched to a specified burning velocity - via t_b.

The laminar burning velocity of a combustible mixture is a function of the gas composition, its temperature and pressure, and may generally be easily specified. However, a small degree of turbulence will affect the flame propagation velocity greatly. The effects of mild turbulence are modelled by introducing the burning velocity correlation of Bradley *et al.* (1992), in a slightly modified form

$$u_B = u_l + 0.88 F \,\mathrm{Ka}^{-0.3} \sqrt{2k}, \tag{C21}$$

where F is a fitting factor, Ka is the Karlowitz stretch factor, and k is the turbulent kinetic energy. The Karlowitz stretch factor is given by

$$\mathrm{Ka} = 0.157 \frac{2k}{u_l^2} \left(\frac{\mu}{\mu_T}\right)^{0.5}. \tag{C22}$$

To enable the model to correctly predict the reaction rate of mixtures of differing equivalence ratios, the laminar burning velocity is obtained from a three point parabolic fit in terms of the equivalence ratio and the maximum laminar burning velocity, Bakke (1986),

$$\frac{u_l}{u_{l,max}} = \frac{(x-x_l)(x-x_r)}{(1-x_l)(1-x_r)}, \tag{C23}$$

where $x = \Phi/\Phi_{max}$. Φ_{max} is the equivalence ratio corresponding to the maximum laminar burning velocity ($u_{l,max}$) and x_l and x_r are the values of x at the lean and rich limits of flame propagation, respectively.

When the flow becomes fully turbulent, the combustion rate is modelled using a form of the eddy break-up expression

$$\bar{\omega}_F = -\rho \frac{\varepsilon}{k} C_R \, C_A \, Y_{min}, \tag{C24}$$

where C_R is given by

$$C_R = 23.6 \left(\frac{\mu \varepsilon}{\bar{\rho} k^2}\right)^{0.25} \tag{C25}$$

and C_A is given by

$$C_A = \begin{cases} 1 & \text{for } Y_P \geq Y_{P,i} \\ 0 & \text{for } Y_P < Y_{P,i} \end{cases}, \tag{C26}$$

where Y_P is the mass fraction of products and $Y_{P,i}$ is an ignition criterion based upon a product mass fraction threshold and Y_{min} which is defined as

$$Y_{min} = min\ (Y_{fu},\ Y_{ox}/s,\ BY_p/(1+s)),$$

where Y_{fu} is the mass fraction of fuel, Y_{ox} is the mass fraction of oxidant, Y_p is the mass fraction of product, s is the stoichiometric mass requirement of oxidant required to oxidise 1 kg of fuel, and B is a model constant. This is introduced to prevent propagation of the flame due to numerical effects. The quenching of the flame is also accounted for in CFX-4. The ratio of quenched and unquenched reaction rates is given by

$$\frac{\bar{\omega}_{F,q}}{\bar{\omega}_F} = \exp\left\{-\frac{D}{D_q}\right\}, \tag{C27}$$

where D is the Damköhler number and D_q is the quenching threshold. For the thin flame model the Damköhler number is the ratio of the turbulent rate of strain to the laminar flame crossing rate, for the eddy break-up model it is the ratio of the eddy dissipation rate to the laminar flame crossing rate. The quasi-laminar, thin flame model is used whenever the burning rate calculated by the thin flame model is greater than that calculated by the eddy break-up model. Hence, the thin flame model is not used only as a forerunner to the eddy break-up calculation, but is used throughout the entire life of the explosion to ensure that all low turbulence regions burn out correctly.

Currently, the turbulence model used in CFX-4 for explosion modelling is the two-equation k-ε model. Originally, the version of this turbulence model included in the standard CFX-4 code, in common with other explosion models and CFD codes, incorporated the effects of turbulence generation due to shear and (optionally) buoyancy only. However, two of the terms omitted from the exact transport equation for k may exhibit a large effect in an explosion situation. These terms appear as additional sources in the k equation and arise from compressibility effects, Jones (1980), not from the Rayleigh-Taylor instability as has been previously stated, Guilbert and Jones (1996). The terms are modelled as follows, see Bradley *et al.* (1988),

$$\overline{P' \nabla \bullet u''} = -\frac{9}{55}\ \bar{\rho}\ k \nabla \bullet \tilde{u} \tag{C28}$$

$$-\overline{u''} \bullet \nabla \bar{P} = -\frac{\mu_T}{\sigma_\rho}\frac{1}{\bar{\rho}^2} \nabla \bar{\rho} \bullet \nabla \bar{P}, \tag{C29}$$

where the term on the right hand side of each equation is the modelled form. These terms have been included in release 3 of the CFX-4 code. A large improvement in over-pressure prediction is noted after inclusion of these terms, the over-pressure increased (typically by an order of magnitude) compared with that predicted by the standard k-ε model, Pritchard *et al.* (1996).

C4. COBRA

The reaction progress variable (c) used in COBRA is bounded between zero and unity and is defined as $c = 1 - Y_F / Y_{F,u}$, where $c = 0$ corresponds to unburnt mixture. The combustion model may be considered as consisting of two distinct parts. The first part prescribes a local turbulent burning velocity based on the local flow properties and the second part ensures that the solution of the transport equations yields a propagating flame front that matches this prescribed burning velocity. The correlations of Bray (1990) and Gülder (1990a) are used to derive the turbulent burning velocity. The correlation of Bray (1990) is used in the regime where $\mathrm{Re}_l > 3200$ and $\mathrm{Re}_\eta > 1.5\,(u'/u_l)$ and is given by

$$\frac{u_T}{u_l} = 0.875\,\mathrm{Ka}^{-0.392}\,\frac{u'}{u_l}\,, \tag{C30}$$

where Ka, the Karlowitz stretch factor, is taken as

$$\mathrm{Ka} = 0.157\left(\frac{u'}{u_l}\right)\mathrm{Re}_l^{-1/2}, \tag{C31}$$

where

$$u' = \left(\frac{2k}{3}\right)^{1/2}.$$

Gülder (1990a) proposes three correlations for different turbulence regime

$$\frac{u_T}{u_l} = 1 + 0.62\left(\frac{u'}{u_l}\right)^{1/2}\mathrm{Re}_\eta \qquad \text{for } \mathrm{Re}_\eta \le 3200 \text{ and } \mathrm{Re}_\eta \ge 1.5\frac{u'}{u_l}, \tag{C32}$$

$$\frac{u_T}{u_l} = 1 + 0.62\exp\left\{0.4\left(\frac{u'}{u_l}\right)^{1/2}\right\}\mathrm{Re}_\eta \quad \text{for } \mathrm{Re}_l \le 3200 \text{ and } 0.6\frac{u'}{u_l} \le \mathrm{Re}_\eta \le 1.5\frac{u'}{u_l}, \tag{C33}$$

$$\frac{u_T}{u'} = 6.4\left(\frac{u_l}{u'}\right)^{3/4} \text{for } \mathrm{Re}_l \le 3200 \text{ and } \mathrm{Re}_\eta < 0.6\frac{u'}{u_l} \text{ or } \mathrm{Re}_l > 3200 \text{ and } \mathrm{Re}_\eta < 1.5\frac{u'}{u_l}, \tag{C34}$$

where the turbulence Reynolds number based on the Kolmogorov length scale (Re_η) is taken to be $\mathrm{Re}_l{}^{1/4}$. An enhancement factor is applied to the predicted burning velocity, based on the geometry of the sub-grid scale obstacles. This factor takes the form

$$E_T = 1 + \frac{\rho_b}{\rho_u}\frac{D}{P}, \tag{C35}$$

where D is representative obstacle diameter and P a representative obstacle pitch. Catlin and Lindstedt (1991) used numerical techniques to determine the burning velocities predicted by mixing controlled reaction models under idealised conditions. Their study focused on the limitation of such models caused by the problem associated with the boundary condition used at the cold front of the flame, i.e. the burning velocity predicted by these mixing controlled models is not uniquely defined unless the reaction rate falls to zero as the cold front is approached. Catlin and Lindstedt (1991) found that a quenching model based on the reaction progress variable was found to predict a limiting steady value for the burning velocity. Following guidelines established by the analysis of Catlin and Lindstedt (1991), the reaction rate in COBRA is specified as

$$\bar{\omega}_c = \bar{\rho} R \tilde{c}^4 (1-\tilde{c})(\tfrac{\rho_u}{\rho_b})^2. \qquad \text{(C36)}$$

The analysis of Catlin and Lindstedt (1991) shows that the turbulent burning velocity and the turbulent flame thickness can be expressed in terms of a turbulent diffusion coefficient (Γ) and the reaction rate constant (R) as

$$u_T = \Lambda_1 (\Gamma R)^{1/2} \qquad \text{(C37)}$$

and

$$\delta_T = \Lambda_2 (\Gamma R)^{1/2}, \qquad \text{(C38)}$$

where Λ_1 and Λ_2 are burning velocity and flame thickness eigenvalues. If the burning velocity is specified and the flame thickness is known, then the values of Γ and R required to reproduce the burning velocity are

$$\Gamma = \tfrac{u_T \delta_T}{\Lambda_1 \Lambda_2} \qquad \text{(C39)}$$

and

$$R = \tfrac{u_T \Lambda_2}{\delta_T \Lambda_1}. \qquad \text{(C40)}$$

Both eigenvalues have been calculated from one-dimensional numerical calculations of a planar flame propagating in a flowfield with constant levels of turbulence. These calculations demonstrate that unique values of these eigenvalues do exist and have the values of $\Lambda_1 = 0.346$ and $\Lambda_2 = 3.575$. In the calculations the flame thickness was taken as being equal to a turbulence length scale given by $l = C_\mu^{3.4} k^{3/2}/\varepsilon$, COBRA also uses this expression for the flame thickness.

C5. NEWT

Earlier work, sponsored by Shell Research Ltd., has applied NEWT to the modelling of two explosion geometries, the HSL baffled box, Connell *et al.* (1996a), and the Shell SOLVEX box, Watterson *et al.* (1996) and Connell *et al.* (1996b). This work highlighted deficiencies in the eddy break-up combustion model employed in NEWT. In particular it was found necessary to apply two constraints to the eddy break-up model. The first was required to yield correct flame behaviour near to walls. The reaction rate predicted by the eddy break-up model is proportional to the reciprocal of the turbulence time-scale ($\omega \propto \varepsilon / k$). Near wall boundary conditions force k to zero whilst ε remains finite, resulting in the combustion rate becoming unbounded as a wall is approached. However, experimental evidence shows that the opposite is true and in fact the combustion rate is decreased near surfaces. To prevent the combustion rate becoming unbounded near solid surfaces the eddy break-up term is modified so that when k becomes small the reaction rate is dependent on the Kolmogorov time scale

$$\bar{\omega}_c = C_{com} \bar{\rho} \tilde{c} (1-\tilde{c}) \left(\tfrac{k}{\varepsilon} + \sqrt{\tfrac{\nu}{\varepsilon}} \right)^{-1}, \qquad \text{(C41)}$$

where C_{com} is a constant and v is the kinematic viscosity of the gas mixture. The second constraint ensures that the combustion rate falls to zero as the leading edge of the flame is approached. This is achieved simply, and crudely, by setting the reaction rate to zero below a certain threshold for the reaction progress variable (leading edge suppression).

Within the HSE funded project, a parametric study has been undertaken to determine the sensitivity of the model to leading edge suppression and the eddy break-up constant. The value of the progress variable threshold, for the leading edge suppression, was set to be 0.001. This value yielded flame shapes that were qualitatively correct. However, with no leading edge suppression (equivalent to setting the threshold to zero) the flame was observed to become more distributed with spurious ignition, especially in high turbulence regions, whereas increasing the progress variable threshold by an order of magnitude was found to prevent flame propagation entirely. The calculations were also found to be sensitive to the eddy break-up model constant, with the flame speed increasing as this constant is increased. Leading edge suppression was found to be more important with higher values of C_{com}, as increasing this constant increased the tendency for the flame to run along the walls.

Further modifications have been made to the eddy break-up model as documented by Guilbert and Jones (1996). The first of these is a Damköhler number based quenching model, the second is a dependence on the turbulence Reynolds number combined with an ignition threshold - see section 2.3.2 for further details.

Presently the ignition treatment in NEWT is fairly simple, a point ignition is modelled by ramping up the value of the progress variable in a single cell at a wall. To more realistically model the ignition process, work is ongoing to implement the flameball approach described by Guilbert and Jones (1996) - see section 2.3.2. The quasi-laminar flame phase is modelled using the approach of Sæter (1994), where the combustion rate term is modified on the basis of an experimental correlation to ensure that the reaction rate over the whole domain is equal to that of the modelled laminar flame. This form of the reaction rate is used whenever the turbulence Reynolds number falls below a critical value - see section 2.2.2.

The deficiencies of the eddy break-up model have led to the inclusion of the alternative laminar flamelet combustion model, Bray *et al.* (1985), for the turbulent flame phase, in NEWT. The reaction zones are assumed to consist of thin, highly wrinkled surfaces that separate unburnt reactants from fully burnt products. These surfaces are stretched and transported by the turbulence, but retain the structure of a strained laminar flame - i.e.. the flame is propagating in a direction normal to its surface at the locally applicable laminar burning velocity. The reaction rate per unit volume may be formed as a product of the reaction rate per unit surface area (R) and the mean flame surface area per unit volume (Σ)

$$\bar{\omega}_c = R\,\Sigma. \qquad \text{(C42)}$$

It is possible to derive an exact transport equation for Σ, which may be modelled and solved. However, solution of this equation involves significant computational expense and the modelling assumptions introduce additional uncertainties. Presently in NEWT a simpler method is implemented whereby Σ is obtained algebraically. An algebraic expression for Σ may be derived by treating the passage of laminar flamelets past a point in space as a stochastic process analogous to a random telegraph signal, Bray *et al.* (1989),

$$\Sigma = \frac{g\bar{c}(1-\bar{c})}{|\bar{\sigma}_y|\hat{L}_y}, \qquad \text{(C43)}$$

where g and $\bar{\sigma}_y$ are model constants with values of 1.5 and 0.5 respectively, and $\hat{L}_y$ is the integral length scale of the telegraph signal process. Abu-Orf (1996) proposes

$$\hat{L}_y = C_L L_L f\left(\frac{u'}{u_l}\right), \qquad \text{(C44)}$$

where C_L is a constant (taken to be unity) and L_L is the laminar flamelet length scale. The empirical function f is included to reproduce experimentally observed behaviour where the turbulent flame speed first increases with the ratio u'/u_l, but then decreases for higher values of this ratio as flame stretch effects begin to cause local extinction. The laminar flame speed is obtained from an empirical correlation - Abu-Orf (1996). Qualitatively, results obtained using this combustion model are in much better agreement with experiment than with the eddy break-up model.

APPENDIX D - DISCRETIZATION OF PARTIAL DIFFERENTIAL EQUATIONS

D1. Introduction

The equations governing the fluid flow, the Navier-Stokes equations, are partial differential equations. It is necessary to cast the pde's into a set of algebraic equations. This is achieved by discretising the terms, both spatially and temporally, in the pde's. All terms are taken at time t_n, as indicated by a small superscript 'n', i.e. f_i^n, in an explicit finite difference formulation. In implicit finite differences, some if not all terms is taken at time step t_{n+1}. There are also semi-implicit schemes which treats some of the spatial directions implicitly while the other directions are treated in an explicit manner. For a more in-depth treatment, see e.g. Hirsch (1988) or Roache (1998). The following sections describe the process of discretising the equations, using some commonly used schemes.

D2. First-Order Discretization Schemes

Partial Taylor series expansion of partial derivatives yields the basic finite difference form. Assume that the problem is in 1D, the extension to 2D or 3D is trivial, and an explicit formulation is sought.

Carry out a forward expansion of a Taylor series of the first derivative, $\frac{\partial f}{\partial x}$ around point 'i', ignoring third-order and higher terms:

$$f_{i+1} = f_i + \left(\frac{\partial f}{\partial x}\right)_i (x_{i+1} - x_i) + \frac{1}{2}\left(\frac{\partial^2 f}{\partial x^2}\right)_i (x_{i+1} - x_i)^2 + \cdots \qquad \text{(D1)}$$

or

$$f_{i+1} = f_i + \left(\frac{\partial f}{\partial x}\right)_i \Delta x + \frac{1}{2}\left(\frac{\partial^2 f}{\partial x^2}\right)_i \Delta x^2 + HOT\,, \qquad \text{(D2)}$$

where HOT refers to higher order terms. Solve eqn. D2 for $\frac{\partial f}{\partial x}$

$$\left(\frac{\partial f}{\partial x}\right)_i = \frac{f_{i+1} - f_i}{x_{i+1} - x_i} + \frac{1}{2}\left(\frac{\partial^2 f}{\partial x^2}\right)_i \Delta x + HOT, \qquad \text{(D3)}$$

or

$$\left(\frac{\partial f}{\partial x}\right)_i = \frac{f_{i+1} - f_i}{x_{i+1} - x_i} + O(\Delta x), \qquad \text{(D4)}$$

where $O(\Delta x)$ refers to terms of order Δx. The finite difference resulting from the forward expansion of the partial derivative is written as

$$\frac{\partial f}{\partial x} \approx \frac{\delta f}{\delta x} = \frac{f_{i+1} - fi}{\Delta x} \qquad \text{(D5)}$$

and has a truncation error of order Δx. A backward expansion around point 'i', following the procedure above,

$$\left(\frac{\partial f}{\partial x}\right)_i = \frac{f_i - f_{i-1}}{x_i - x_{i-1}} + \frac{1}{2}\left(\frac{\partial^2 f}{\partial x^2}\right)_i \Delta x + HOT \qquad \text{(D6)}$$

gives another finite difference

$$\frac{\partial f}{\partial x} \approx \frac{\delta f}{\delta x} = \frac{f_i - f_{i-1}}{\Delta x}. \qquad \text{(D7)}$$

An analogous procedure can be followed for the temporal discretization. It can be shown that the forward differencing scheme is numerically unstable for all grid spacings, $\Delta x > 0$, and for all time steps, $t_n > 0$, and can, therefore, not be used to discretize the partial derivative. The backward, or more commonly referred to as first-order upwind, differencing on the other hand is stable for all $\Delta x > 0$ and for all time steps, $t_n > 0$. This upwind differencing scheme is frequently used because it is inherently numerically stable. However, the stability is achieved through the truncation error, which has the same effect as diffusion, and is hence referred to as numerical diffusion. An initial step change in a variable would soon be diffused, or smeared out.

D3. Second-Order Discretization Schemes

D3.1. Central Differencing Scheme

Higher order discretization schemes should nominally be more accurate as the truncation error will be of order Δx^2. However, there are other issues to consider, such as whether the discretization scheme is stable. A second order accurate differencing scheme can be obtained by subtracting eqn. D7 from eqn. D5

$$\frac{\partial f}{\partial x} \approx \frac{\delta f}{\delta x} = \frac{f_{i+1} - f_{i-1}}{2\Delta x}. \qquad \text{(D8)}$$

This formulation is often referred to as the central differencing scheme. The expression is stable for $\mathrm{Re}_{cell} < 2$, where the cell Reynolds number is based on the cell width as the characteristic length. The scheme exhibits an unphysical, oscillatory behaviour for cases where $\mathrm{Re}_{cell} \geq 2$. This makes the central differencing scheme unsuitable unless the mesh is sufficiently fine so that the cell Reynolds number is below 2.

A solution to the problem of too much diffusion, when using the first-order upwind scheme, and unphysical wiggles, when using the central differencing scheme, is to use the more accurate central differencing method, where the scheme is stable, and use the upwind scheme everywhere else. It is often referred to as hybrid differencing. Considerable effort has gone into devising blending functions so that central differencing scheme is used to as large an extent as possible.

D3.2. Total Variation Diminishing Schemes

The discretisation schemes, discussed above, are not well suited to compressible flows. A number of different discretisation methods were devised, where sensors which would detect an incipient build up of a shock wave and then locally apply a weighted first order method in the vicinity of the shock wave, in order to avoid overshoots, Roache (1998). Total Variation Diminishing (TVD) schemes were shown, Lax (1973), to have a functional to the solution, called total variation, which will not increase with time for (linear and non-linear) scalar conservation laws. TVD schemes are always first order near the shock but can be higher order

accurate away from the shock. Please see Roache (1998) and references therein for a more detailed discussion of the TVD methods.

D4. References

Hirsch, C. (1988)
Numerical Computation of Internal and External Flows. Volume 1 : Fundamentals of Numerical Discretization
John Wiley & Sons, Guildford, U.K.

Lax, P. D. (1973)
Hyperbolic Systems of Conservation Laws and the Mathematical Theory of Shock Waves
SIAM, Philadelphia, U.S.A.

Roache, P.J. (1998)
Fundamentals of Computational Fluid Dynamics
Third Edition, Hermosa Publishers, New Mexico, U.S.A.

APPENDIX E - COMMUNICATIONS WITH CHRISTIAN MICHELSEN RESEARCH

E1. Introduction

The comments in Sections E2 and E3 are taken verbatim from communications with Christian Michelsen Research in Norway. Lines beginning with '**HSL**' in Section E3 are the questions posed by HSL to the code developers, while lines beginning with '**CMR**' are the answers (verbatim) from CMR. All the views expressed in Appendix E are those of CMR; HSE' s comments and views can be found in Section 2.3.3.

E2. Comments from J. R. Bakke on 20 June 2001

When simulations of dispersion and explosions in large areas like chemical plants or offshore installations are performed the geometry is meshed with a grid of cells of one cubic metre in volume. This is done for practical reasons (acceptable runtimes). FLACS can also be used for other simpler applications, in which case the gridding procedure may be very different.

It is true that for explosion simulations the code can be said to be calibrated for cells of the order one metre cubed. However, grid size sensitivity simulations are performed - not to ensure that the solution is grid independent but rather to see if the grid dependence is acceptable. It is not expected for these kinds of problems that full grid independence can be achieved.

E3. Reply from O.R. Hansen on 9 July 2001

HSL : What control does the user have when it comes to meshing? (Cell size and distribution)

CMR : The user of FLACS will choose the grid embedding himself. The FLACS manual and FLACS-I and FLACS-II course handouts give relatively rigid guidelines on how the gridding should be performed, in order to avoid mistakes. Essential is close to cubical grid cells in combustion regions, and also outside the geometry if far field blast is considered. Stretching of grid towards boundaries is OK, and there are some demands wrt grid resolution relative to geometry and gas cloud size.

1m x 1m x 1m grids was required up to 1993, as FLACS-89 combustion models were calibrated for this. FLACS-93, -94, -95, -96, -97, -98 and FLACS-99 have no requirements on grid size, but rather that the grid resolution is a certain number of grid cells across the room or gas cloud (if less then (sic) the room). In a typical offshore module, we would still use 1m x 1m x 1m, but also 0.5m or less. For large offshore modules, and onshore plants, 2m x 2m x 2m is also sometimes used. For other situations, like explosions inside pipes or equipment, much smaller control volumes than this will be used.

HSL : Dr Bakke said that FLACS has been used to carry out blind predictions with acceptable results. Have any of these calculations been published in the open literature so that I can read it and reference the work?

CMR : Generally most of the work done is confidential in one way or the other. Usually experiments are not shared outside the sponsorgroup of the experiments. A range of different blind tests have been performed (but the degree of blindness vary).

A) During the MERGE and EMERGE projects, some tests were simulated prior to performance of the tests. Some of the tests with initial turbulence were published (see chapter 6 in the EMERGE final report for reference to paper). These were blind, but a range of tests carried out prior to the tests made it not so hard to guess the outcome of the blind tests, and the value is thus questionable.

B) During the Blast and Fire Campaign blind tests were carried out. The first round lost most of its value as the project did a poor job describing the geometry, so that the blind tests and experiments were carried out at quite different geometries. The test 24, 25, 26 and 27 were simulated blind with FLACS. The project did not report test 24 in the final report from SCI, as the rig was destroyed. The SCI final report from the Blast and Fire project (1998) you will easily find at HSE or order from the SCI.

C) 1996 we carried out some simulations in a 20m and a 200m tunnel in South Africa. One year later the experiments were performed by CSIR, and FLACS predicted with good accuracy the outcome of the tests. One of these comparisons from the report from South Africa (CSIR AERO 97/299) is published at a paper from a conference held in Poland 1999:

Hansen, O.R., Storvik, I., and Wingerden, K. van, "*Validation of CFD-models for gas explosions, FLACS is used as example. Model description, experiences and recommendations for model evaluation*", **European Meeting on Chemical Industry and Environment III** pp 365-382, Krakow, Poland September 1999.

D) In a lot of experimental projects we are involved in, we carry out simulations prior to or during experiments. This is also the case for the Blast and Fire Phase 3B project, where we have performed a range of simulations before getting knowledge about the results. In general the results are quite good.

HSL : What criteria do you use to deem the results to be acceptable?

CMR : It is very difficult to set up criteria that makes comparisons acceptable or not. In our validation work, hundreds of simulations are carried out and compared, using different grids, and doing a range of parameter variations (experimentally as in simulations). For pressures we are typically happy if the pressures are predicted within +/-30%, and still find it acceptable with a factor of two deviation in pressure. But this vary with the tests. Some tests sponsored by the HSE showed local pressures to vary with more than a factor of 10 in identical experiments, whereas the average pressures varied by almost a factor of 2. Under these circumstances it is difficult to demand +/-30% from the simulator. In a closed vessel explosion, higher precision is expected.

In one of our studies where 30-40 full scale explosion experiments were simulated and compared with experiments (more than 1000 monitor point comparisons) we find a good trend in general, but still find tests where the deviation is larger than we would like. HSE sponsored this work (report CMR-98-F30058).

With FLACS guidelines and pre-settings of choices are quite strict, so that the user have limited opportunities to influence the results by choosing non-physical parameters. Very often BP or Norsk Hydro perform validation simulation at the same time as ourselves, and get similar answers.

Other CFD-simulators may have strength parametres as input when starting the simulation. A validation work by such a simulator will have limited value.